

UNCLASSIFIED

AD 281 948

*Reproduced
by the*

**ARMED SERVICES TECHNICAL INFORMATION AGENCY
ARLINGTON HALL STATION
ARLINGTON 12, VIRGINIA**

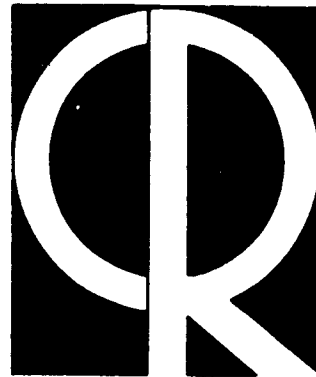


UNCLASSIFIED

NOTICE: When government or other drawings, specifications or other data are used for any purpose other than in connection with a definitely related government procurement operation, the U. S. Government thereby incurs no responsibility, nor any obligation whatsoever; and the fact that the Government may have formulated, furnished, or in any way supplied the said drawings, specifications, or other data is not to be regarded by implication or otherwise as in any manner licensing the holder or any other person or corporation, or conveying any rights or permission to manufacture, use or sell any patented invention that may in any way be related thereto.

62-4-5

281 948



Research Report

**AFCRL Studies of the November 1960
Solar - Terrestrial Events**

**Edited By
J. AARONS AND S. M. SILVERMAN**

Requests for additional copies by Agencies of the Department of Defense, their contractors, and other government agencies should be directed to the:

Armed Services Technical Information Agency
Arlington Hall Station
Arlington 12, Virginia

Department of Defense contractors must be established for ASTIA services, or have their 'need-to-know' certified by the cognizant military agency of their project or contract.

All other persons and organizations should apply to the:

U. S. DEPARTMENT OF COMMERCE
OFFICE OF TECHNICAL SERVICES,
WASHINGTON 25, D. C.

ABSTRACT

A conference on the November 1960 solar-terrestrial events was held at the Air Force Cambridge Research Laboratories, Hanscom Field, Bedford, Massachusetts, February 15 to 17, 1961. Data on solar and geophysical observations and their theoretical interpretations by the scientific staff at AFCRL are presented. The solar-terrestrial events are unique in that they provide information on solar particles of cosmic-ray energies and on geophysical and propagation effects of the cosmic-ray flares.

PREFACE

This collection of papers is a representative selection of the research done at the Air Force Cambridge Research Laboratories relating to the November 1960 Solar-Terrestrial Events. Some of this material was presented at, or arose from, the Conference on the November 1960 Solar-Terrestrial Events held at Bedford, Massachusetts in February 1961. Furthermore, a number of these papers have been, or are in process of being, published in other journals. They have been collected here in order to give an integrated picture of AFCRL work in this area. Additional material not yet fully analyzed has been omitted in order to avoid further delay in publication. Two of the authors represented here, T. Obayashi and B. Sandford, were visiting scientists at the Geophysics Research Directorate.

It is hoped that this collection will be useful to others working in this fascinating area of the geophysical effects of solar flares.

CONTENTS

1. Resume of the Conference on the Solar-Terrestrial Events of November 1960, T. Obayashi	1
2. Solar Effects on Propagation With Special References to the November 1960 Cosmic-Ray Flares, J. Aarons	27
3. Polar-Glow Aurora in Polar-Cap Absorption Events, B. P. Sanford	65
4. Irregular Lunar Reflection Polarization Changes Noted in the Presence of Aurora, J. Klobuchar, J. Aarons, H. Whitney, and G. Kantor	93
5. Emission of Carbon Group Heavy Nuclei From A 3+ Solar Flare, H. Yagoda, R. Filz, and K. Fukui	101
6. Backscatter Measurements at 19 Mcps During the November 1960 Events, C. Malik and R. Hartke	107
7. Radiation Studies From Nuclear Emulsions and Metallic Components Recovered From Polar Satellite Orbits (Abstract), H. Yagoda	113
8. Radioactivity Produced in Discoverer XVII by November 12, 1960, Solar Protons, J. T. Wasson	115
9. X-Band 84-Foot Radio Telescope, S. Basu and J. Castelli	125
10. Photometric Observations of 6300 A O I at Sacramento Peak, New Mexico During November 1960, S. M. Silverman, W. Bellew, and E. Layman	131
11. Radioactive Cobalt and Manganese in Discoverer XVII Stainless Steel, J. T. Wasson	147
12. Magnetic Activity Associated With the 12 November 1960 Event, E.J. Chernosky	157

RÉSUMÉ OF THE CONFERENCE ON THE SOLAR-TERRESTRIAL EVENTS OF NOVEMBER 1960*

Tatsuzo Obayashi[†]

ABSTRACT

A conference on the November 1960 solar-terrestrial events was held at the Air Force Cambridge Research Laboratories, Hanscom Field, Bedford, Massachusetts, February 15 to 17, 1961. The results obtained at the conference are summarized and include data of solar and geophysical observations and their theoretical interpretations. It has been concluded that the solar-terrestrial events of November 1960 are unique in that they provide not only information on solar particles up to cosmic-ray energy ranges, but also knowledge of existing interplanetary magnetic fields. Some important discoveries made in the November events are also described briefly.

1. INTRODUCTION

A conference on the November 1960 solar-terrestrial events was held at the Air Force Cambridge Research Laboratories, Hanscom Field, Bedford, Massachusetts, on February 15 to 17, 1961. This conference was organized by J. Aarons and S. Silverman of the Air Force Cambridge Research Laboratories, and the author who represented the Arctic Institute of North America. Approximately one-hundred scientists participated, and fifty-seven reports were presented on solar observations, cosmic rays, rocket and satellite measurements in outer space, ionospheric soundings, geomagnetism, and aurorae. At the completion of the conference, interpretations and theoretical discussions of the events were summarized.

This report is mainly concerned with a brief description of the events and a model of the solar-geophysical disturbances which has emerged from the discussions at the conference. Since the meeting was held only a few months after the events, observational materials are provisional

* Published as Arctic Institute of North America Research Paper No. 14.

[†] Arctic Institute of North America; now at Ionosphere Research Laboratory, Kyoto University, Kyoto, Japan.

and conclusions are still incomplete. It may be very important, however, to report the overall picture of the events and the tentative conclusions, which to date appear to be consistent. It is hoped that this report may stimulate further studies on the November events in order to reach a better understanding of solar-terrestrial disturbances.

2. PHENOMENOLOGICAL DESCRIPTION OF THE NOVEMBER EVENTS

A series of events occurred during November 1960 which were undoubtedly the most outstanding and complicated solar-terrestrial phenomena in recent years. Three solar cosmic-ray events were observed which were associated with intense solar flares. The geomagnetic storms that followed were extremely severe. The upper atmosphere was very disturbed and displayed unusually bright aurora and airglow.

The major events that have been reported so far are listed in Tables 1 and 2. There were at least eight important solar flares that have been identified as the possible source of major terrestrial disturbances. All flares except those on November 6 originated from the same active region, the McMath Plage Region 5925, which passed the central meridian of the sun around November 12. Three of them, on November 12, 15, and 20, produced energetic solar cosmic rays detected at sea level. Three major geomagnetic storms occurred that were accompanied by large Forbush-type decreases of cosmic rays. Solar phenomena, geomagnetic activity, and records of cosmic rays and ionospheric absorptions (f_{min}) near the geomagnetic pole are illustrated in Fig. 1. Details of these phenomena are given in subsequent individual descriptions.

2.1 November 12 Event

An intense flare started 1323 UT on November 12 near the central meridian of the sun, which a few days earlier had had an active region. The flare developed from 1325 UT, and reached a maximum at 1330 UT. An outburst of solar radio emission of spectral Type II was observed between 1327 to 1331 UT at 200 Mcps, and then a strong outburst of Type IV (continuum radiation) followed, reaching a maximum from 1330 to 1350 UT and fading out by 1800. The $H\alpha$ intensity curve at McMath-Hulbert Observatory and radio outbursts at Nera, Netherlands are reproduced in Fig. 2.

TABLE 1. Major Events, November 6 to 22, 1960

DATE	FLARE		RADIO OUTBURST		SWF(SID)		COSMIC RAY INCREASE ^f	
	Imp.	Time and position	Type	Time*	Imp.	Time	$\Delta I\%$	Time
6	III	1752-2030 07E 13N	Maj. +	1827-1858	I	1708-1815	-	-
10	III	1011-1430 28E 29N	- Maj. +	1020-1116 1116-1200	II	1022-1152	-	-
11	II+	0305-0428 12E 29N	III II IV	0316-0330 0332 0340-0730	III+	0311-0616	-	(PCA)
12	III+	1323-1922 4W 26N	II IV	1327-1331 1330-1800	III+	1325-1600	65 120	1340- 1900-1030 (13th)
14	II+	0246-0520 19W 27N	- IV	0318-0335 0335-0700	III	0300-0500	-	(PCA)
15	III+	0207-0427 33W 26N	II IV	0221-0225 0225-0700	III+	0220-0630	85	0240-22..
19	II	1543-1649 90W 28N	III (IV)	1559-1602 1636-1723	-	-	-	(PCA)
20	III	2017-2024 (110W) 25N	II IV	2023-2035 2027-2046	III-	2023-2145	5	2100-18.. (21st)

* Time at 200Mcps,

[†] Deep River

TABLE 2. Major Events, November 6 to 22, 1960

DATE	SC MAG. STORM*		MAIN PHASE		Associated Cosmic Ray Forbush Decrease	Probable Origin Solar Flare	Delay Time hours
	Time	(ΔH)av.	Time	(ΔH)av.			
11	11-0033	12	11-....	110	11-00.. M	6-1752 III	102.7
12-13	12-1348	42	12-17..	450	- -	10-1011 III	51.6
12-13	12-1846	36	12-19..		12-1930 S	11-0305 II+	39.7
13-14	13-1021	(200)	13-11..	(250)	13-1035 S	12-1323 III+	21.0
15-16	15-1304	22	15-17..	240	15-1330 M	14-0246 II+	34.3
15-16	(15-2155)	(10)	15-22..		(15-2200) (M)	15-0207 III+	19.8
21-22	21-0632	15	21-07..	110	(21-06..) (M)	19-1543 II	38.8
21-22	21-2147	20	22-00..	70	(21-22..) (M)	20-2017 III	25.5

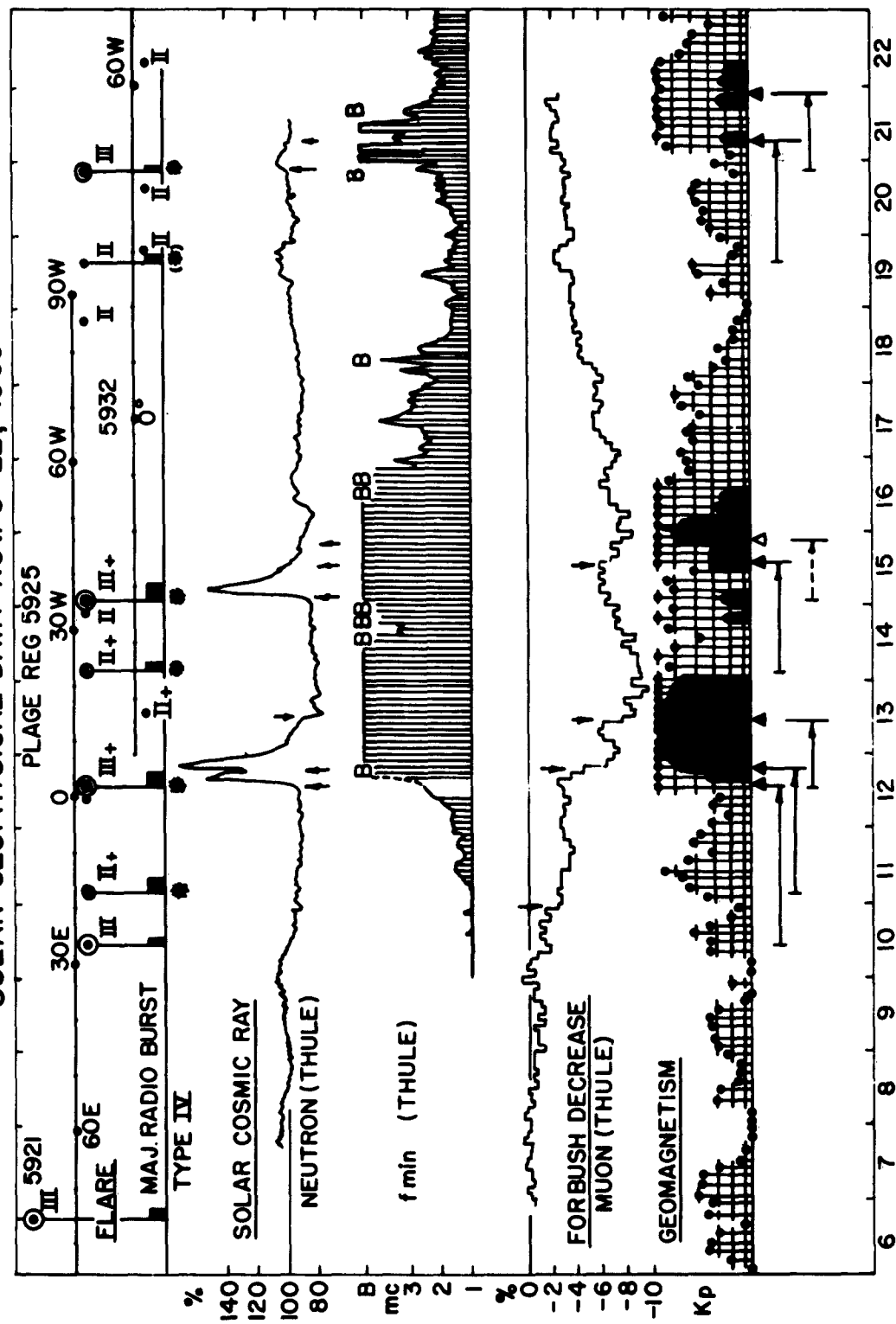
* Average of several low-latitude stations, ΔH in gamma.

As some observers pointed out, the H α record of this flare resembles closely that of cosmic ray produced flares such as those of February 23, 1956 and July 16, 1959. In fact, the most outstanding feature of this flare was the production of energetic solar cosmic rays. At 1340 UT, about 10 minutes after the onset of the major radio outburst of Type IV, a distinct increase in the cosmic-ray flux was observed at most neutron monitor stations in high latitudes. As shown in Fig. 3 from the record at Deep River, after a gradual rise the flux intensity reached a maximum in about 2.5 hours and then decreased until a sudden rise occurred near 1900 UT. The second increase had a maximum at 2000 UT exceeding 100 percent above the normal level and then a smooth recovery followed until about 1030 UT on November 13.

It has been noted that the solar flare and radio outburst intensities were substantially reduced after 1500 UT, and that there was no resurgence or new flare outbreak between 1800 and 2000 UT that could provide an obvious solar explanation for the second increase in cosmic rays. Therefore, the complex time variation of cosmic rays observed in this event must be understood in terms of the modulation effect upon the original flux of solar cosmic rays.

In this respect, geomagnetic storms which occurred in this period are of particular importance, because they provide the information on any existing solar plasma cloud in space and on the outer geomagnetic field where solar cosmic ray particles might interact and likely be modulated. In fact, two sudden commencements (SC) of geomagnetic storms were noticed in the earlier part of the event at 1348 and 1846 UT on November 12. Magnetograms obtained at Hiraizo Radio Observatory are shown in Fig. 4. Unlike the first SC of the geomagnetic storm, the second one occurred right after the beginning of the main phase of the preceding storm. It was clearly seen, however, in magnetograms obtained at most equatorial stations. Furthermore, a very sharp Forbush decrease of cosmic-ray flux, which was observed in meson monitor records, followed soon after the second SC. Since almost all sudden Forbush decreases follow SC's of geomagnetic storms within a few hours, it is rather

SOLAR GEOPHYSICAL DATA NOV. 6-22, 1960



NOVEMBER 1960

FIG. 1. Solar and geophysical data, November 6 to 22, 1960.

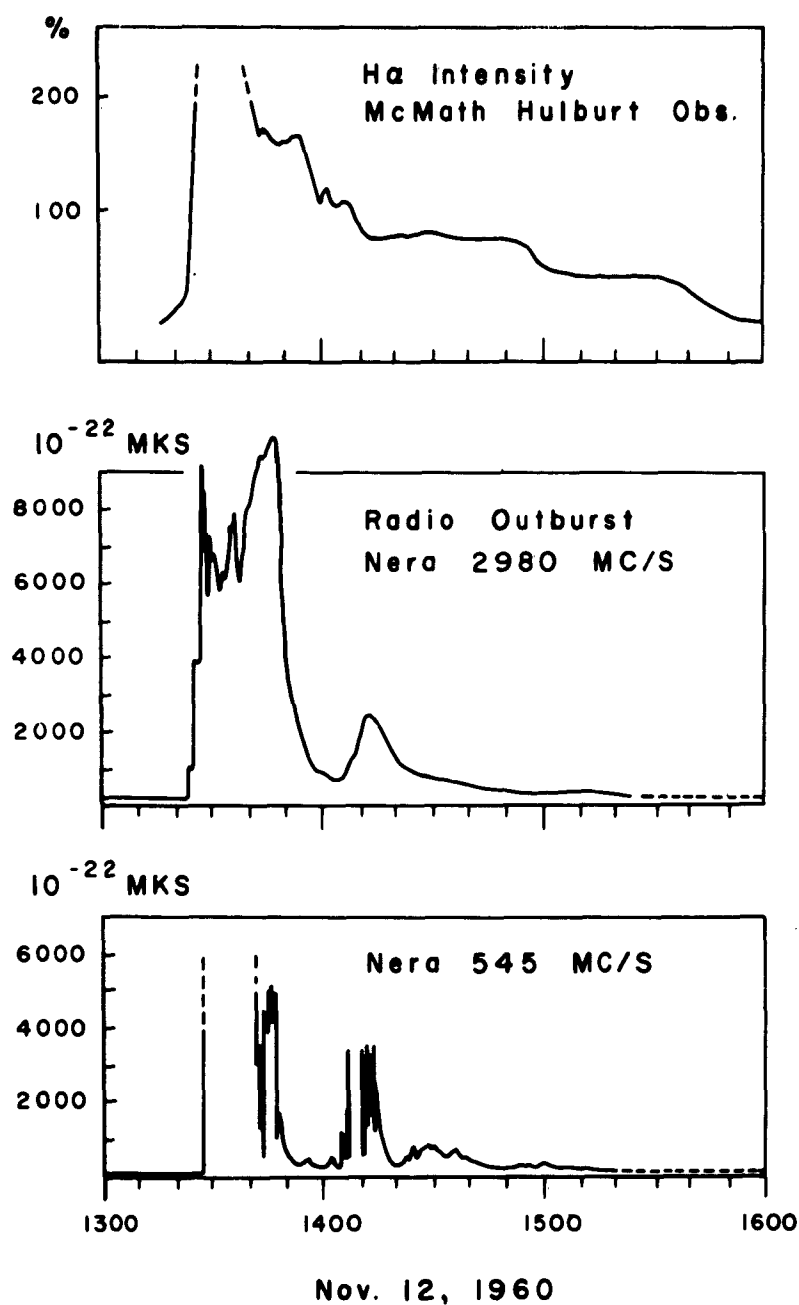


FIG. 2. H α and radio outbursts records of the solar flare on November 12, 1960. (H. W. Dodson, McMath-Hulbert, Obs., and A. D. Fokker, P. T. T., Netherlands)

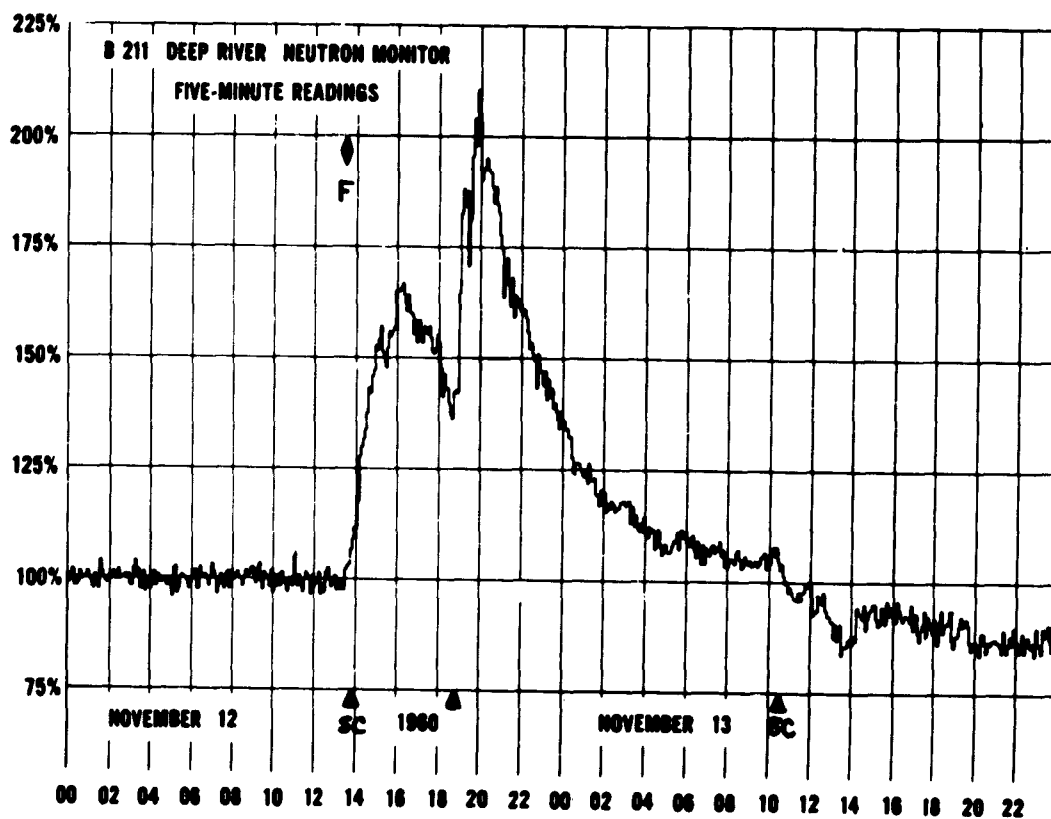


FIG. 3. Record of the standard neutron monitor at Deep River on November 12 to 13, 1960. (J. F. Steljes and H. Carmichael, Atomic Energy of Canada Ltd.)

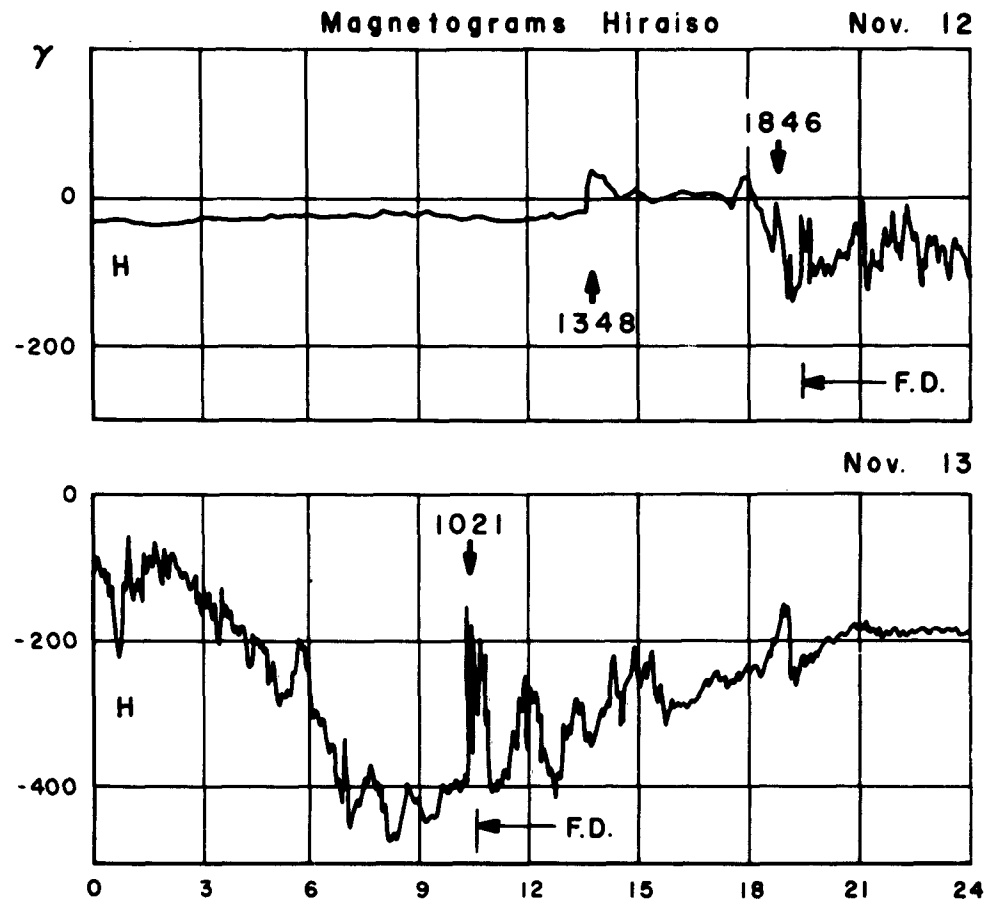


FIG. 4. Magnetograms of H-component observed at Hiraiso Radio Observatory geomagnetic latitude 26°N , on November 12 to 13, 1960.

convincing that the SC at 1846 UT is a really important one. It should be noted that the second large increase of cosmic-ray flux coincides with nearly the time of onset of a geomagnetic storm. As will be discussed later, this fact is essential in order to explain the complicated structure of this solar cosmic-ray event.

As has been noted in Table 2, these SC's probably originated from the earlier flares on November 10 and 11, respectively. Therefore, at the time of the flare of November 12, solar plasma clouds responsible for these storms were in the vicinity of the earth, but not yet enveloping it. It appears also reasonable to presume that a conspicuous sharp SC and a Forbush decrease at 1021 UT on November 13 were caused 21 hours later by a plasma cloud ejected from the flare relevant to the solar cosmic-ray event.

In the polar ionosphere, soon after the solar flare of November 12, the polar-cap absorption event, which was noted by riometers as well as vertical ionosondes, started. There was also some indication that a weak polar-cap absorption had already been in progress near the geomagnetic pole as early as 0100 UT on November 12. A more pronounced increase of absorption was, however, certainly started around 1400 UT. The riometer records at Cape Jones (Fig. 5) illustrate that the absorption at 30 Mcps went up steadily and reached beyond the dynamic range (12db) by 1800 UT. The 60 Mcps riometers at Ottawa and Churchill, however, showed a sharp increase in absorption at approximately 1900 UT, coinciding with the time of the second cosmic-ray increase. Most other stations also showed similar time variation, indicating again a close association with the onset time of a geomagnetic storm.

It is generally accepted that polar-cap absorptions are caused by the precipitation of low-energy solar cosmic rays of ≈ 10 to 100 Mev. High altitude balloon and rocket measurements made in this event revealed the existence of an enormous amount of low-energy solar cosmic rays. The result from the Explorer VII also confirmed this. The estimated peak proton flux above 30 Mev exceeded $10^5 \text{ cm}^{-2} \text{ sec}^{-1}$ and the exponent of integral spectrum in this energy range would be approximately -2 to -3.

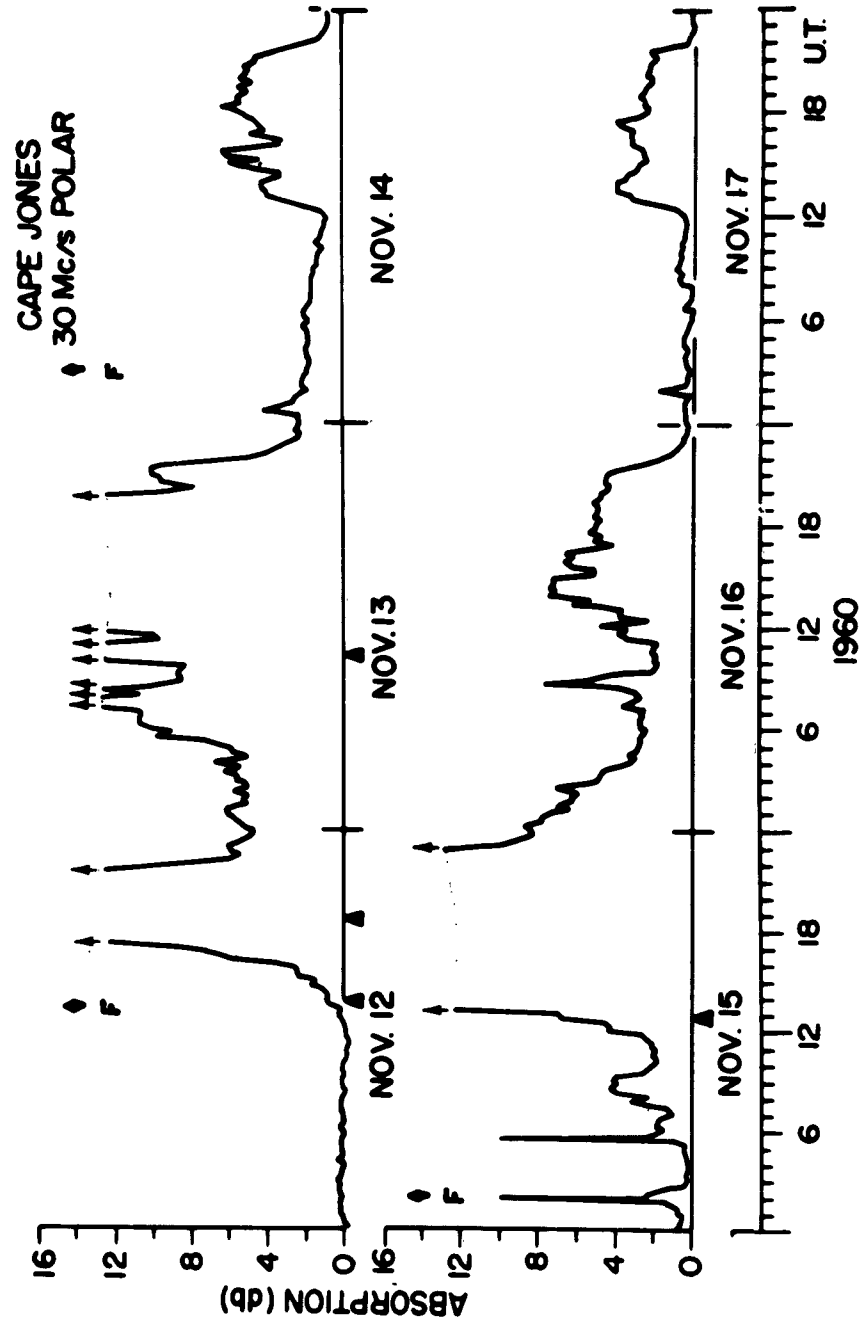


FIG. 5. 30 Mcps riometer record observed at Cape Jones on November 12 to 17, 1960, (E. L. Vogan, Radio Physics Lab., DRB, Canada).

Both polar cap and auroral absorption were extremely intense during the active phase of the geomagnetic storm of November 12 and 13, and a remarkable red aurora was seen at as low as 40° geomagnetic latitude. The F-2 layer appeared to be completely wiped out during a period of several hours, as indicated by ionosonde records and by lunar reflection experiments at Jodrell Bank and Sagamore Hill.

2.2 November 15 Event

A very similar, almost identical, intense flare was observed on November 15 at 0207 UT. Radio outbursts which appeared as Type II, started at 0221 UT and then almost immediately a gradual build up of a Type IV continuum followed from 0225 to 0700 UT. The records of $H\alpha$ intensity and of radio outbursts observed in Japan are reproduced in Fig. 6. A combined dynamic spectrum drawn by using point frequency records is shown in Fig. 7.

The cosmic-ray increase associated with this flare (Fig. 8) started very sharply near 0240 UT and rose in 15 minutes to a rather flat jagged top. A smooth recovery began about 0500 UT at a rate similar to that of the event of November 12. Unlike the previous event, there was no SC of a geomagnetic storm until November 15 at 1304 UT, and apparently the solar cosmic-ray flux did not show any appreciable geomagnetic storm effect.

On the other hand, the polar-cap absorption observed by the riometer at Cape Jones showed that a very gradual rise after the flare continued until the time of SC of the geomagnetic storm. At about 1300 UT the absorption increased to very high values. Since there exists a marked sunrise effect in absorption, it is not certain whether the time variation of this polar-cap absorption event well represents the change of solar cosmic-ray flux in outer space, or the effect in the ionosphere itself.

Though a geomagnetic storm started at 1304 UT, the magnetic activity was fairly moderate until 2155 UT when a sudden outbreak of activity commenced (Fig. 9). This might have been the moment when the plasma cloud, emitted from the flare of November 15, arrived at the earth after

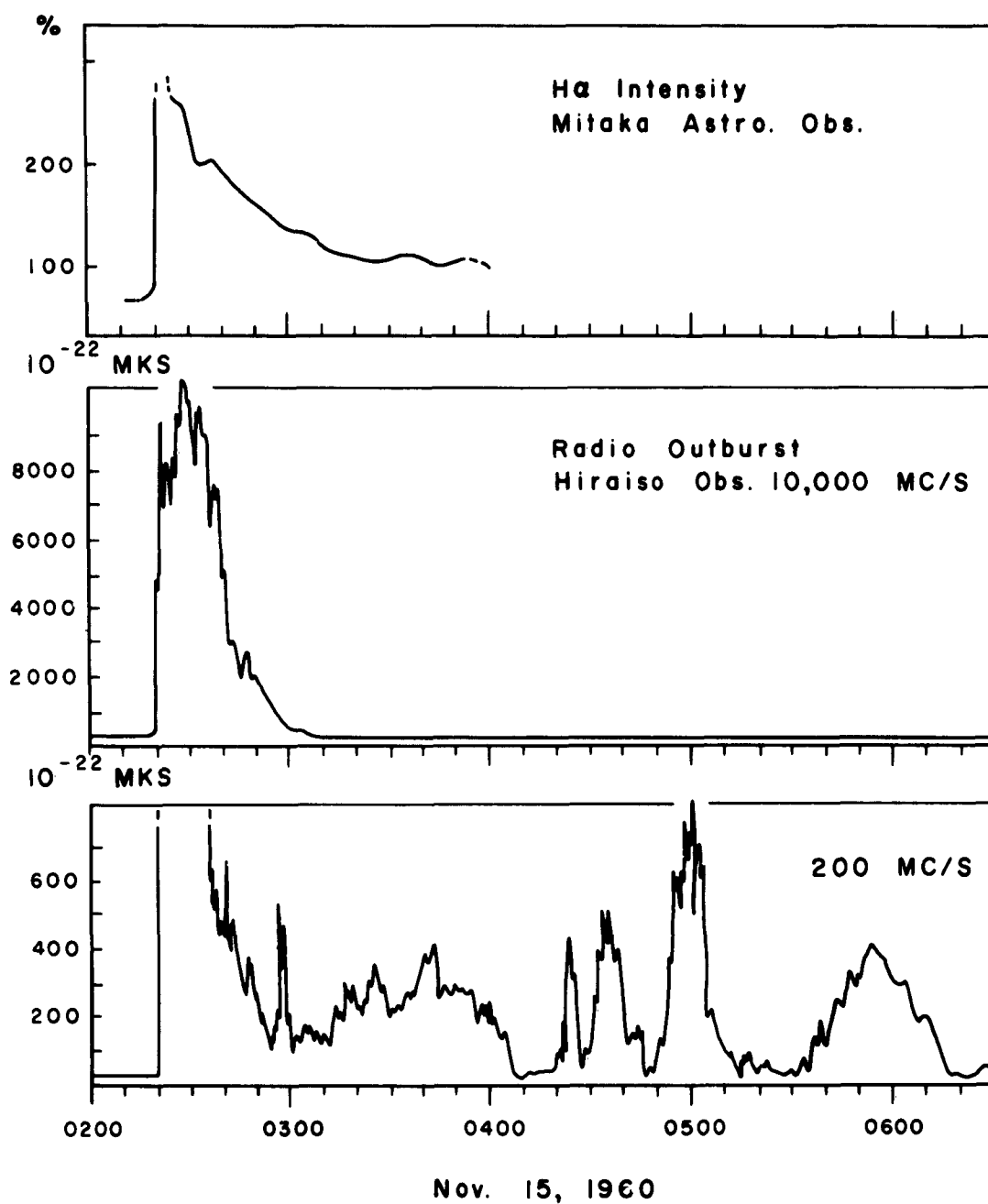


FIG. 6. H α and radio outbursts records of the solar flare on November 15, 1960. (S. Nagasawa, Tokyo Astr. Obs., and F. Yamashita, Hiraiso Radio Obs.)

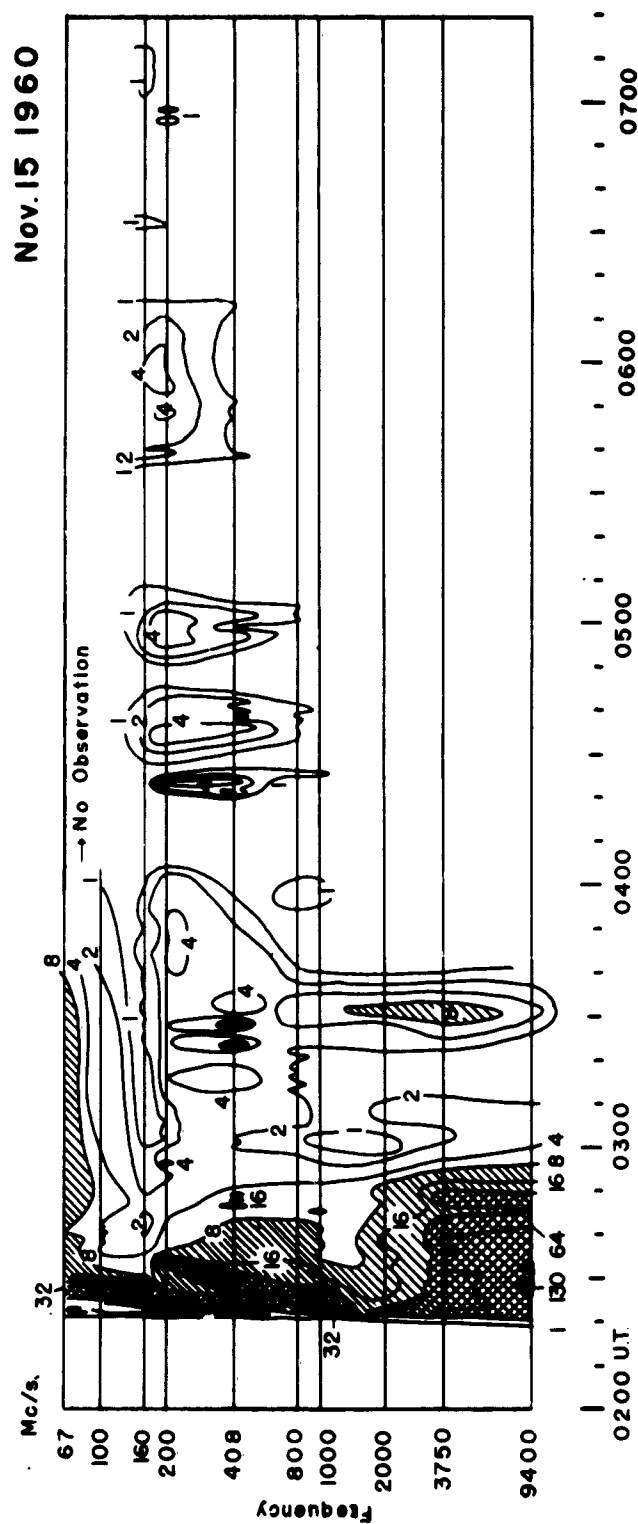


FIG. 7. Dynamic spectrum drawn by using point frequency records.

Numbers on the contour lines in units of $10^{-20} \text{ Wm}^{-2} (\text{c/s})^{-1}$ (T. Takakura and A. Tsuchiya, Tokyo Astr. Obs., and H. Tanaka, Research Inst. Atmospherics, Nagoya University).

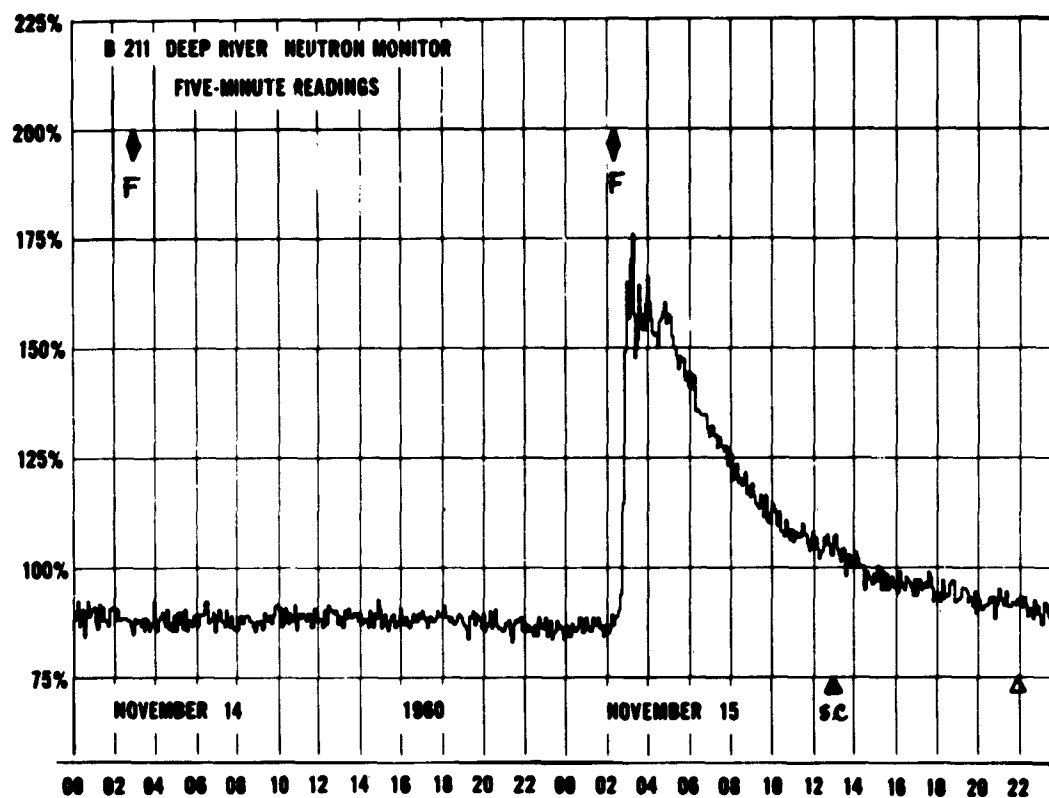


FIG. 8. Record of the standard neutron monitor at Deep River on November 14 to 15, 1960. (J. F. Steljes and H. Carmichael, Atomic Energy of Canada Ltd.)

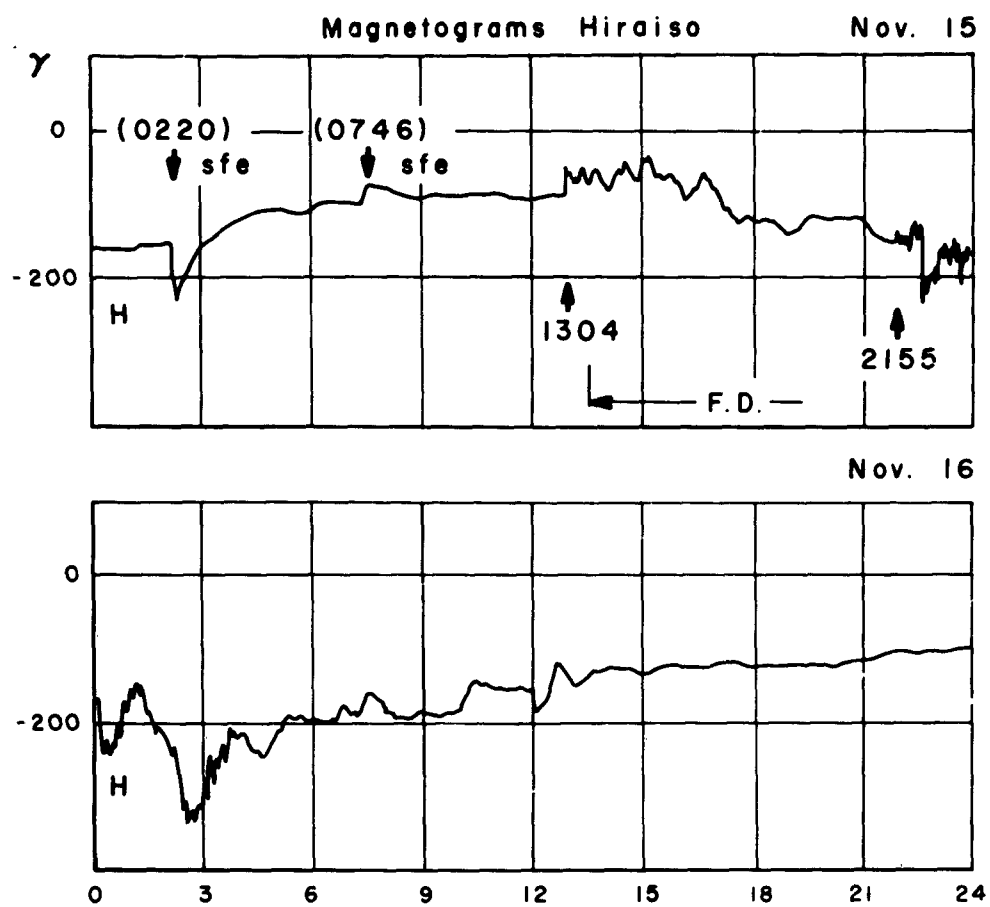


FIG. 9. Magnetograms of H-component observed at Hiraiso Radio Observatory, Japan on November 15 to 16, 1960.

a delay of about 20 hours. This geomagnetic storm was rather small compared with the one of November 12 and 13. Therefore, auroral and ionospheric disturbances were moderate and the southward extension of the auroral zone was not as remarkable as that of the previous storm.

2.3 November 20 Event

About November 19, the active region 5925 had turned around the western limb of the solar disk, and yet the third cosmic-ray increase was observed at 2100 UT on November 20. In fact, a spectacular limb flare was observed, coinciding with the time of the cosmic-ray event. As shown in Fig. 10, this flare appeared about 2000 UT as a small mound on the limb, and then a sudden outbreak of brightness occurred between 2017 to 2024 UT. The flare was certainly beyond the limb, and its position has been estimated to be about 20° off the west limb. A strong radio outburst of continuum radiation accompanied the flare from 2027 to 2046 UT. During this period, a remarkable ascending prominence was seen above the limb with a velocity of the order of a thousand km/sec.

A distinct yet very small cosmic-ray increase began at about 2100 UT, after a delay of about 30 minutes from the start of the radio outburst (Fig. 11). The rise time of approximately one hour was comparatively slow and after 2300 UT a gradual decay followed until approximately 1800 UT on November 21. This is the first solar cosmic-ray event whose source has been identified outside the visible solar disk.

3. THEORETICAL INTERPRETATIONS OF THE EVENT

The most outstanding feature of the November events is the emission of energetic solar cosmic rays. Three of the events, on November 12, 15, and 20, involved particles above the relativistic energies. There are some good reasons to believe that the flares on November 11, 14, and 19 produced the particles of subrelativistic energies (low-energy solar cosmic rays).

It has been known that most solar cosmic-ray events are closely related to intense solar flares associated with Type IV solar radio outbursts. In this respect, it is consistent that all Type IV outbursts

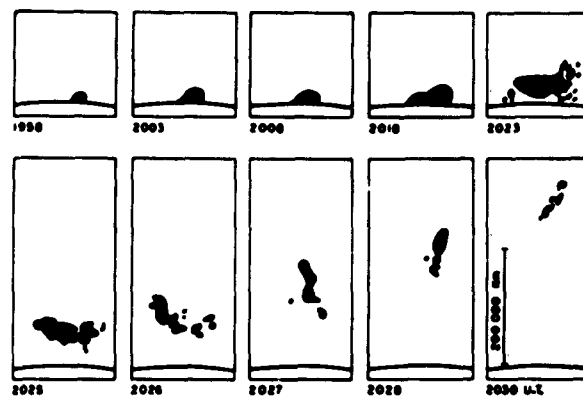


FIG. 10. The solar limb flare on November 20, 1960. West limb, 25° North. (R. T. Hansen, High Altitude Obs., Univ. Colorado).

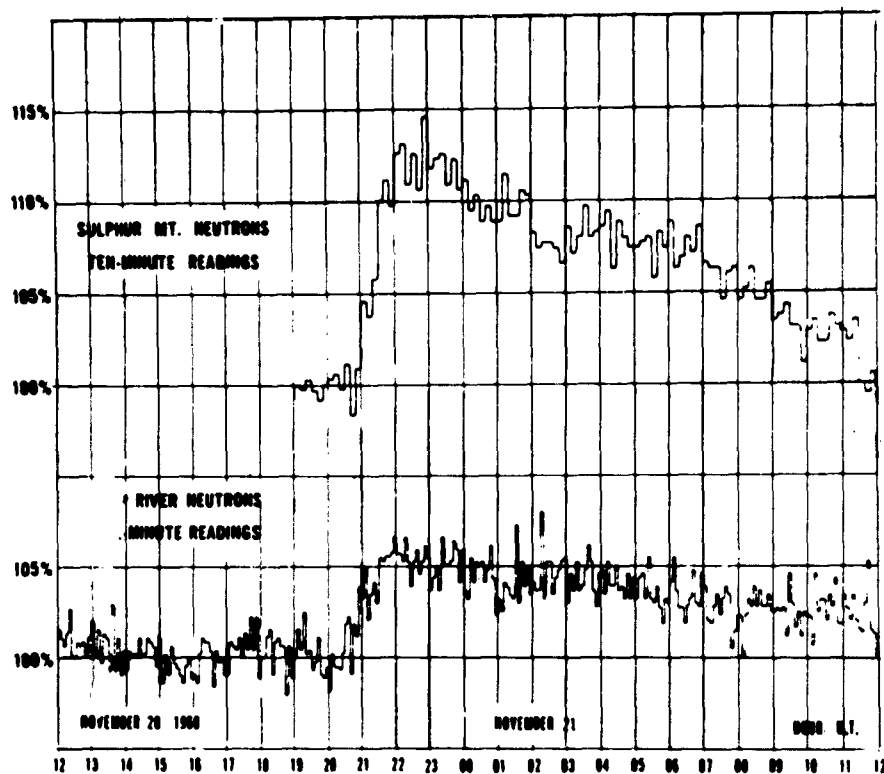


FIG. 11. Records of neutron monitors at Sulphur Mt. and Deep River on November 20 to 21, 1960. (H. Carmichael and J. F. Steljes, Atomic Energy of Canada Ltd., D. C. Rose, Nat. Res. Council, Ottawa, and B. G. Wilson, University Alberta).

observed in this period were followed either by the cosmic-ray increase of relativistic energies or by the polar-cap absorptions that are presumably produced by the particles of ≈ 10 to 100 Mev. Since Type IV outbursts are believed to be the synchrotron radiation from relativistic electrons spiralling in magnetic fields, it is also likely that such agitated solar plasma-bearing magnetic fields may be capable of accelerating solar protons from thermal to very high energies. It is not yet clear, however, why only three of them produced relativistic solar cosmic rays. As has been mentioned, the flares of November 12 and 15 had features very distinct from other intense flares; they show the development, after flare maximum, of a very complex loop-type prominence of absorption features and of large coverage of the nearby spots by a structureless extensive glow. The flare of November 15 was also seen by the naked eye in pearly white color, which might be of the synchrotron origin. These facts are very encouraging for further studies of this problem.

The time variation of cosmic rays on November 12 is unusual among other solar cosmic-ray events in the past. The feature of double peaks is of particular interest because of its unique shape. As has already been pointed out, any obvious solar origin as the cause of this variation was ruled out since there was no resurgence or a second flare which might provide a new source for the second increase of cosmic rays. Therefore, the time variation of solar cosmic rays on November 12 must be understood by means of the modulation of flux in interplanetary space or in the outer geomagnetic field.

Since a geomagnetic storm started soon after the flare, a depression of the geomagnetic cutoff because of the distortion of the field may have caused an increase of incoming cosmic-ray flux to the earth. It is, however, rather difficult to conceive the fact that a large second increase was also observed at Thule, near the geomagnetic pole where the effect is expected to be very scarce. Hence, this mechanism may explain a part of the increase observed at latitudes outside the polar cap, but certainly not be responsible for the substantial part of the second cosmic-ray

increase. Thus, the modulation of cosmic-ray flux must be taking place somewhere in outer space beyond the geomagnetic field.

The argument follows that magnetic plasma clouds existing in interplanetary space play an important role in the modulation of solar cosmic rays. It has already been suggested by several investigators that the solar plasma cloud ejected from the flare may draw out any magnetic field existing in the vicinity of the sun, since the cloud itself has a high conductivity. As the plasma cloud advances into interplanetary space, it must form an expanding bulge of magnetic lines of force, such as shown in Fig. 12a. Supposing that solar cosmic-ray particles are injected into this magnetic bulge, then most particles are trapped inside by magnetic field lines, and advance in interplanetary space essentially with the same speed as the front of the magnetic cloud but not with the speed of the particle itself. When such a magnetic cloud evolves about the earth, as is indicated by the onset of a geomagnetic storm, a substantial rise of solar cosmic-ray flux is expected. On the other hand, a magnetic cloud will also act equally to exclude the cosmic-ray particles coming from outside the solar system. This phenomenon is the so-called Forbush decrease of cosmic rays. The condition of this trapping or exclusion of cosmic-ray particles will depend upon the magnetic field strength, the rate of expansion, and the geometrical shape of the cloud. From the statistics of solar flares, geomagnetic storms, polar cap absorptions, and Forbush events, it is known that the magnetic cloud must occupy a substantial fraction of a hemisphere centered at the sun.

The event of November 12 was exactly the same situation as described above. The flare shot out solar cosmic-ray particles when two magnetic clouds, presumably produced by earlier flares, were advancing in the vicinity of the earth but not yet enveloping it. Judging from the onset of two SC's of geomagnetic storms, their distances from the earth at the time of particle injection were 10^6 km and 2×10^7 km ($1 \text{ AU} = 1.5 \times 10^8$ km), respectively. Since the first SC was not followed by an appreciable Forbush decrease, there might be little magnetic field associated with it. The second one, however, had a strong field so that it

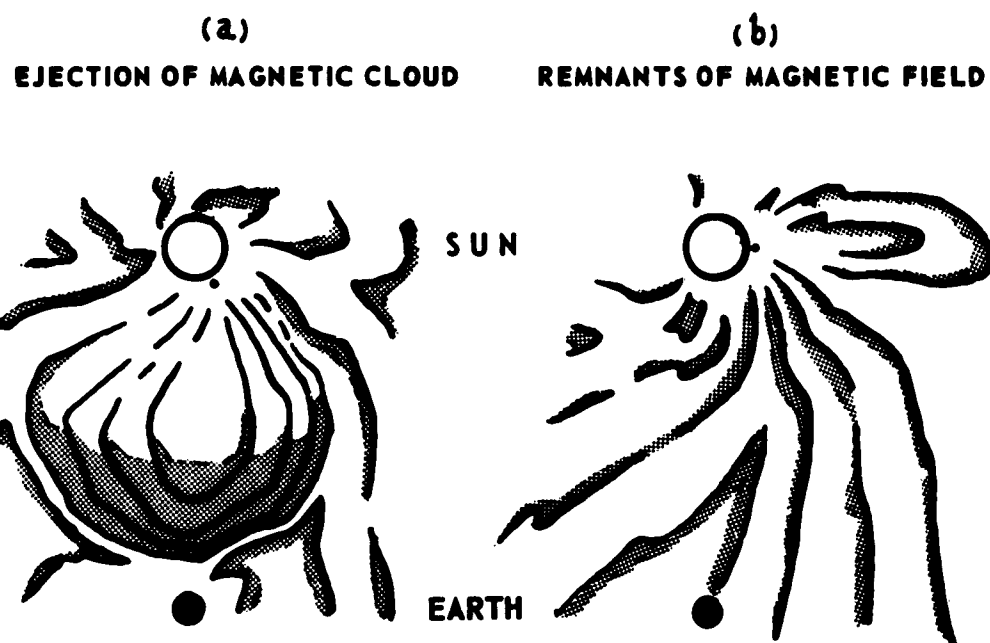


FIG. 12. Schematic diagrams of the interplanetary magnetic fields:
a) Magnetic cloud associated with a solar eruption.
b) Remnants of magnetic fields.

induced a large Forbush decrease.

The majority of solar cosmic-ray particles ejected from the sun were stopped by the inner (second) magnetic cloud and were trapped. Some of the particles, however, presumably high energy ones, could leak out through the magnetic barrier and reach the earth before the arrival of the magnetic cloud. A slow rise and subsequent fall of observed cosmic-ray flux can be explained by this mechanism. The maximum energy of particles produced the first part of the increase and would be 5 Bev. The integral spectrum was undoubtedly very steep (approximately E^{-4}).

Immediately after the arrival of the second magnetic cloud, a very sharp rise in particle flux was attained. Although the rise was steep, the increase was simultaneously world-wide, and there was no impact-zone effect because the particles had already well migrated from the entire magnetic cloud. The large Forbush decrease, observed after 1930 UT by meson monitors, certainly indicated that the earth entered within the magnetic cloud from which cosmic-ray particles coming from the outside of the cloud were excluded. During the period of this second increase, the low-energy solar cosmic rays became abundant. This condition was detected by rocket and balloon measurements.

The time variation of polar-cap absorption followed a very similar pattern with two steps of the increase coinciding with the arrival of the magnetic clouds. This can be explained consistently by the trapping mechanism of solar particles though the energy range relevant to this is ≈ 10 to 100 Mev, considerably less than that detected by neutron monitors at sea level.

The flare of November 12, which produced this cosmic-ray event, also ejected its own magnetic plasma cloud. The cloud arrived at the earth 21 hours later and induced an extremely sharp SC and a sudden Forbush decrease as well. Although the SC occurred during a very active phase of the previous geomagnetic storm, the sudden impulse was noticeably recognized all over the world. It was of considerable interest that the solar cosmic-ray flux suddenly disappeared after the arrival of this

plasma cloud. By examining the energy spectrum of incoming particles it was found that the steep spectrum characteristic for solar cosmic rays disappeared and a shallow spectrum remained which is common for galactic cosmic rays.

This fact gives further support to the theory of the existence of the third magnetic cloud. Solar cosmic-ray particles remained in interplanetary space and were swept out by this magnetic cloud. In other words, the third magnetic cloud excluded both solar and galactic cosmic-ray particles, and thus the solar cosmic-ray particles were completely trapped between two magnetic clouds. It is quite possible that solar particles may be piled up in front of the sweeping magnetic cloud. This was found to be the case since the polar-cap absorption showed a sharp increase just before the SC of the geomagnetic storm.

On November 15 there was another increase of solar cosmic rays associated with an intense flare with a strong Type IV radio outburst. Unlike the previous one, this had a much sharper increase and attained a single maximum within an hour. There was no geomagnetic storm until late on November 15. At the time of the flare, however, the effect of Forbush decreases produced by previous magnetic clouds had not yet recovered. Thus, the earth was still within the huge magnetic cloud and was connected directly to the sun by fairly well-ordered magnetic lines of force as illustrated in Fig. 12b. Any particles ejected from the flare should be able to reach the earth quickly by spiralling down such lines of force. Also, their impact zones may be well-defined since the lines of force would direct and collimate the particles. In fact, the result of a careful study has revealed that there was a discrete impact zone, and the particles were coming apparently from the direction of about 60° west of the sun-earth line.

Nevertheless, there is a puzzling fact. An SC of geomagnetic storm occurred at 1304 UT on November 15. Judging from its delay-time, the plasma cloud responsible for this storm should have originated from the flare at 0246 UT on November 14. If so, the plasma cloud would have been about $1/3$ AU from the earth in the sun-earth line at the time when

the solar cosmic-ray particles were injected. Therefore, solar particles must have encountered this cloud before reaching the earth. The time variation of polar-cap absorption did show some indication of this effect, a very slow rise of absorption until about the onset time of the geomagnetic storm. No appreciable effect was seen, however, in the records of neutron monitors. Perhaps the magnetic field in the plasma cloud was very weak, since the Forbush decrease associated with this geomagnetic storm was comparatively small. Then the plasma cloud would be rather transparent for cosmic-ray particles, but still have enough magnetic fields to interact and trap low-energy solar cosmic-ray particles.

The November 20 event provides still another interesting fact. The ejection of solar cosmic-ray particles covers a fairly wide angular spread from the source, and an appreciable number of particles can arrive beyond the visible solar disk. This statement may be valid, however, only for the case of the flare in the western limb. Of course, statistically, it seems to be likely that solar cosmic-ray events are larger for the source near the central meridian.

It may also be worthwhile to note that the delay-time of geomagnetic storms originating from the cosmic-ray producing flares was unusually short, 21, 20, and 26 hours, respectively, for the present three cases. Further, these geomagnetic storms occurred while the preceding storms were still in the very active phase. There is some statistical evidence that when two plasma clouds are ejected from the sun one after another the second cloud travels at a much faster speed than the first one. This might be related to some complicated situation in the interplanetary magnetic fields, although a suitable explanation has not yet appeared.

Several interesting discoveries related to the November events have also been reported. A strong enhancement of molecular nitrogen bands, especially the first negative band of N_2^+ , at 3914\AA has been detected in the polar-cap region during the polar-cap absorption events. The luminosity curve at 3914\AA was very similar to that of the polar-cap absorption, essentially starting right after the solar flare. The variation

was very steady reaching a maximum approximately one-hundred times above normal at the onset of the geomagnetic storm, and then decaying to normal levels over the next two days. It appeared as an extensive glow rather than discrete auroral forms. The source of the emission exists at an altitude of 100km or below, and it seems likely that it is excited by incoming solar cosmic-ray particles.

Anomalous propagation of VLF radio waves has been confirmed during these solar cosmic-ray events. It is believed that the radio waves propagate via an ionized layer formed by incident solar cosmic rays well below the ionosphere.

The material recovered from Discoverer XVII, which was exposed to the solar cosmic-ray event of November 12, has been under very careful study. An analysis shows that a considerable number of radio isotopes were produced by the impact of energetic particles, presumably by solar cosmic-ray particles. A large amount of tritium content was also found. Since the observed ratio of tritium to argon 37 was much larger than that expected from the experiment of particle bombardments, it has been concluded that production of the large tritium content was not from the bombardment by solar protons, but from tritium in the flare itself.

Severe geomagnetic disturbances during the November events have offered the opportunity of investigating the geomagnetic storm effect on the air density of the upper atmosphere as revealed by the orbital motion of satellites. Appreciable increases in air density at the 200 km level occurred on November 13 and 15 to 16, coinciding with two maxima of the geomagnetic activity.

Other prominent phenomena noted in the November events were strong absorptions in VHF ionospheric scatter propagation in the polar region, hydrogen emission in auroral spectra, and formation of remarkable auroral red arcs. Such phenomena seem to be associated with unusually severe disturbances during this period.

SOLAR EFFECTS ON PROPAGATION WITH SPECIAL
REFERENCE TO THE NOVEMBER 1960 COSMIC-RAY FLARES

Jules Aarons
ELECTRONICS RESEARCH DIRECTORATE
AIR FORCE CAMBRIDGE RESEARCH LABORATORIES

ABSTRACT

The slowly varying changes and the flaring actions superimposed on the periodic variation of the sun are discussed and their effects on the propagation of radio waves and on the ionosphere in general are illustrated by outlining some of the solar-terrestrial events ascribed to plage region 5925. Specific reference is made to the cosmic-ray-producing flares of November 12, 15, and 20, 1960, and the effects of the particle and radiation emission comprising their flaring action are touched on. These effects include the sudden ionospheric disturbances resulting from the ionizing action of the X-ray radiation, the polar-cap absorption following the arrival on earth of the protons, the magnetic storms accompanying the corpuscular streams, and the unusual low-frequency propagation and electron-distribution conditions resulting from the arrival of the high-energy particles.

1. INTRODUCTION

An understanding of the variability of solar processes is a basic prerequisite to the study of upper-atmosphere physics. The sun goes through its sunspot cycle in 11 years, changing during this period from a quietly radiating body without sunspots to one with many sunspot groups visible on its surface. Superimposed on this periodic variation are slow changes and flaring actions.

The theories advanced to explain solar-terrestrial physics have undergone the same cyclic and explosive changes that characterize the sun itself. Within the space of a few years, our knowledge of the effects of the sun on the upper atmosphere has changed with dynamic force. For example, texts in cosmic-ray physics written before 1956 have only rather vague statements about the solar-terrestrial relationship. Physical measurements of the ionosphere above the F layer have been obtained only within the last few years. The advent of the rocket, the satellite, and the

International Geophysical Year has extended observations in many disciplines – in a sense adding a third dimension. As a result, some of our errors in understanding the structure of the atmosphere and solar physics have been corrected.

Because this dynamic reconstruction of upper-atmosphere physics is a continuing process, this paper will undoubtedly become outdated before it becomes a printed page. With this fact in mind, the description of solar-terrestrial observations has been oriented towards explaining the effects on the earth's atmosphere of one particular disturbed solar region. The solar-terrestrial history of this sunspot group will be used to illustrate the usual and the unusual in solar variations.

2. THE QUIET SUN

The term 'quiet sun' is a misnomer since the sun is never completely quiet but is only less disturbed during some periods than it is during others. What is actually meant by the term 'quiet sun' is the absence of spot groups. If the sun is observed with a telescope having neutral density filters to cut down on visible light, sunspots or cold regions may be seen on the disk of the sun. At times when such spot groups disappear completely from the disk, the sun is said to be quiet. The solar temperature observed during so-called quiet periods may vary greatly, however, from one time to another. If the temperature of the sun, observed during periods of total absence of spots from the sun during a sunspot-minimum year such as 1954, is compared with the observed temperature measured during a time of total absence of spots at another phase of the sunspot cycle, such as from 1958 to 1960, there may be a factor-of-two variation. In order for the solar temperature to reach its lowest values, the sun must be free of sunspots for many months. Even when no visible sunspots are present, dynamic processes are taking place near the surface level of the sun.

The observable disk of the sun is called the photosphere. This is the coldest layer of the sun and the one of minimum ionization. If only

the photosphere is considered, the solar radius is 700,000 km. When the sun is quiet, radiation of thermal origin is emitted from the photosphere. The required energy for this radiation comes from the convective heating of the solar surface by the higher-temperature regions inside the sun. The convective process is transformed into radiation both on the photosphere and within the layers of the outer atmosphere of the sun. The radiation of the sun has been observed at wavelengths varying from 1 Angstrom unit (AU) in the X-ray region to 40 meters in the high-frequency radio spectrum.

The layers of the outer atmosphere of the sun are the chromosphere and the corona. The chromosphere lies above the disk of the sun extending to a height of perhaps 15,000 km and is at a higher temperature than the photosphere. The centimeter radio-astronomy observations measure in part radiation of chromospheric origin. Above the chromosphere is the corona. Decimeter- and meter-wavelength radiation originates in this region. The radiation centers of importance for radio-frequency observations lie at heights above the sun ranging from 100,000 to 200,000 km. The corona extends into interplanetary space. Measurements showing coronal effects up to twenty solar radii beyond the surface of the sun are part of the radio-astronomy literature. In particular, the annual June measurements of the discrete source in Taurus as it is occulted by the solar corona show the extent of the corona.

Although energy is radiated from the quiet sun at wavelengths ranging from those of the short X rays to those of the long high-frequency waves, only two bands of the spectrum penetrate the earth's atmosphere, with some attenuation from water vapor and oxygen in the low atmosphere. These are the visible wavelength region from 4000 Å to the infrared, and the radio band from 24 mm to the long wave upper limit where radio waves are reflected by the ionosphere (approximately 10 Mcps). The upper atmosphere, on the other hand is penetrated to varying altitudes by X rays and ultraviolet radiation. The very act of absorbing the X-ray and ultraviolet solar radiation and the consequent ionization process produces the layers of the upper atmosphere.

The lowest layer, the D layer, ranges in height from 55 km to 80 km above the surface of the earth. The particles in this layer are ionized for the most part by ultraviolet line radiation, Lyman α at 1216A emanating from the quiet sun. In the field of propagation this layer and the earth act essentially as the two surfaces of a waveguide for the transmission of waves in the low-frequency range from 10 kcps to 150 kcps. The D layer is also important because of its attenuation effect on all radio signals, which are partially absorbed when they pass through it. When an electromagnetic wave probes this layer, the electrons that it excites in this relatively dense medium collide with neutral particles and lose energy.

The next two layers, the E and F layers, are produced by X rays and ultraviolet radiation. They are the portion of the ionosphere most used for communication purposes. Their diurnal change, their height variation, and their variation with latitude all depend on the solar-terrestrial relationship.

The E layer is the ionized region in the height range of 80 to 120 km above the earth. Through various processes the radiation in the 10-to 100-A region of the X-ray band is absorbed in this layer. Ultraviolet radiation in the range from 100 to 910 A is absorbed at heights below 220 km, with the maximum absorption rate taking place at 180 km, in the F layer.

The impact of recent scientific developments on making possible the understanding of the processes of the upper atmosphere is very great. Although it has long been known that there is solar radiation throughout the electromagnetic spectrum, the intensity of that portion of the radiation stopped in the upper atmosphere can be measured only by rockets and satellites. Probes are the only means of accurately obtaining a direct measure of the composition of the upper atmosphere. The number and density of the atoms and molecules available for ionization are thus revealed. Before these measurements were possible, much of the theoretical work in this field was based on conjecture, since it dealt with two unknown quantities, — the intensity level of the ionizing radiation and the

exact composition of the upper atmosphere. Because of the paucity of observational material, many theories appeared to be possible. After the satellite and rocket measurements were made, the validity of the theoretical and laboratory work could be tested and the number of conjectured theories was drastically reduced.

3. THE DIURNAL VARIATION

Not only does the character of the solar radiation vary with time, but the observer's relationship to the sun also changes. The observer is stationed at a particular latitude on a rotating planet, and therefore his position vis-a-vis the sun varies considerably during the course of a day. The general subject of this diurnal effect is more suitably covered elsewhere. The importance of one type of solar observation, however, the total solar eclipse, in shedding light on the process responsible for the diurnal variation and other solar effects, might well be mentioned here. As the moon covers and uncovers different parts of the sun, it is possible to get a detailed picture of how various solar phenomena affect propagation parameters at particular heights. The ionization process normally associated with sunrise, and therefore with low angles of elevation, may in many eclipses take place at high elevation angles since the time immediately following totality is similar to sunrise from the ionospheric point of view. Then, too, it is possible to study the effect on the ionosphere of the eclipsing of sunspot regions, the ionization and attachment processes in the atmosphere, and at totality, the extent of the outer atmosphere of the sun, the corona. The time of an eclipse remains an important occasion for studying propagation and solar parameters.

4. THE SLOWLY VARYING COMPONENT

As has been indicated, the character of the solar radiation from the quiet sun and its terrestrial effects are complicated. This complication is extended manyfold when the sun is active, that is, when spots are present. Not only are there sudden and spectacular explosive changes due

to flares from spot regions, which will be discussed in detail in a later section, but there is also a relatively slow variation associated with the region surrounding the magnetically complicated sunspots. It has long been known that sunspots are surrounded by very high magnetic fields up to several thousand gauss in magnitude. In most cases, the field is bipolar with both north- and south-seeking magnetic fields embedded in one sunspot group, but occasionally a unipolar magnetic field is present. The slowly varying component of solar radiation may change within a few hours at the fastest or it may take several solar rotations, several months, for any change to be apparent.

For many years it has been possible to observe optically the details of spots on the surface of the sun. More recently, radio-astronomy observations have revealed a high density column through the solar chromosphere and corona with the sunspot as its base. Considering the portion of the spectrum below the visible region, rockets have supplied a picture of these concentrated solar areas and measured their intensities at X-ray and ultraviolet wavelengths. In the radio-frequency band, interferometers have shown high apparent temperatures in the solar chromosphere and corona above the sunspot.

One of the most basic quantities in solar-terrestrial physics is the sunspot number R .

$$R = k (10g + f) ,$$

where f is the number of sunspots, g is the number of groups, and k a factor dependent on the observer's telescope. The sunspot number R may vary from 0 to 300 during the course of the sunspot cycle, an average period of 11 years.

As the sun rotates on its axis, its position with respect to the earth changes. From observations of individual sunspots or other details on the solar surface, it has been found that the rotation of the sun is a function of the latitude of the solar position. At the solar equator, the sun's period of rotation is 25.38 mean solar days. The equatorial sunspots have a greater angular velocity, however, and therefore a shorter rotation

period, than those near the poles. For practical purposes a mean rotation period of 27 days is usually used in geophysics.

5. PLAGE AREAS

If optical observations of the sun are made with narrow-band filters whose transmission is centered on the calcium and hydrogen line emissions, bright enhanced regions are noted in the vicinity of the sunspot groups. In a solar photograph or spectroheliogram, the plage area resembles a bright beach or sandy region standing out from the dark background (see Fig. 1). If the sun is observed by radio astronomical techniques in the wavelength range between 1 cm and 100 cm, enhanced radiation is detected in the area above the optical plage (see Fig. 2). This radiation, which changes only over a minimum period of time of a few hours and may remain constant for days, results from condensation in the coronal and upper chromospheric regions.

The solar processes taking place in the radiation from the region above the plage areas are somewhat similar to the quiet-sun radiation. In both cases, a part of the outward flow of energy near the solar surface is carried by convection to the surface. A portion of this energy passes, with very little dissipation, through the surface region and into the solar atmosphere where it is later dissipated in the form of radiation in the chromosphere and corona.¹ The radio-frequency radiation of the quiet sun and of the slowly varying plage region are both of thermal origin. The quiet-sun radiation is due to free-free transitions of the electrons in the field of the ions. Centimeter wavelengths originate in the chromosphere, and decimeter and meter wavelengths are radiated from higher regions of the corona. The slowly varying component arises from a condensation in the coronal and upper chromospheric regions. World-wide radio astronomical observations of a particular plage region² have shown the apparent rf thermal radiation in the center of activity regions to be 10^5 °K at heights of 10,000 km above the photosphere (the chromospheric limits), rising to perhaps 2×10^6 °K at 15,000 km, and falling again to 1.5×10^6 °K at 300,000 km. Individual plage regions will vary both

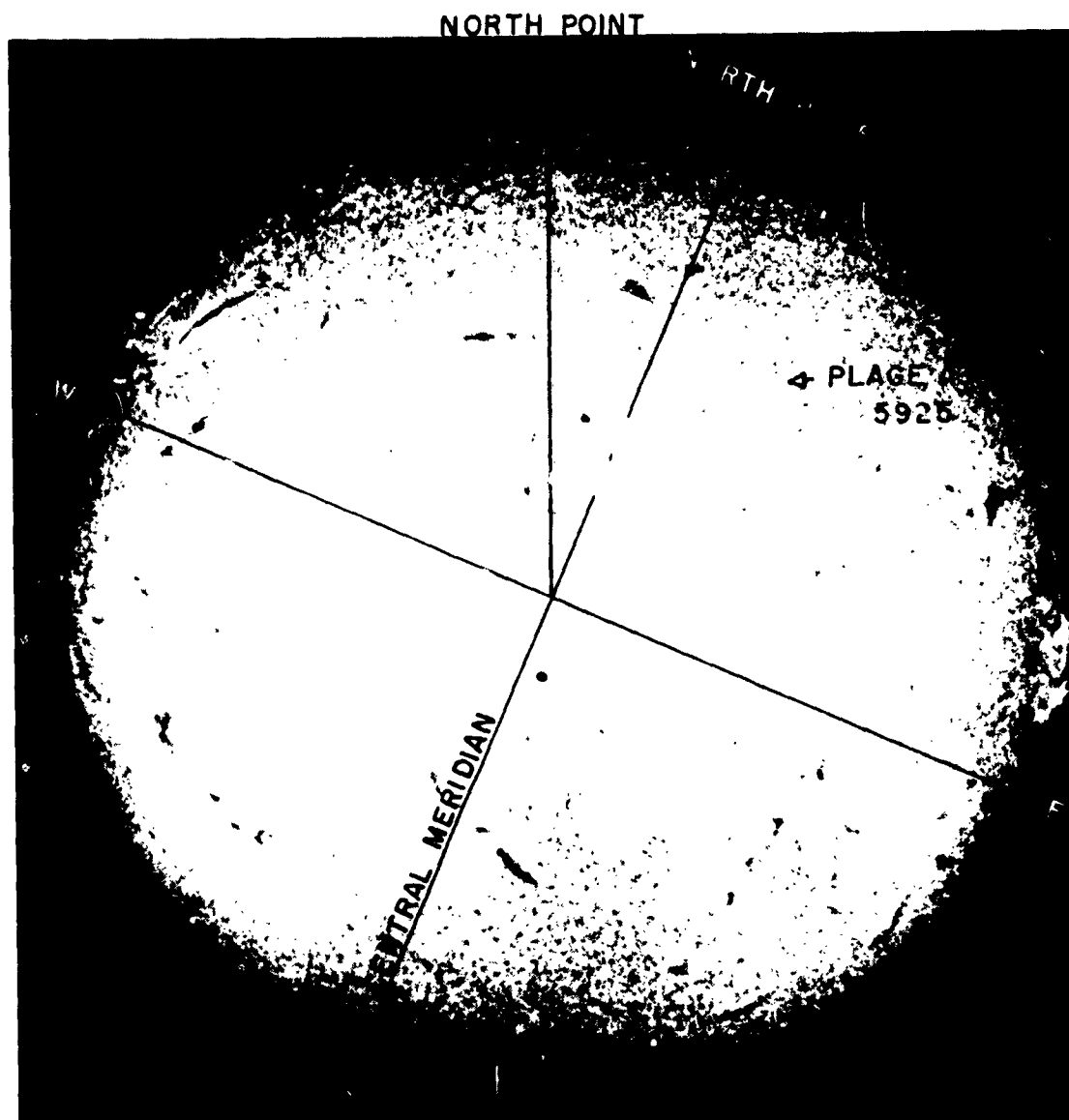


FIG. 1. $H\alpha$ photograph of sun on November 11, 1960. Plage area 5925 is clearly seen. (Courtesy of Sacramento Peak Observatory, Sunspot, N. M.)

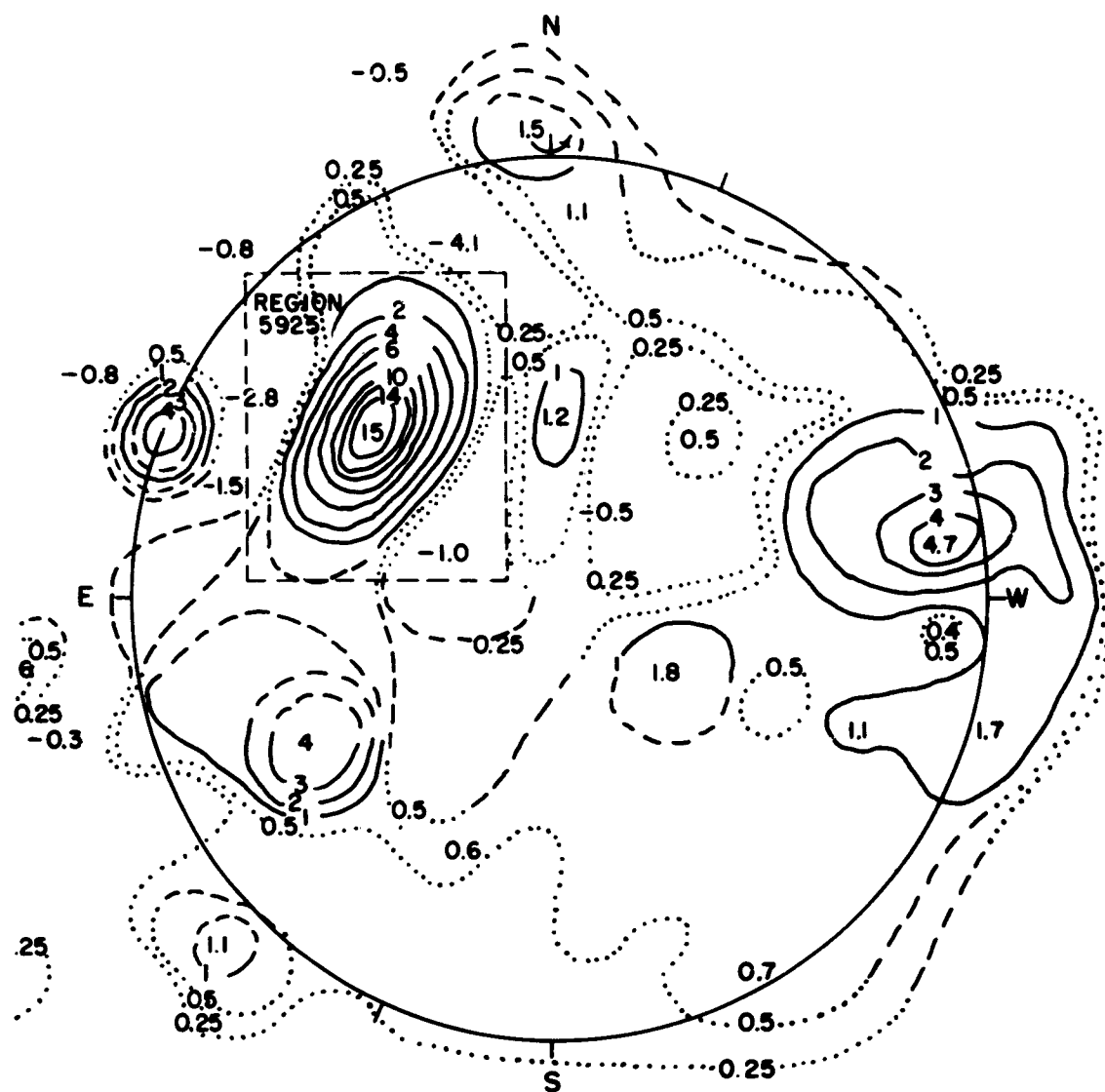


FIG. 2. Stanford University spectroheliogram at 9.1 cm November 9, 1960 (1900-2000 UT). Contour brightness unit 6.2×10^4 °K. (Courtesy G. Swarup)

in their diameter and in the temperature associated with them.

Within the condensation region responsible for the slowly varying component, densities are higher than in the surrounding corona. When the most energetic particles in the coronal atmosphere attain a sufficiently high kinetic energy so that their velocities are greater than that needed to overcome resistance and the solar gravitational field, these particles are emitted from the corona.³ As the temperature and therefore the kinetic energy increases, the percentage of particles that can escape grows in number. The high-velocity particles from plage regions may well form a low-level corpuscular envelope reaching out into interplanetary space.

The picture of the CA or center of solar activity, then, is of a dense region of higher apparent temperature than its surrounding, which may be observed on the disk and in the chromosphere in the light of the visible band, in Lyman α , and in X rays. When microwave interferometric equipment is used to observe the area of the plage region, the radiation of upper layers of the chromosphere and of the corona are recorded; at these solar altitudes, the radiating source gets wider and hotter. But when the observations are made at still longer wavelengths (frequencies of 169 Mcps), the source energy has become extremely diffuse and frequently is not considerably hotter than the surrounding coronal region. Thus, at centimeter wavelengths the plage region has an apparent temperature many times hotter than the background sun but at meter wavelengths it is just slightly hotter than the surrounding coronal region.

6. FLARES

The plage-sunspot areas are the seat of the more spectacular solar phenomena that have a short duration such as flares, which eject streams of charged particles into which magnetic fields are frozen. Flares are a sudden brightening of the plage areas observed optically at chromospheric levels. Their intensity is estimated at each observing station on a scale of area and brightness. The predominant measure is the area, with the largest flares labelled 3+ on a scale of 1, 2, and 3. The lifetime of a

flare varies from a few minutes to a few hours, with its brightness increasing sharply at the beginning of this time but decreasing more gradually at the end of the period. A disturbed region of the sun may produce many flares of varying intensity and area.

When solar observations are made with H α filters, the presence of a flare is first indicated by a sudden brightening in the solar chromosphere outline against the quiet photospheric and chromospheric features of the sun. Radio equipment can be employed to deduce the motion of the flare outward from the solar chromosphere by using radio receivers tuned to different frequencies in the range from 7.5 Mcps to 9300 Mcps and noting the difference in time at which enhanced signals (indicating the brightening of the flare) are received at the individual frequencies. The maximum signals are observed first at the high-frequency end of the spectrum; later the lower frequency bursts are seen.

The plasma frequency of the completely ionized solar atmosphere is proportional to the square root of the number of electrons it contains. Each layer in the solar chromosphere and corona has a plasma frequency associated with it. When the radio signals associated with a flare show enhanced bursts at a certain frequency, it is an indication that the shock wave or particle stream emitted by the flare is, at that time, exciting the solar layer associated with that particular frequency. The difference in time at which enhanced signals are received at various frequencies can be translated into height differences in the solar atmosphere, from which the velocity of the exciting shock wave can be found.

One type of flare of particular importance to terrestrial disturbances is the Type II-Type IV flare. A slow drift of the maximum solar signals from the high-frequency to the low-frequency end of the radio spectrum, corresponding to a slow excitation or shock wave, is denoted as a Type-II burst. After the shock wave reaches a certain altitude in the solar atmosphere, the nature of the radio-frequency radiation changes. All frequencies radiate from the same position in the solar corona. This radiation of energy in the radio band from at least 7.5 Mcps to 9300 Mcps is called

continuum or Type-IV radiation. The combination of Type-II shock wave and Type-IV continuum is the radio-burst configuration most closely associated with solar-terrestrial events. The continuum radio radiation is due to synchrotron radiation produced by trapped relativistic electrons in the solar corona.

When a solar flare develops, the increase of synchrotron radiation is enormous, perhaps by a factor of 10^5 . The electrons above a sunspot are accelerated to their relativistic velocities and kept in a tight spiral by the magnetic field surrounding the sunspot. Electrons radiate a good deal of the kinetic energy they have acquired by synchrotron radiation in the direction of the starting velocity. Protons, on the other hand, are responsible for only a small amount of radiation since, when they have acquired the same kinetic energy as electrons, their velocities are much smaller. Relativistic electrons radiate energy that is proportional to E^2 , where

$$E = \frac{mc^2}{\sqrt{1 - v^2/c^2}}$$

Protons, however, radiate a power proportional to their kinetic energy. Synchrotron energy from the electrons extends down to the X-ray bands. The protons that have not lost energy by radiation may well be the source of the increasing flux of protons observed in the polar-cap region of the earth within one to seven hours after a Type II-Type IV flare.

7. THE SOLAR-TERRESTRIAL HISTORY OF PLAGE AREA 5925

In order to illustrate the effect of the various types of solar phenomena already described on terrestrial parameters, the history of the passage of one particular solar region, plage area 5925, across the disk of the sun will be examined in detail from the time that it came into view both on the solar disk and as a coronal condensation, through its flaring stages, up until the time it receded beyond the west limb of the sun.

Plage region 5925 appeared on the eastern limb of the sun on November 6, 1960 in the Northern hemisphere (see Fig. 2). It passed the central

meridian of the sun on November 12 and disappeared around the western limb of the sun November 19. During its passage, it gave rise to a number of large and outstanding flares, which in turn produced a series of noteworthy terrestrial disturbances, including magnetic storms, auroras, airglow displays, and blackouts of radio communications. Some of the most important events^{4, 5} are summarized in Table 1.

Shortly after radio observers had noted the high apparent temperature of this region, flare activity started. The most startling fact was that three increases in cosmic rays were recorded near sea level during the passage of this area. Two of the flares responsible for these increases could be seen in white light when the sun was observed through neutral density filters.

These three cosmic-ray-producing flares (November 12 — 1322 UT, November 15 — 0217 UT, and November 20 — 2000 UT) were only the 9th, 10th, and 11th such flares observed since 1942. They took place in the space of eight days. In white-light observations of solar flares, only 17 had been observed before this series although optical observations have been carried on over an even greater span of years than have the cosmic-ray measurements.

Not only were these flares unusual because such rare occurrences followed each other in rapid succession, but they were also much more widely observed with a greater variety of equipment than had been the case with previous cosmic-ray flares. The first flare of the November 1960 group was observed in astronomical and atmospheric observatories in Europe and North and South America; the second flare was seen in Australia, Japan, and the U.S.S.R. The after-effects of the flares, the geophysical and propagation events following them, were observed all over the world. Among the newer types of measurement that were made were satellite observations of the cosmic-ray flux at various intensity levels and ground observations of satellite orbital periods. Sweep-frequency solar measurements, cosmic-noise recordings, auroral radio

TABLE 1. Solar Terrestrial Events, November 10 to 21, 1960

DATE	FLARE		SOLAR NOISE OUTBURST		SWF(SID)		COSMIC RAY, INCREASE†	
	Imp.	Time and position	Type	Time*	Imp.	Time	$\Delta I\%$	Time
10	III	1011-1430 28E 29N	— Maj. +	1020-1116 1116-1200	II	1022-1152	—	—
11	II+	0305-0428 12E 29N	III II IV	0316-0330 0332 0340-0730	III+	0311-0616	—	Polar-Cap Absorption
12	III+	1323-1922 4W 26N	II IV	1327-1331 1330-1800	III+	1325-1600	65 120	1340- 1900-1030 (13th)
14	II+	0246-0520 19W 27N	— IV	0318-0335 0335-0700	III	0300-0500	—	(PCA)
15	III+	0207-0427 33W 26N	II IV	0221-0225 0225-0700	III+	0220-0630	85	0240-22..
19	II	1543-1649 90W 28N	III (IV)	1559-1602 1636-1723	—	—	—	(PCA)
20	III	2017-2024 (110W) 25N	II IV	2023-2035 2027-2046	III-	2023-2145	5	2100-18.. (21st)

* Time at 200Mcps

† Deep River

reflections, and reflections from the moon on radio frequencies were used to study the solar bursts and the ionospheric medium. These and many other observations are now available for study and for use in evolving an integrated picture of the processes at work during this period.

8. THE EARLIER NONCOSMIC-RAY FLARES

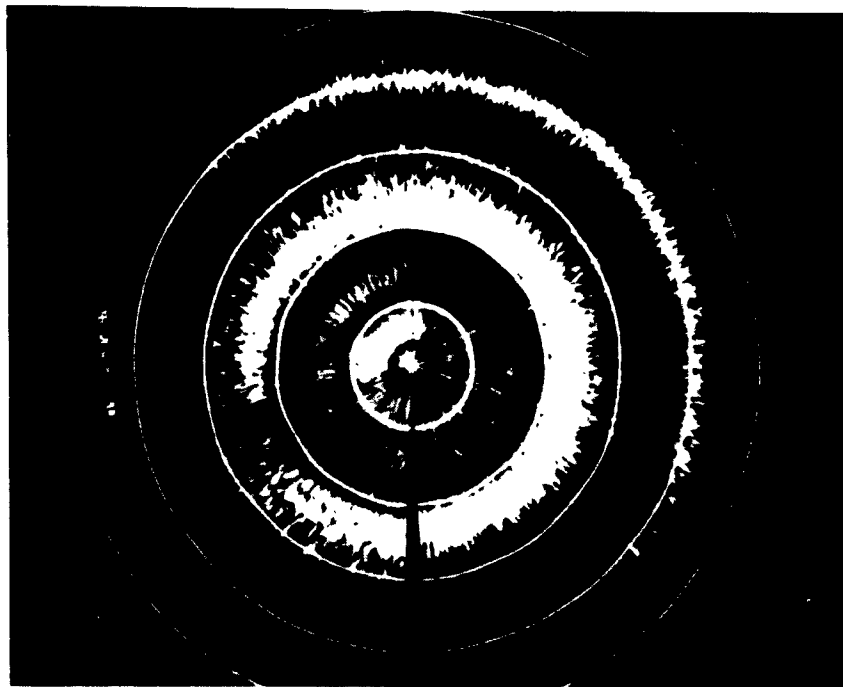
Before the detailed history of the first cosmic-ray flare, that of 1322 UT on November 12, can be fully understood, the earlier solar-terrestrial events associated with plage 5925 must be examined. Flare activity started soon after the appearance of this plage region. Two of the early flares are of direct interest: the November 10 flare of importance 3, observed from 1009 to 1400 UT and the flare that started at 0311 UT on November 11 beginning with a smaller area-intensity product but lasting longer than the November 10 flare. Although both of these flares were important in forming the magnetic and particle link between the sun and the earth that influenced the terrestrial effects of the subsequent cosmic-ray flare, the November 11 flare had higher energy in the 10-cm radio-wavelength region⁵ and will be described in detail.

The available evidence points to the November 11 flare as the source of a later and important magnetic storm. It was observed optically in the U.S.S.R. and with radio equipment in Australia and Japan, starting at 0315 UT. The Netherlands world-wide chain of stations, NERA, also observed it in many regions of the radio spectrum. Radio observations of this large flare showed small burst signals suddenly changing at 0318 UT to a Type-II enhanced outburst of solar radio-frequency emission, followed by a Type-IV continuum signal at 0330 UT. The Type-II burst signals indicated that the shock wave from this flare was moving slowly through the solar atmosphere with a velocity of 500 to 2000 km/sec. The adverb 'slowly' is used because some types of burst that are not as well correlated with geophysical disturbances move with velocities of 0.2 to 0.7 the velocity of light. Continuum radiation lasted until the close

of observations in Australia at 0700 UT. The Nançay Observatory of the French Observatoire de Meudon continued to record the Type-IV continuum. The French group also measured the diameter of the source of radio radiation and found it to be 2 minutes of arc. This value holds for all frequencies since, as has been explained in the section on flares, the continuum is due to synchrotron radiation originating in the same area of the solar corona for all frequencies in the radio band from 7.5 Mcps to 9300 Mcps and is not due to the excitation of the various plasma frequencies at different heights above the photosphere.

Both the earlier November 10 flare and the November 11 flare produced Sudden Ionospheric Disturbances, called SIDs. When a high-frequency wave used for long-distance communications passes through the D layer as it is probing the ionosphere, it sets into motion electrons in this layer. Collisions in this dense atmospheric region between the oscillating electrons and neutral particles result in absorption of radio-frequency signals. The emission of X rays from a flare produces an unusually large number of electrons in the D layer of the earth's ionosphere, at a height of from 60 to 80 km in middle and high latitudes. Increased absorption of short-wavelength radio waves, called short-wave fadeout, occurs over the sunlit portion of the earth. An example of the type of backscatter return observed during a SID is shown in Fig. 3. Since the causal agent is the flare radiation at X-ray wavelengths, the fadeout ends when the flare ends. The beginning and end of the intense radiation producing the Sudden Ionospheric Disturbance (SID) can thus be sharply timed.

The Riometer, or Relative Ionospheric Opacity Meter, is one of the newer techniques for ionospheric measurements. As it is now used, this instrument is designed to record the variations at the earth's surface of cosmic rf noise in the frequency range of 18 Mcps to 60 Mcps. The main interest in these measurements, however, is that they provide information about the intervening ionospheric medium and its effect on the amplitude of the signal level. Absorption in the D and the F-1 layers of



(a) END OF CLOCKWISE SWEEP
IS 0825. SID STARTS AT 0826.



(b) TRACE STARTING IN WEST
STARTED AT 0825 AND ENDED
AT 0833.

FIG. 3. PPI scope photographs showing 19 Mcps backscatter returns of Plum Island, Mass., observed on November 12: (a) at 1325 UT just preceding the SID, and (b) at 1333 UT during the SID. Second photo shows the complete absorption of signals after 0826 UT. (C. Malik and R. Hardke)

the ionosphere will reduce the cosmic-noise signal by varying amounts. By means of the cosmic-noise measurements, the SID, auroral absorption, and polar-cap absorption, as well as the normal diurnal variation, may all be measured quantitatively more accurately than was possible by earlier methods. Until the widespread use of this technique, observers frequently reported short-wave fadeout or polar blackout, without having any idea of the decibel decrease in signal level associated with these phenomena or of the fine-scale variations present within the period of absorbed or blackout signals. On some types of transmission circuit, for example, a 3-db decrease in signal level in the 12-to 20-Mcps range might represent a fadeout; in polar regions, absorption of 26 db has been observed at even higher frequencies.

When all the available measurements are studied, it can be seen that the noncosmic-ray flare emitted energy in the X-ray spectrum and produced the SID, one effect of which was the short-wave fadeout; radiation in the H α line was observed with optical telescopes; and plasma radiation in different regions of the solar atmosphere and synchrotron radiation in one region of the solar corona were produced.

These are the immediate effects. Two other effects have already been referred to briefly – the emission of protons of slower velocity than the X-ray radiation, and the plasma cloud.

The flare protons that have not lost energy by radiation are channeled by the earth's magnetic field into the polar-cap region, producing ionization in the lower ionospheric levels. After several hours have elapsed, the ionization reaches proportions sufficient to black out all short-wave transmissions in the polar-cap area.

The high-velocity particles escaping from the corona as the result of a flare form a corpuscular stream reaching out into interplanetary space. This corpuscular or plasma cloud travels even more slowly than does the proton stream. It arrives at the earth from 10 to 45 hours after the flare. Its effect is to produce a magnetic storm. Such a magnetic storm started at 1345 UT on November 12, 34 1/2 hours after the November 11 flare, and probably can be ascribed to the plasma cloud

from this flare. The November 10 flare could have been the causal agent, however; no tags exist to determine this with surety.

The plasma clouds have been followed outward from the sun to perhaps four solar radii. Within the plasma cloud is a frozen magnetic field extending back to the sunspot region from which the flare originated. In the case of the November 11 flare, the solar particles trapped within the magnetic field were of low energy. On the other hand, particles of cosmic-ray energy were trapped within the plasma cloud emitted from the cosmic-ray flare of November 12. The magnetic lines of force within the cloud, stretching back to the active sunspot region, form a magnetic bottle.

9. THE COSMIC-RAY FLARE OF NOVEMBER 12, 1960

The Increase in Cosmic-Ray Count

The large flare that began at about 1322 UT on November 12 was the first flare from plage region 5925 to result in a large increase of cosmic rays at sea level.

In Table 1 are summarized some optical and radio observations of the flare which, although of relatively short duration, was of sufficient intensity to force almost all radio equipments to go off scale. The flare, as observed by Sacramento Peak Observatory with an $H\alpha$ filter, is shown in Fig. 4. Neutron counters over the world recorded an increase which built up slowly over a span of hours.⁶ The increase was much more gradual than that observed during other cosmic-ray flares, including the two later flares from plage area 5925 (see Fig. 5). The reason for the slow buildup was that the magnetic bottles created by the noncosmic-ray flares of November 10 and 11 did not yet include the earth within their configuration. Therefore, in order to reach the earth, the solar cosmic-rays from the November 12 flare had to diffuse slowly across the existing magnetic-bottle lines of force extending from the sun into interplanetary space. In contrast to the slow buildup time of hours on November 12, neutron counters recorded an increase which rose to maximum in a matter of minutes following the November 15 cosmic-ray flare.

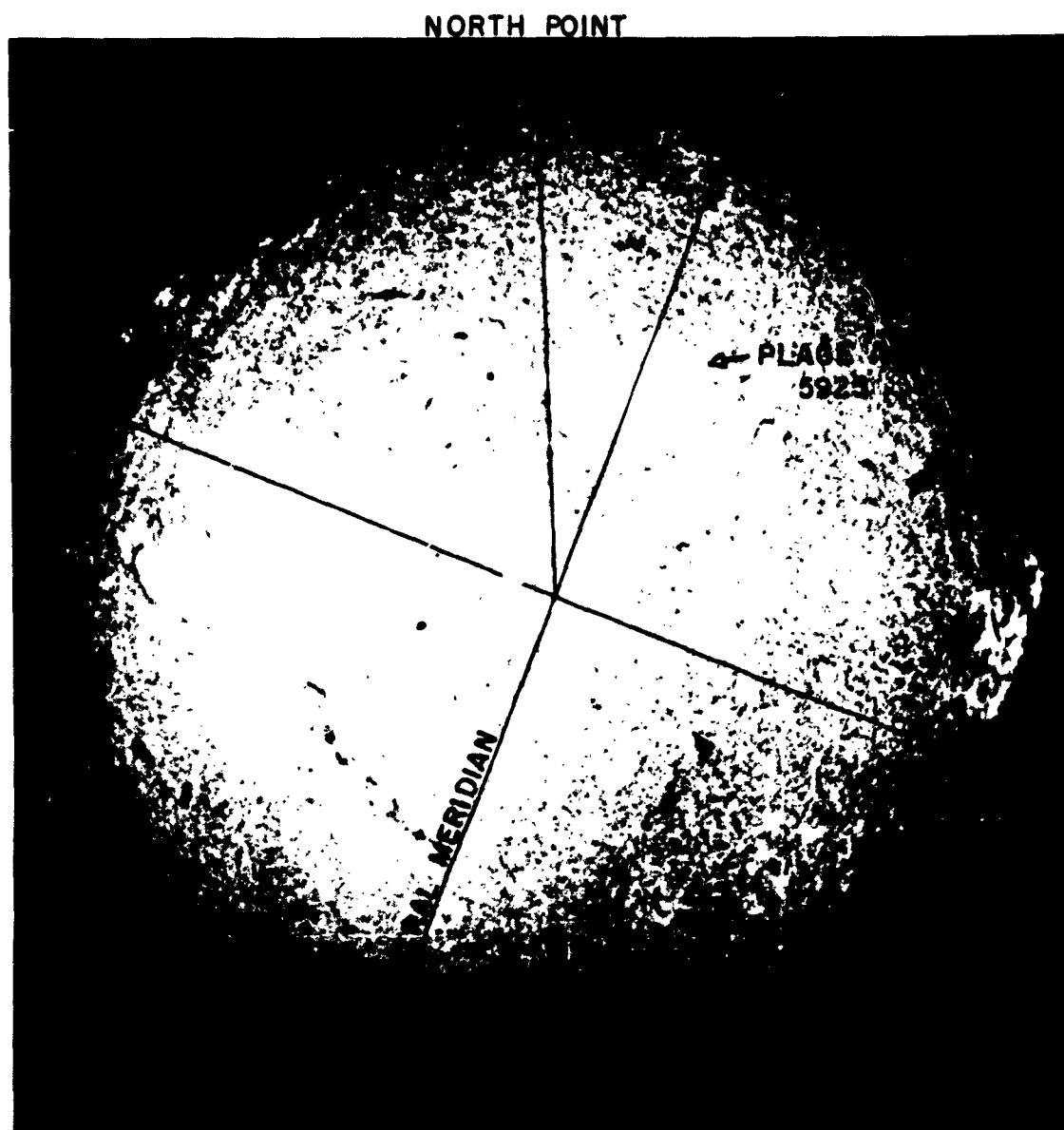


FIG. 4. $H\alpha$ photograph of sun at 1435 UT on November 12. Plage area 5925 is just passing the central meridian of the sun. The November 12 cosmic-ray flare can be clearly seen obscuring the sunspots of Fig. 1. (Courtesy of Sacramento Peak Observatory, Sunspot, N. M.)

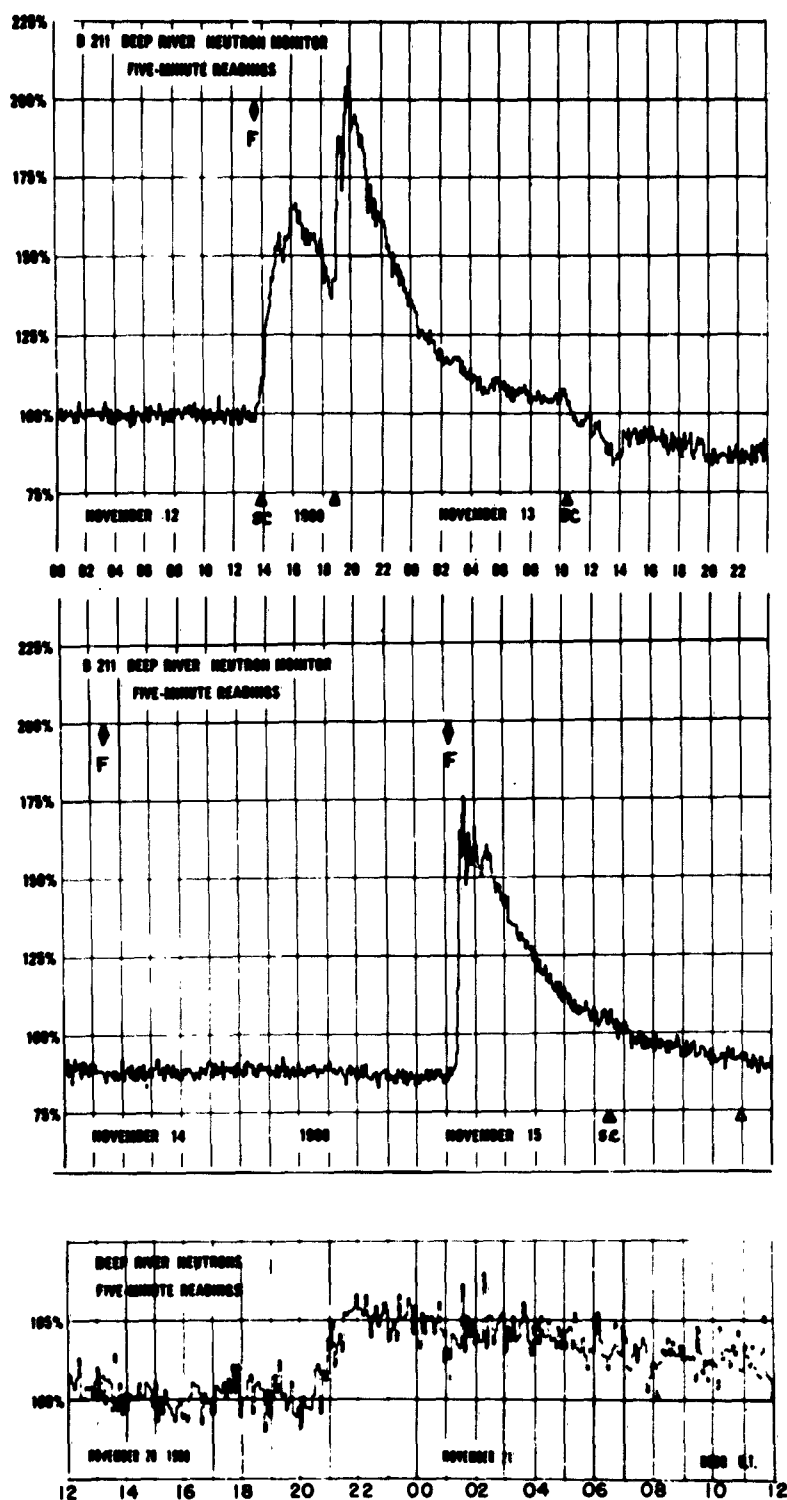


FIG. 5. Records of standard neutron monitor at Deep River for the periods Nov. 12 to 13, Nov. 14 to 15, and Nov. 20 to 21, 1960. Note the gradual increase starting at 1325 UT on Nov. 12 in contrast to the steep slope at 0207 UT on Nov. 15. Because of the very slight increase noted on Nov. 20, the scale of the graph has been expanded for ease of reading. (J. F. Steljes and H. Carmichael, Atomic Energy of Canada, Ltd.)

The Ionospheric Disturbances

The SID, produced by X rays ionizing the D layer, was observed at 1323 UT over the sunlit portion of the earth, except in regions where the sun was at very low angles of elevation. Riometer data were taken at 18 Mcps at Troy, N. Y.; Ann Arbor, Michigan; and Boulder, Colorado. Similar units recorded observations at 30 Mcps and 60 Mcps at Athens, Greece; Ottawa, Canada; Kiruna, Sweden; College, Alaska; Oslo, Norway; and many other areas. Illustrated in Fig. 6 are observations of absorption at 10 Mcps taken at Sagamore Hill, Massachusetts.

The SID, which usually brackets the flare observations, is a short-lived affair. The ionosphere ordinarily returns to something akin to its normal diurnal variations at the end of the intense radiation from the flare. The sudden-commencement (SC) magnetic storm resulting from the flares of either November 10 or 11 started only twenty minutes after the first optical sighting of the November 12 cosmic-ray flare. Therefore, fresh ionospheric disturbances and the resultant absorption seen on November 12 to 13 followed hard on the November 12 SID.

At receiving stations above the Arctic Circle, such as Kiruna, Sweden,⁷ the sun was not above the horizon at 1323 UT. They therefore did not observe the SID. About an hour and a half after the November 12 flare had been observed, a decrease in cosmic-noise power with a gradient of 1.5 db per hr was noted, however. This decrease was not related to the X-ray-produced SID. It was, rather, a new event which signalled the arrival of high-velocity protons from the November 12 flare. When these solar particles, traveling at speeds of 0.1 the velocity of light, pour into the polar regions, polar-cap absorption is produced. The continuous bombardment of the atmosphere by the protons produces a high degree of ionization which, in turn, causes the first phase of the polar blackout of high-frequency signals. Although polar-cap absorption is usually confined to geomagnetic latitudes greater than 60°, it may occur at lower latitudes following some large perturbations of the earth's magnetic field such as those accompanying the 1345 UT November 12 geomagnetic storm caused by an earlier flare.

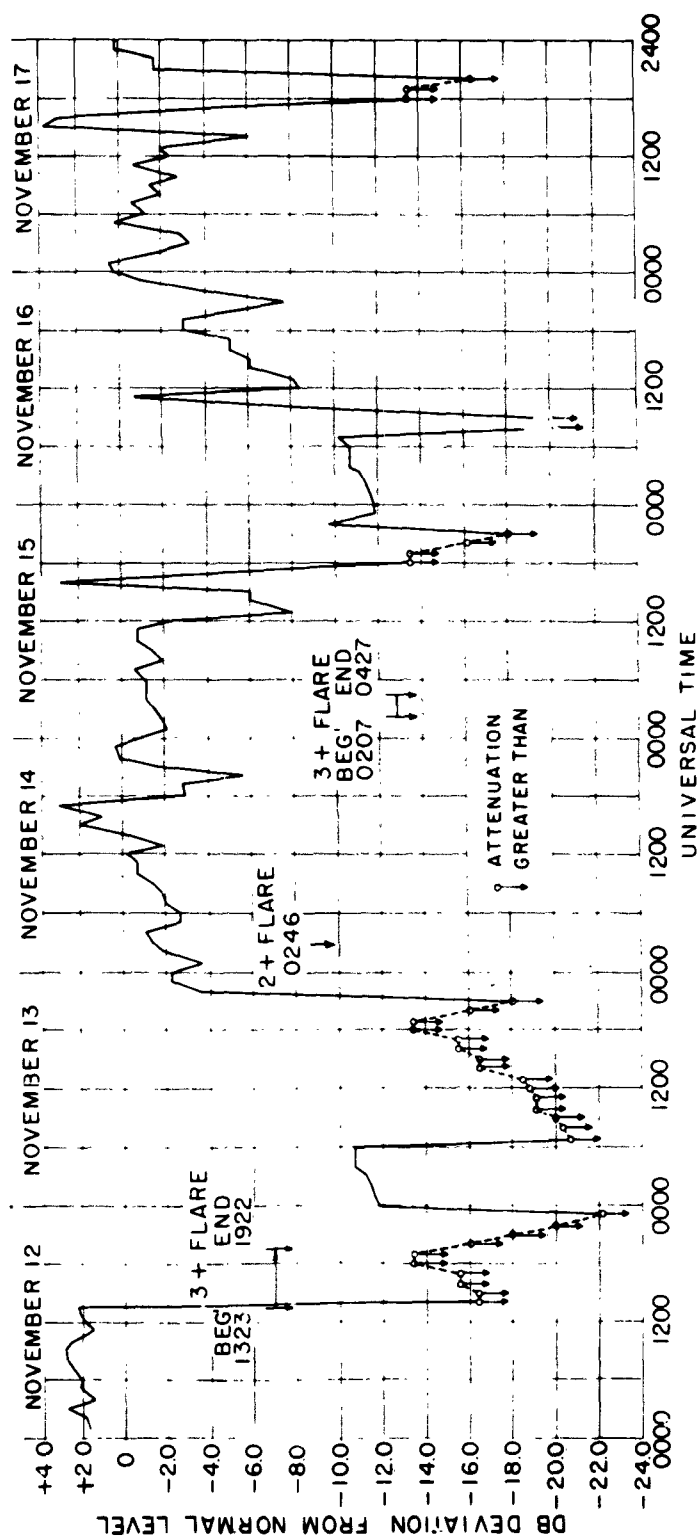


FIG. 6. Cosmic-noise absorption at 10.004 Mcps observed at Sagamore Hill Radio Observatory Nov. 12 to 17. (R. Straka)

By 1600 UT, the ionosounders at Kiruna were unable to detect the high-frequency signals reflected from the ionospheric layers. Somewhat south of this observatory at Lycksele, Sweden, a blackout was also recorded. It was not until two hours later, however, that the ionosounder at Upsala, Sweden (near Stockholm) recorded blackout conditions. The same slow motion of the polar-cap-absorption protons toward the south was noted by the Canadians in their chain of cosmic-noise receiving stations.

As time went on, the main phase of the geomagnetic storm, combined with the visual aurora spreading south, became the most significant factor in the ionospheric storm. The Canadian chain of stations observed an increase of absorption at 1900 UT. Kiruna's observations of VHF auroral reflections between 1755 and 1925 UT coincided with the strongest geomagnetic activity of the day. H. V. Serson and B. C. Blevins of Canada's Defense Research Telecommunications Establishment report reflections from the radio aurora at 944 Mcps at 1830 to 1900 and 2200 to 2230 at approximately the same universal time as the Kiruna observations were made. Rapidly moving auroral echoes were detected by Stanford Research Institute during this period.⁸

Very-Low-Frequency Propagation Effects

In order to circumvent the intense absorption of high-frequency propagation during auroral and ionospheric disturbances, long-wave radio transmission (15 to 300 kcps) are often used during these periods. In the case of these wavelengths the earth-ionosphere acts as a waveguide. An intense noncosmic-ray flare will result in a narrower waveguide with a more highly conducting surface. This is due to the fact that the incoming protons from a large noncosmic-ray flare produce lower reflecting layers in the auroral zone. The layer height is reduced about 10 km so that signals are then being reflected from 50 or 55 km or lower. The protons maintain this layer height both day and night during a polar-cap event. As a result, long-wave propagation in or near the auroral zone maintains uniform intensity levels. There is no diurnal variation.

But the events of November 12 and November 15 were not normal

polar-cap events. The high-energy cosmic-ray particles bombarded the atmosphere and, as a result, the signal level of the long-wave transmissions was not increased but was reduced significantly, especially across the polar cap.

These facts indicate that the energy and the flux of the bombarding particles are the overriding factors in determining the structure of the D layer in the auroral zone. The energy spectrum of the bombarding particles sets the propagation parameters for low-frequency waves regardless of the normal nighttime processes such as attachment of free electrons to form negative ions.⁹

The 1900 to 2000 UT Period of November 12, 1960

If all the records are used for intercomparison, it is found that the following events occurred in the period from 1900 to 2000 UT on November 12: a large increase in magnetic disturbance, an increase in cosmic-ray intensity, increased ionospheric absorption, and auroral reflections. (Figures 5, 6, 7, and 9 illustrate some of the changes observed.) No new solar burst was recorded during that time, however. One possible explanation of these events is that a new magnetic storm started at this time and contributed to the effects of the PCA and the magnetic storm already in progress. Such a storm may have been produced by the arrival of the corpuscular stream from the flare of November 11, in which case the 1345 UT storm would have to be ascribed to the November 10 flare. Another possibility is that these effects were due to some modulation of the 1345 UT magnetic storm.

Electron-Density Effects

A most vital study for understanding propagation effects is the determination of the electron-density structure of the upper atmosphere. Radar techniques of sweeping in the 0.5 to 25 Mcps frequency range and reflecting pulses off the ionosphere make it possible to calculate the electron density vs. height above the earth's surface up to the point in the ionosphere where the electron concentration is a maximum. The highest frequency to be reflected at a given height is the plasma frequency or the critical frequency of the layer; it is proportional to the

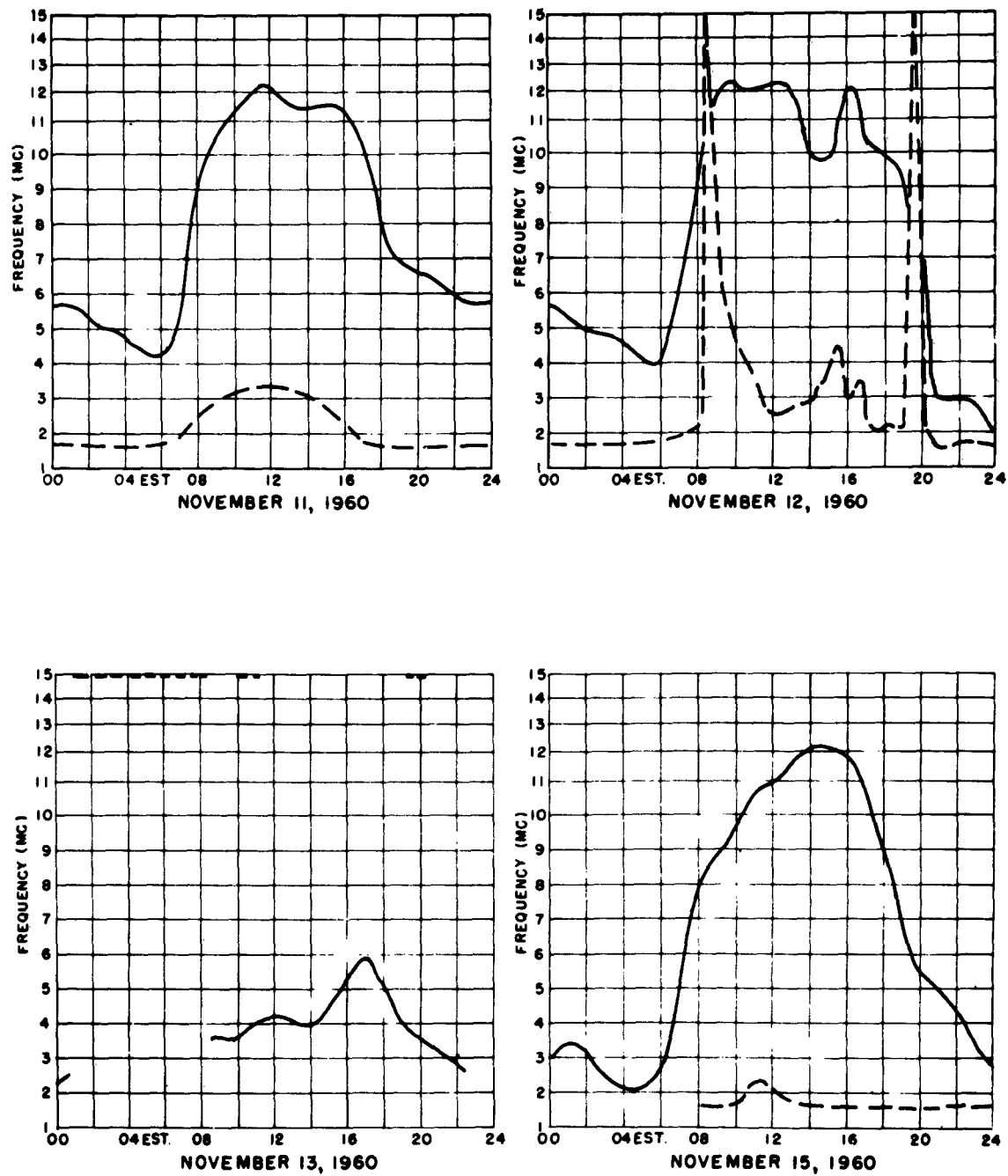


FIG. 7. Fort Belvoir, Virginia ionospheric data f-plot for Nov. 11, 12, 13, and 15. (CRPL, National Bureau of Standards.) Continuous line is f_oF_2 ; dashed line is f_{min} . (J. Virginia Lincoln)

square root of the electron density. Newer techniques, described later, have made it possible to obtain information as to the electron distribution above the maximum-concentration point in the atmosphere.

Electron-density studies were made at many places during the November events. World-wide records of November 13 indicate a decrease in the critical frequency at all sites except those within about 15° of the geomagnetic equator. The National Bureau of Standards' records¹⁰ at Cheltenham, Maryland from November 11 to 15 (illustrated in Fig. 7) show the variations in critical frequency during the November 12 period as well as the lower critical frequencies that were obtained all day on November 13. By way of contrast, a critical frequency 1.5 times normal was reported on November 13 over the geomagnetic equator at Concepcion, Chile. It appeared that the maximum electron density had decreased considerably everywhere but in the equatorial zone.

Since these studies provide no picture of the ionospheric electron density above the point of maximum electron concentration, they do not reveal whether the shape of the complete electron-density curve had changed, with the electrons redistributing themselves and spreading out in the upper layer, or whether there had been an actual decrease in the total number of free electrons.

More recent techniques, designed to provide an answer to this question, use the rotation of the plane of polarization of signals reflected from the moon to determine the total number of electrons in the ionosphere. Jodrell Bank, England, using this technique during the November period,¹¹ noted that the total number of electrons had decreased on November 13 by a factor of 3 to 5 (see Fig. 8). Whistler observations¹² confirm the reduction in electron density above the F-2 maximum for November 13. This information, combined with the ionosound data, reveals that the electrons had not been distributed in a different manner within the earth's atmosphere but had actually decreased in total number. In other words, in the regions somewhat distant from the equator, there had been a scaling down of the whole

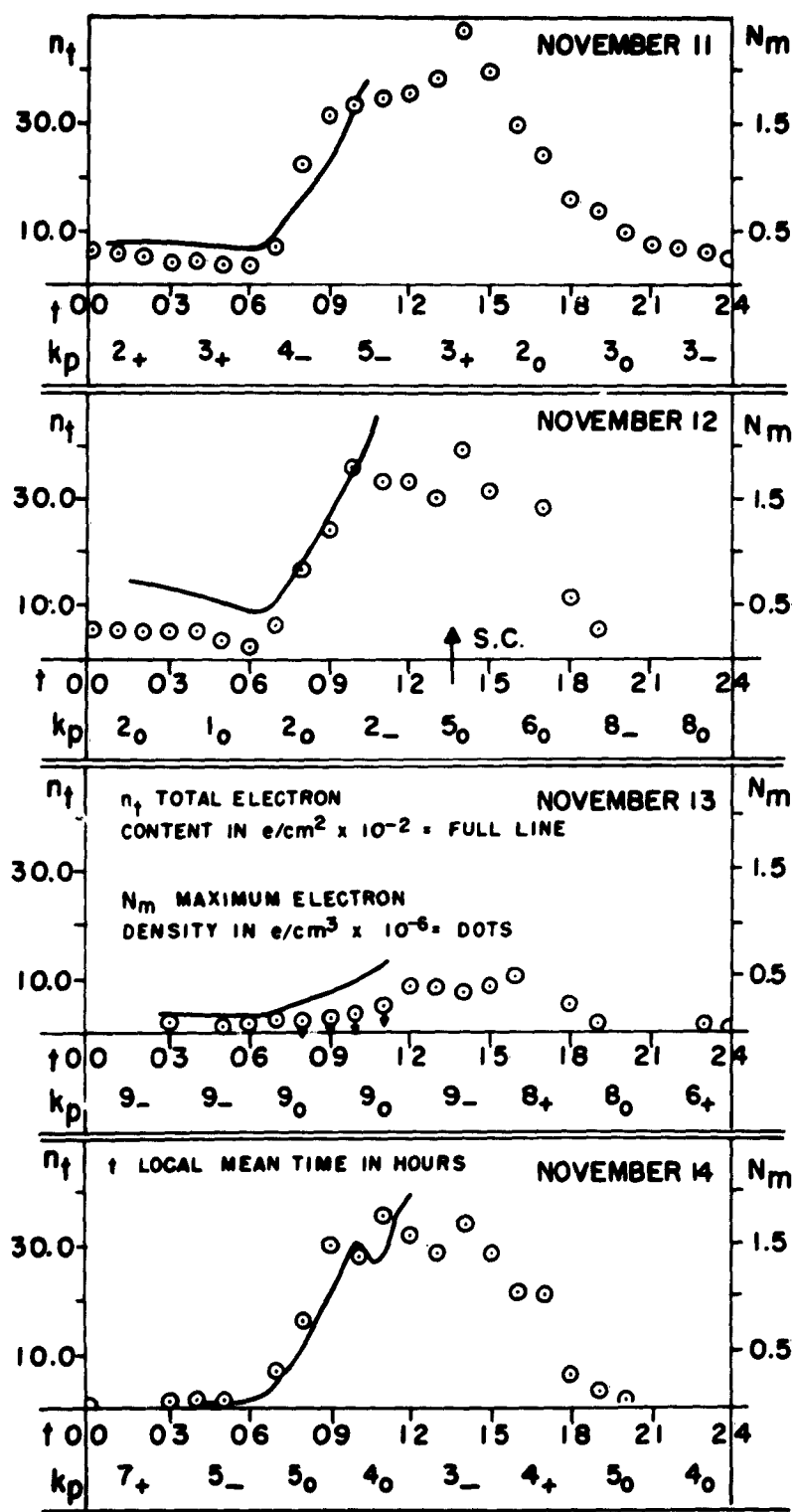


FIG. 8. Curves of n_t (total electron content of the ionosphere) vs. time for each of the days from Nov. 11 to 14. Curves have been corrected for local mean time at the sub-ionospheric point and the mean sub-ionospheric latitude is 50° N. (G. N. Taylor, Jodrell bank.)

ionosphere rather than a vertical redistribution of the ionization.

At first glance, this appears to be contrary to what one would expect. Two possible explanations, the introduction of another mechanism for attachment and association of the electrons produced by the increased ionizing radiation, and the postulation of a decrease in the atmospheric density itself so that the ionizing radiation encounters less atmosphere to ionize in the northern regions, are discussed at greater length with reference to the November 15 flare.

10. THE NOVEMBER 15 COSMIC-RAY FLARE

Although the ionospheric picture on November 15 and 16 in many ways echoed that of November 12 and 13, each solar flare and its X-ray, proton, electron, and plasma corpuscular streams has different effects on the earth's atmosphere. The factors affecting the end results are the intensity and size of the flare, its position on the solar disk relative to the sun-earth line, the interplanetary configuration of existing electrons, protons, and frozen magnetic field, as well as the state of the ionosphere just preceding the flare.

The 3+ flare at 0207 UT on November 15 was almost immediately followed by an increase in cosmic-ray intensity at the ground level. Neutron counters recorded a rapid increase which reached its maximum within a period of minutes in contrast with the slow buildup observed on November 12 (see Fig. 5). The intensity level remained essentially constant for about two hours. The cosmic rays from the 0207 UT flare apparently spiralled down lines of force of magnetic fields from previous flares. These magnetic lines of force were still connecting the earth and the sun and therefore rapidly channeled the well collimated solar cosmic rays to the earth.

A short-wave fadeout (SID) accompanied the flare. The H α enhancement lasted from 0207 to 0427 UT, the short-wave fadeout from 0220 to 0630 UT. Radio-astronomy observations of the sun revealed Type-II radiation from 0221 to 0225 UT, followed from 0225 to 0700 UT by Type-IV continuum radiation at all frequencies from the meter to the centimeter

wavelength region. Japanese scientists observed the flare in white light and Australian radio astronomers recorded this as the major outburst of 1960.

At 1304 UT an SC magnetic storm started. Whether the 0207 UT cosmic-ray flare was the source of this storm or whether the plasma cloud originating in the 2+ flare of 0246 UT on November 14 could have caused it, is a matter of conjecture.

The ionospheric changes, on the other hand, may be clearly defined. On November 16 ionosound data indicated that the critical frequency of the F-2 layer had decreased considerably North of geomagnetic latitude 54° but had changed little to the south. Ionosound records at Slough, England at 54° latitude showed a decrease whereas Cheltenham, Maryland and White Sands, New Mexico records did not show any significant change in critical frequency. The backscatter results at Sagamore Hill, Massachusetts, geomagnetic latitude 54° , (illustrated in Fig. 9), showed a gap in the north. This indicates that the ionization was insufficient to give backscatter in that direction but that in the directions of east, south, and west the ionosphere could sustain backscatter.

As mentioned previously, two possible explanations have been advanced for the bunching of electrons around the equator and the deficiency of electron content near the poles during a severe magnetic storm. The first—the decrease in recombination rate because of the introduction of another mechanism for attachment and association—has been considered by several authors.^{13, 14} Satellite observations during the November events made it possible to obtain measurements to test the second hypothesis (that the density of the atmosphere changed so that the ionizing radiation encountered less atmosphere to ionize in the northern regions).

When a denser atmosphere is encountered, a satellite's orbit is changed by frictional forces. The encounter with neutral atoms and molecules forces it to approach the earth's surface. The principle of Kepler's second law (a satellite will sweep out equal areas in equal time periods) therefore causes the shortening of the satellite's orbital period when the density increases.

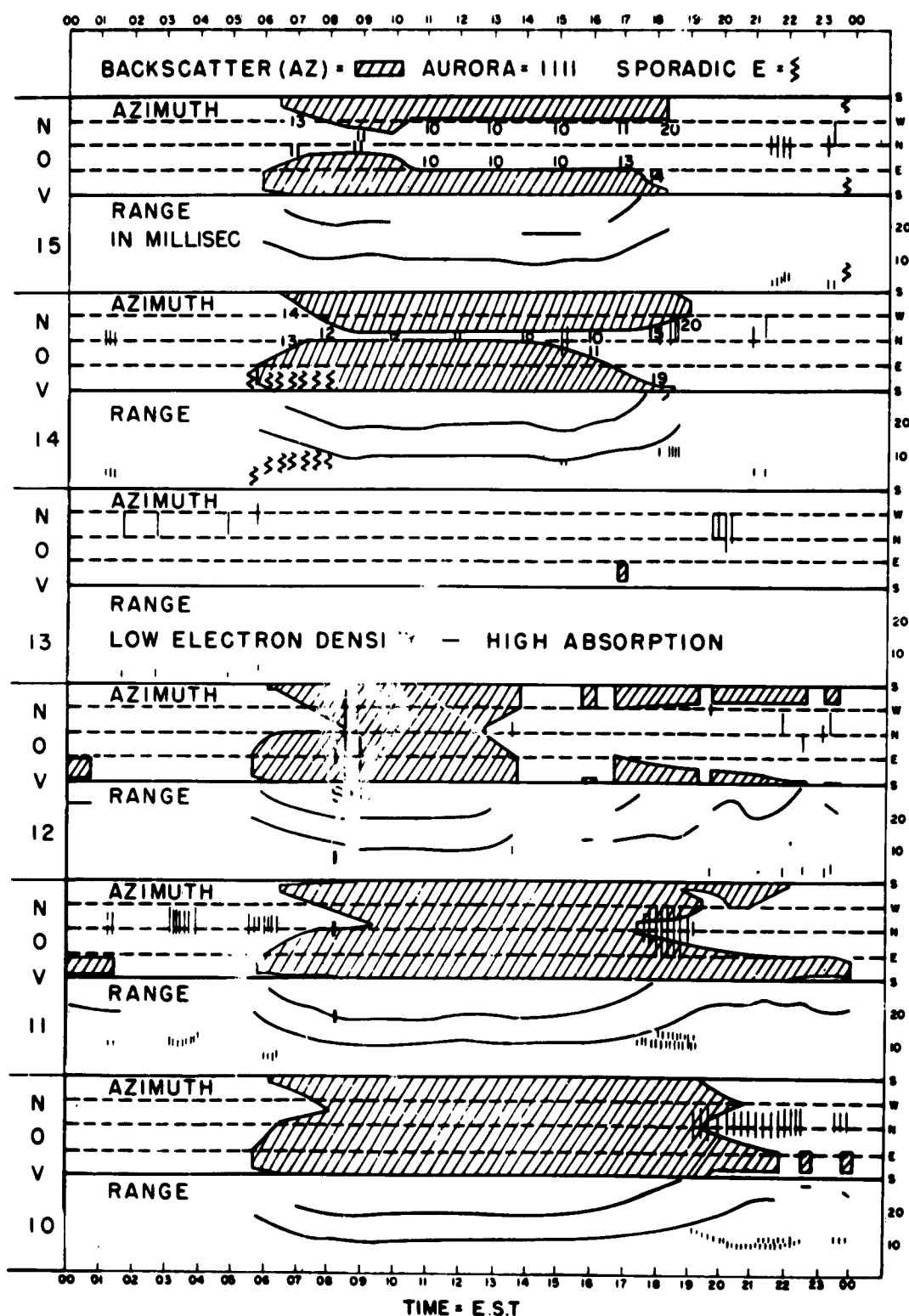


FIG. 9. Backscatter signals at 19 Mcps, Nov. 10 to 15, 1960, Plum Island, Mass. Note absence of signal return in the northerly direction all day on Nov. 15. Nov. 10 and 11 records show typical undisturbed diurnal variations. (C. Malik and R. Hardke)

On a long-term basis, there is evidence that perturbations in satellite period may be correlated with the 10.7-cm flux from the sun. This flux is basically the slowly varying component. On a short-term basis, the large magnetic storms produce increases in atmospheric density at all altitudes. During November 12, 15, and 16, satellite observations at altitudes from 200 km to 1100 km indicated that, although there was an increase in density relative to normal at all altitudes in this range, the increase was greater at the higher than at the lower altitudes. These atmospheric density changes are associated with the magnetic storms rather than with the flares.¹⁵

Although these observations showed atmospheric-density changes, no fine-scale changes were discerned with respect to latitude. On the contrary, the indications were that, on the days of November 12 to 13 and November 15 to 16, the atmospheric density had increased on a world-wide basis. This would seem to indicate that, at least during this period, the hypothesis that the atmospheric-density variations were responsible for the equatorial bunching and the polar deficiency of electrons was not valid.

11. THE NOVEMBER 20 COSMIC-RAY FLARE

The disappearance of the center of plage region 5925 beyond the west limb of the sun took place on November 19. Yet, at 1956 UT on November 20, a flare was observed rising from beyond the limb into the solar atmosphere. The University of Colorado High Altitude Observatory photographs of this limb flare are shown in Fig. 10. A swept-lobe interferometer of Rensselaer Polytechnic Institute at Troy, N. Y., operating at 517 Mcps first recorded the event at 2020 UT when the particles had penetrated the lower corona. By 2030 UT, when the corpuscular cloud or shock wave could be observed optically at 250,000 km beyond the limb, the radio center of gravity was approximately 6 minutes from the optical limb. At 2037 UT, the radio measurements indicated that the intensity had increased to 5.5 times the quiet-sun level;

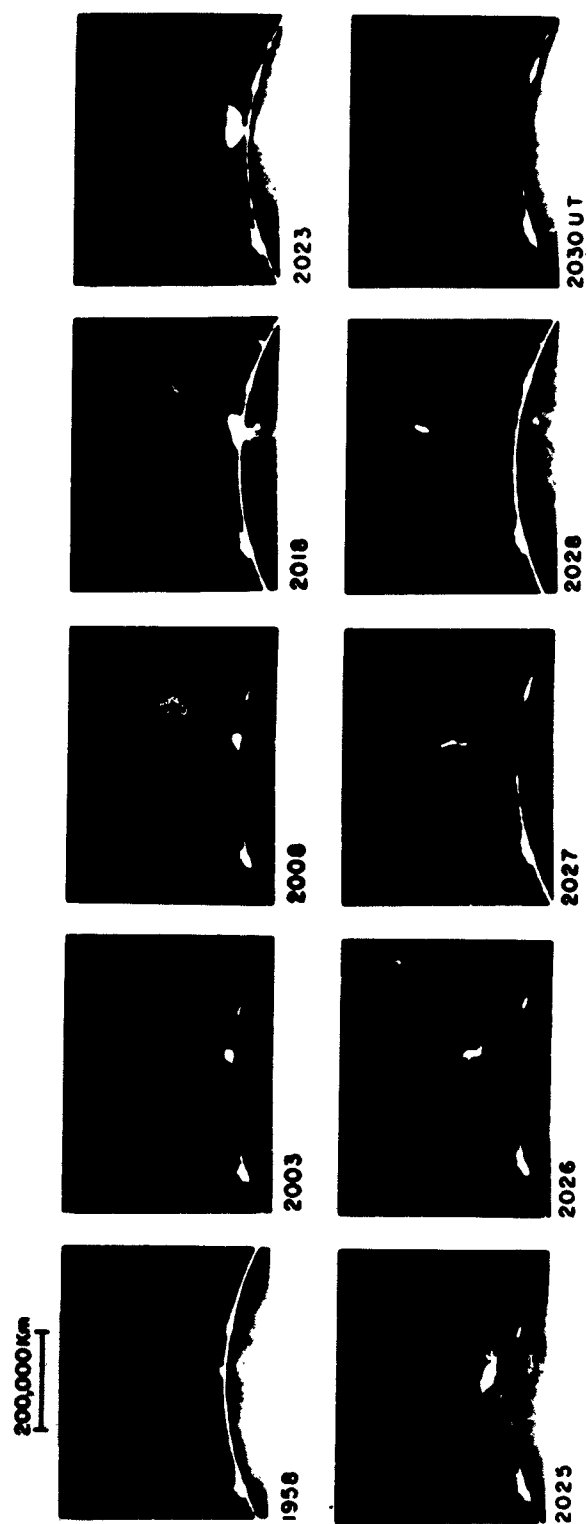


FIG. 10. The solar limb flare of Nov. 20, 1960. West limb, 25° north.
(R. T. Hansen, High Altitude Observatory, University of Colorado.)

the position of the burst had dropped back to about 13 minutes from the solar center.¹⁶

The limb-flare observations graphically illustrate the movement of the flare, that is its slow movement into the solar corona and finally the movement of the center of gravity of the cloud or shock wave back to the solar disk.

In the case of the November 20 flare, the cosmic-ray count observed on the earth at satellite heights was small compared to that accompanying the November 12 and November 15 events. There was an increase from 21 to 980 particles per cm^2 above the threshold of the measuring instruments in contrast to counts¹⁷ of 21,000 particles per cm^2 on November 12 and 14,000 on November 15.

Very-low-frequency communications showed an increase in intensity at 0300 UT indicating that a polar-cap layer of the normal variety had been produced rather than the absorbing layer observed on November 12 to 13 and November 15 to 16.

The ionospheric and propagation effects of this flare did not greatly differ from those of typical large noncosmic-ray flares.

12. SUMMARY

Plage region 5925 has been chosen as the medium for illustrating the full range of effects of the sun on the propagation of radio waves and on the ionosphere in general. It first appeared on the eastern limb of the sun as an enhanced source of radio energy, the type of signal associated with a center of activity. Such a center of solar activity appears as sunspots on the disk of the sun, as a plage region in the chromosphere, and as a region of high apparent temperature in the upper chromosphere or the corona.

From this center of activity, flares originate. X-ray radiation, radio signals, and particle emission all form part of the flaring action. The X-ray radiation from the flares results in intense ionization in the D layer of the atmosphere, causing absorption of radio waves and consequent fadeout of communication signals. The protons from flares have

both great intensity and distinctive velocity characteristics. They spiral down the lines of force of the earth's magnetic field and produce, in the polar-cap regions, intense absorption which lasts for a period of days. About 10 to 45 hours following a flare, the corpuscular stream gives rise to a magnetic storm with its resulting ionospheric storm, visual auroral displays, and other effects.

Plage region 5925, which passed the central meridian of the sun on November 12, produced three flares which were followed by ground-level observations of an increase in the count of particles of cosmic-ray energies. The effect of the arrival of the high-energy particles from these flares was a complicated one. In some cases, the ionospheric effects normally resulting from large flares were further enhanced. In other cases, the usual flare effect was nullified. An example of the latter situation is the distinct reversal in the polar-cap enhancement of very-low-frequency propagation normally observed following a large flare.

There have been two very important recent contributions to an understanding of the sun's effect on propagation parameters:

(1) the increase in the number of observations available to a student of the world-wide effects,

(2) the development of new techniques for solar observation such as the sweep-frequency radio receiver and the interferometer, the use of moon reflections for measuring the total electron content in the earth's atmosphere, the measurement by satellites of cosmic-ray counts, and the study of satellite orbital variations.

REFERENCES

1. R. G. ATHAY, J. Geophys. Res., 66: 385 (1961).
2. W. N. CHRISTIANSEN, et al., Annal d'Astrophysique, 23: 75 (1960).
3. V. A. AMBARTSUMIAN, Theoretical Astrophysics, p. 395
Pergamon Press, N. Y., 1958.
4. T. OBAYASHI, Resume of the Conference on the Solar Terrestrial Events of Nov. 1960, Arctic Institute of No. America Research Paper No. 14, June 1, 1961.
5. P. SIMON, L'Activite Radioelectrique Solaire Pendant la Periode du 7 au 20, Novembre 1960, presented at AFCRL Conference, Feb. 1961.
6. J. F. STELJES, H. CARMICHAEL and K. G. McCracken, J. Geophys. Res., 66: 1363 (1961).
7. J. ORTNER, A. EGELAND and B. HULTQUIST, The Great Earth Storms in Nov. 1960 as Observed at Kiruna Geophysical Observatory, Scientific Report No. 1, Contract AF61(052)-418, 7 Feb. 1961.
8. R. L. LEADABRAND, W. E. JAYE and R. B. DYCE, J. Geophys. Res., 66: 1069 (1961).
9. J. S. BELROSE, and D. B. ROSS, Canadian Journal of Physics, 39: 609 (1961).
10. CRPL, National Bureau of Standards, Detailed Values of Ionospheric Characteristics and F-plots for Washington, Nov. -Dec. 1960.
11. G. N. TAYLOR, Nature, 189: 740 (1961).
12. R. A. HELLIWELL, private communication, 1961.
13. S. SILVERMAN, W. BELEW and E. LAYMAN, Photometric Observations of 6300 A OI at Sacramento Peak, N. M., during Nov. 1960, presented at AFCRL Conference, Feb. 1961.
14. M. J. SEATON, J. Atm. and Terr. Phys., 8: 122 (1956).
15. L. G. JACCHIA, Research in Space Science, Smithsonian Institute Astrophys. Observatory Special Report No. 62, Cambridge, Mass., May 26, 1961.

REFERENCES (contd)

16. R. FLEISCHER, and M. OSHIMA, 517-Mc Burst Positions on Nov. 20, 1960, presented at AFCRL Conference, Feb. 1961.
17. J. A. VAN ALLEN, Preliminary Survey of Explorer VII Observations of Solar Cosmic Rays, 12-23 Nov., 1960, State U. of Iowa Report, 1961.

POLAR-GLOW AURORA IN POLAR-CAP ABSORPTION EVENTS*

Brian P. Sandford[†]
 Arctic Institute of North America

ABSTRACT

During polar-cap absorption events, an extensive auroral glow called the polar-glow aurora is observed. The geographical extent and time variations behave in the same manner as the polar-cap absorption. The glow is excited at heights below 100 km by protons in the energy range 0.5 to 100 Mev. It is estimated that the energy of the incoming protons exceeds 2×10^{13} ev/cm² col sec. There appear to be relatively few protons with energies below 1 Mev and the maximum particle flux of about 10^7 protons/cm² col sec is in the energy range of 1 to 10 Mev.

1. INTRODUCTION

An extensive auroral glow which covers the whole sky in polar regions during a polar-cap absorption event has been observed by Sandford.¹ The time variations of the intensity of this glow correlate closely with the variations in cosmic-noise absorption, measured at a frequency of 30 Mcps but the correlation with the intensity of the magnetic disturbance is not as close. Data has been collected from a number of stations in an attempt to discover the origin and extent of this type of aurora.

The auroral spectra have been obtained from patrol spectrographs operated in 1959 and 1960 by the Air Force Cambridge Research Laboratories, the University of Saskatchewan, the University of Chicago, Cornell University, and the New Zealand Dominion Physical Laboratory. The zenith intensities of the spectral emissions have been determined by the methods previously described by Sandford.^{2,3}

* Published as Arctic Institute of North America Research Paper No. 18 and in J. Atmos. Terr. Phys., in press (1962).

[†] On special leave from Dominion Physical Laboratory Auroral Station, Omakau, New Zealand.

During the great solar flare events there were often periods when the sky was overcast making it necessary to measure spectra recorded during cloudy weather in order to obtain sufficient data. Clouds do not reduce the measured intensities by any significant amount. During some nights of variable cloudiness, the recorded intensity of the auroral emissions did not increase during the clear periods. In cloudy weather, the sky light will be integrated by scattering in the cloud. The reduction of the zenith brightness (zenith angle $< 20^\circ$) by the cloud obscuration appears to be approximately compensated for by scattering of light originating at large zenith angles. This is true only if the sky is covered by an extensive and fairly uniform glow, the very condition being observed here.

2. THE POLAR CAP ABSORPTION EVENT

Some flares on the sun give rise to large fluxes of solar cosmic rays that cause disturbances of the earth's upper atmosphere. One type of event, generally called the polar cap absorption event, has been described by Bailey,⁴ Reid and Leinbach,⁵ Collins, Jelly and Matthews,⁶ Obayashi and Hakura,⁷ Reid and Collins⁸ and Warwick and Wood.⁹ In these events, energetic solar cosmic rays cause high absorption of radio frequencies over the polar regions (geomagnetic latitude $> 60^\circ$), ionosondes (1 to 25 Mcps) show blackout conditions, and riometers show very high absorption of cosmic noise at 30 Mcps.

These effects begin within a few hours after the flare on the sun has been observed and they are accompanied, within about forty-eight hours, by a large geomagnetic storm with extensive auroral displays. The polar cap absorption effects are observed for three or four days following the solar flare, whereas, the geomagnetic storm and visual aurora last only for a day or so after the sudden commencement of the geomagnetic storm.

During the main phase of the geomagnetic storm, an intense visual aurora is observed in the auroral and subauroral zones. In the polar-cap region, aurora is commonly not observed during the magnetic storm. Anderson¹⁰ has reported that no aurora is observed that can be associated

with polar cap absorption behavior. The author, who made visual observations during the July 1959 storms at Scott Base, Antarctica, saw no discrete aurora during the main phase of the magnetic storm on July 15 except some very faint isolated rays. On July 11 and 17, some active aurorae were observed during only a short period of the main phase of the magnetic storms. Feldshtein¹¹ reported similar behavior of aurorae at the south geomagnetic pole during these storms.

The observations reported here indicate that an extensive auroral emission does occur. The term 'polar-glow aurora' will be used to describe this phenomenon which manifests itself as a uniform glow. During the peak of the storm, the polar-glow aurora reaches such a brightness that observation of the Milky Way is difficult. Extensive but faint pinkish glows have been reported during these events by Hatherton and Midwinter.¹² Color photographs of the night sky taken with an all-sky camera by Sandford,¹³ also show significant changes in the night-sky brightness during such storms. The glow is so uniform over the whole sky that it is not possible, unless the sky appears colored, for an observer to say for certain there is aurora. Spectroscopic evidence indicates that there is intense auroral emission throughout these events, even though there has been an absence of discrete visual aurora. The brightest feature of the polar-glow auroral spectrum (in the visible region) is the first negative bands of ionized molecular nitrogen.

In July 1959, three polar-cap absorption events occurred following flares on the sun on the 10th, 14th, and 16th of July. Some observations of geophysical phenomena during the period 7 to 23 of July are displayed in Fig. 1. The zenith intensity (logarithmic scale) of the 0-0 first negative band of ionized molecular nitrogen at 3914A and the zenith intensity of the atomic oxygen line at 5577A observed at Scott Base, Antarctica, (geomagnetic latitude 79° S), are shown in a time sequence. The cosmic-noise absorption measured by a 27.6 Mcps riometer at Thule, Greenland, (geomagnetic latitude 88° N) has been taken from data reported by Leinbach and Reid.¹⁴ These are typical stations in the polar-cap region. It should

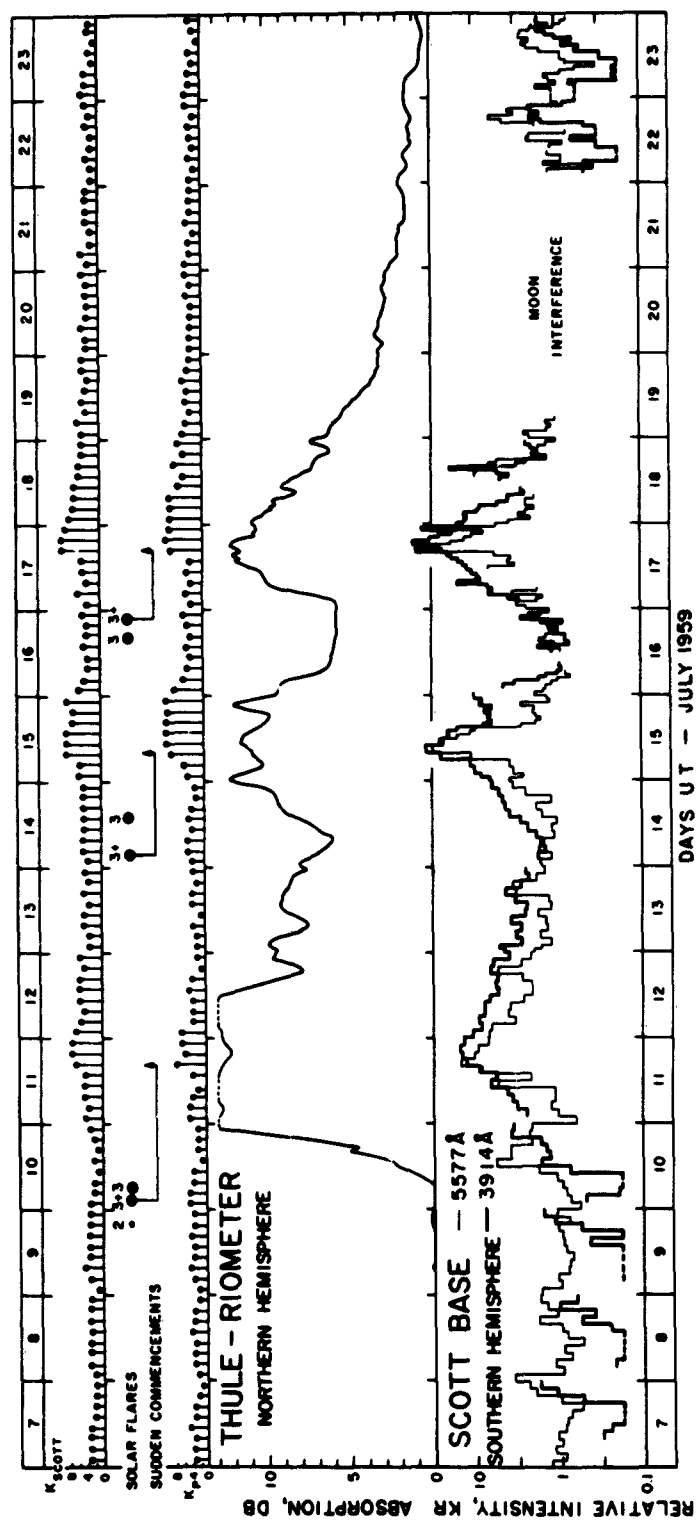


FIG. 1. Solar flare, magnetic, cosmic noise absorption (Leinbach and Reid, 14) and zenith auroral emission data during 7 to 23 July 1959.

be noted that Scott Base is a southern hemisphere station and that Thule is a northern hemisphere station. No riometer records were available from Antarctica.

The planetary magnetic K_p index, the Scott Base magnetic K index, the times of onset of the major flares and the times of the magnetic storm sudden commencements are also shown.

About four hours after a 3+ solar flare began at 0210 UT on July 10, the Thule riometer showed a large increase in cosmic-noise absorption. About eight hours after the flare, the intensity of 3914A began to increase at Scott Base. A similar effect occurred following the flares on July 14 and 16. The Universal Time of the onset of the flares (Shapley and Trotter, ¹⁵), of the start of the cosmic-noise absorption (Leinbach and Reid, ¹⁴), of the start of the increase in intensity at 3914A and of the sudden commencement, SC, of the geomagnetic storm (Bartels, ¹⁶), are given in Table 1. The delay times to the nearest hour, ($\Delta A, \Delta Q, \Delta SC$), between the onset of the solar flare and the onset of the associated terrestrial effects are also listed.

TABLE 1.

Flare Onset Date - UT		Cosmic-Noise Absorption Onset UT ΔA , Hours		3914 Intensity Onset UT ΔQ , Hours		Sudden Commencement UT ΔSC , Hours	
July 10	0210	0700	5	1000	8	11 1625	38
14	0319	0700	4	0700	4	15 0803	29
16	1604	2250	7	1700	1	17 1638	25
16	2118	2250	2	1700	-4	17 1638	19

Two flares were observed on July 16. Shapley and Trotter¹⁵ report that both were associated with Type IV radio noise and other radio effects commonly associated with flares that give rise to major geophysical disturbances. The increase of the 3914A emission started before the second of these flares, suggesting that the first flare at 1604 UT may have been more important than Shapley and Trotter suggest. The cosmic-noise

absorption did not increase until some hours after the second flare, leaving the question in some doubt. It must be remembered that the optical data is from the southern hemisphere and the radio data is from the northern hemisphere.

The intensity of the 3914A emission in each of these events increased steadily from the time of onset, reaching a peak close to the time of the sudden commencement of the magnetic storm. The intensity was then at least one hundred times greater than the normal nighttime minimum of an undisturbed period. At this time it was the brightest feature in the visible region auroral spectrum. The 3914A emission then decayed steadily over a period of forty-eight hours or more. With a time resolution of one hour the polar-glow aurora exhibited no large fluctuations, but there may have been large fluctuations on a shorter time scale.

The variations of the cosmic-noise absorption behaved in a manner very similar to the intensity variations of the 3914A emission although the points of observation were nearly antipodal. At Thule, there was continuous daylight during this observation period, thus day-night variations were not observed. (Reid and Collins,⁸ show that after sunset in the ionosphere, cosmic-noise absorption is greatly reduced, probably due to electron removal in the D region by negative-ion formation.) The 3914A emission is measured during nighttime and shows no twilight variations during the polar-glow aurora (resonant scattering of sunlight might be expected). It is interesting to find that the nighttime intensity of the 3914A emission in one hemisphere is closely related to the daytime cosmic-noise absorption in the other hemisphere. This suggests that the origin of the cosmic-noise absorption and of the polar-glow aurora are very closely related.

Intensity measurements at 3914A, made during the polar-glow aurora when moonlight did not interfere with observations (1000 UT July 10 to 0800 UT July 18, 1959), compared with the Scott Base magnetic K index (Fig. 2) gave a correlation coefficient of 0.77. The polar-cap absorption

events are always accompanied by large magnetic storms. Since the peak of the polar-glow aurora occurs during the main phase of the magnetic storm, the glows have been thought to be directly connected with the magnetic disturbance. The high degree of correlation is somewhat misleading. At low K indices, a very large scatter is evident (Fig. 2). From the time of onset of the flare until the time of the sudden commencement, the K index remains low while the polar-glow aurora increases steadily so that there is actually a low correlation during this particular period of the storm. Since the polar-glow aurora starts soon after the flare and lasts for three or more days, it is evident that the relationship between auroral emissions, magnetic storms and polar-cap events requires a more careful investigation.

A comparison of the intensities of the atomic oxygen 5577A (Fig. 1) and 6300A emissions and the magnetic activity showed that even in the absence of discrete visual aurora there were large enhancements of the 5577A and 6300A emissions during the main phase of the magnetic storm. These emissions also exhibit then a type of glow aurora, but only during the magnetic storm. This suggests that different particles excite these emissions. This difference may only be one of incident particle energy however. On the other hand, there was only a small correlation during the polar-glow aurora between the intensity at 3914A and the intensities at 6300A (correlation coef. is 0.5) and 5577A (correlation coef. is 0.4). Visual inspection of the curves in Fig. 1 suggests a possible small variation of the 5577A emission that follows the 3914A behavior but there is insufficient data to show that this has any statistical significance.

3. EXTENT OF THE POLAR-GLOW AURORA

From a station in the polar region, the polar-glow aurora is seen as a glow covering the whole sky. On a global scale it has been possible to estimate the extent of the polar-glow aurora from a study of auroral patrol spectrograms taken at Canadian and U.S. stations during the November 1960 solar-flare events.

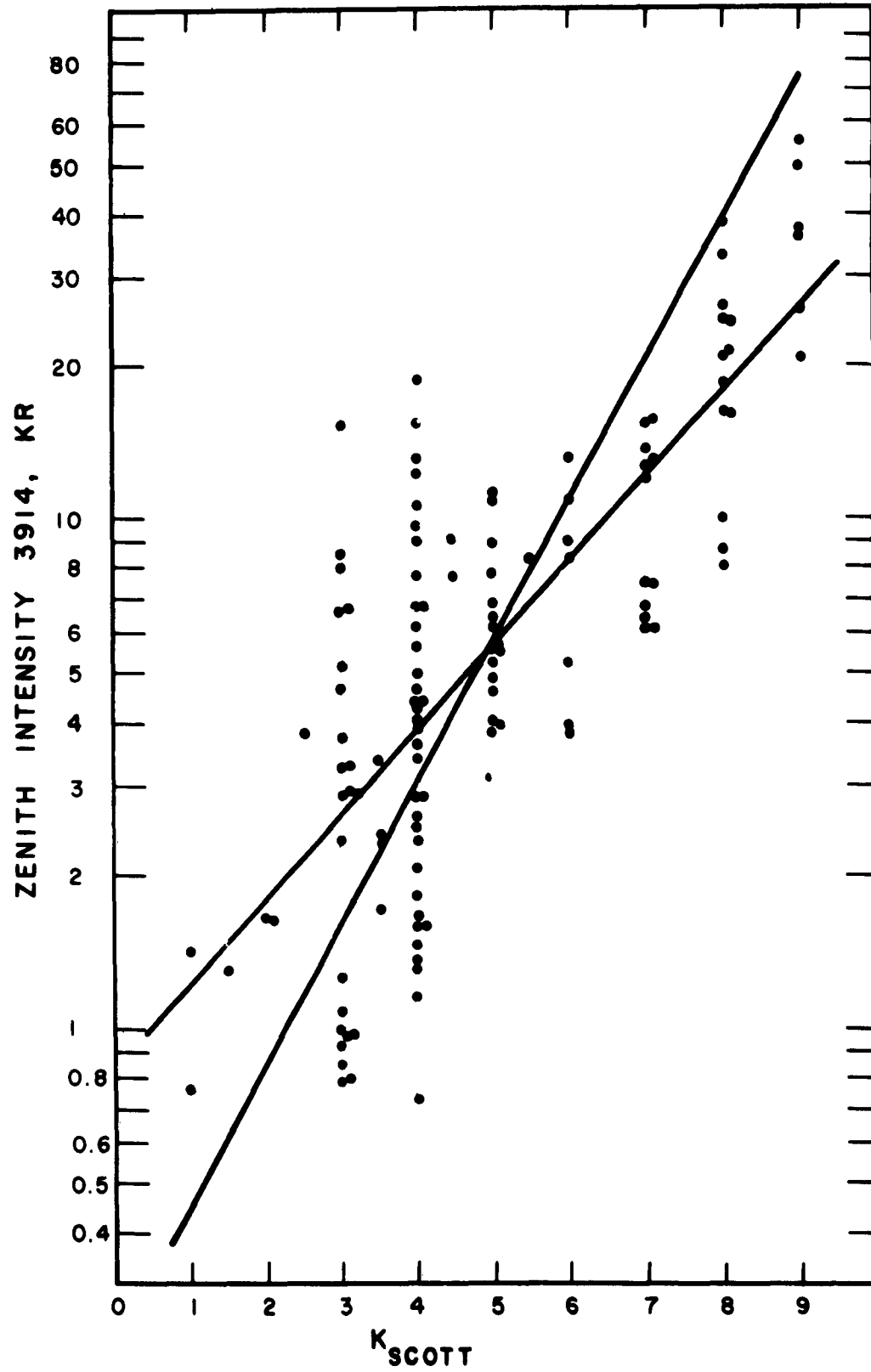


FIG. 2. Intensity of 3914A emission versus Scott Base magnetic K index from 1000 UT 10 July to 0800 UT 18 July 1959. The regression lines are shown. Correlation coefficient is 0.77.

In Fig. 3, the zenith intensity (logarithmic scale) of the 3914A emission has been plotted for the period 10 to 20 November 1960 for five stations; Thule (geomagnetic latitude, $\varphi = 88^\circ$), Meanook ($\varphi = 62^\circ$), Saskatoon ($\varphi = 60^\circ$), Ithaca ($\varphi = 54^\circ$), and Yerkes ($\varphi = 53^\circ$). At some stations, many exposures lasted for a few hours. Dotted lines indicate that the intensity was less than the level shown. The onset times of major solar flares and magnetic storm sudden commencements are also shown. The positions of the stations are shown in Fig. 4.

At Thule, a station well inside the auroral zone, the behavior was similar to that already discussed for the July events. On the 12th of November, a sudden commencement not associated with polar-cap absorption and a flare that caused a polar-cap event occurred together, causing some confusion.

The intensity of the 3914A emission increased rapidly a few hours after the 3+ solar flares on the 12th and 15th of November. A maximum was reached about the time of the sudden commencement of the associated magnetic storm and the intensity then decreased uniformly over a period of about 48 hours.

At Meanook, a station close to the maximum of the auroral zone, the nighttime level of the 3914A emission is very often high due to the common occurrence of discrete auroral forms. On the 11th of November, a moderate magnetic disturbance was associated with a higher than usual level of 3914A emission.

During the solar-flare events, the intensity of 3914A at Meanook, appears to follow fairly closely the behavior observed at Thule. The onset of the second storm on the 15th was particularly marked at Meanook. On the 16th, the level remained high throughout the night while it decreased at Thule. During this time, the magnetic activity was very high. In the auroral zone, bright aurorae are always observed during major magnetic storms, thus, a high proportion of the 3914A emission can be expected to originate from discrete auroral forms. On the nights of the 14th and 17th the magnetic storms had ended and the minimum intensity at 3914A followed the behavior at Thule.

At Saskatoon, only 1.3° of magnetic latitude south of Meanook, the

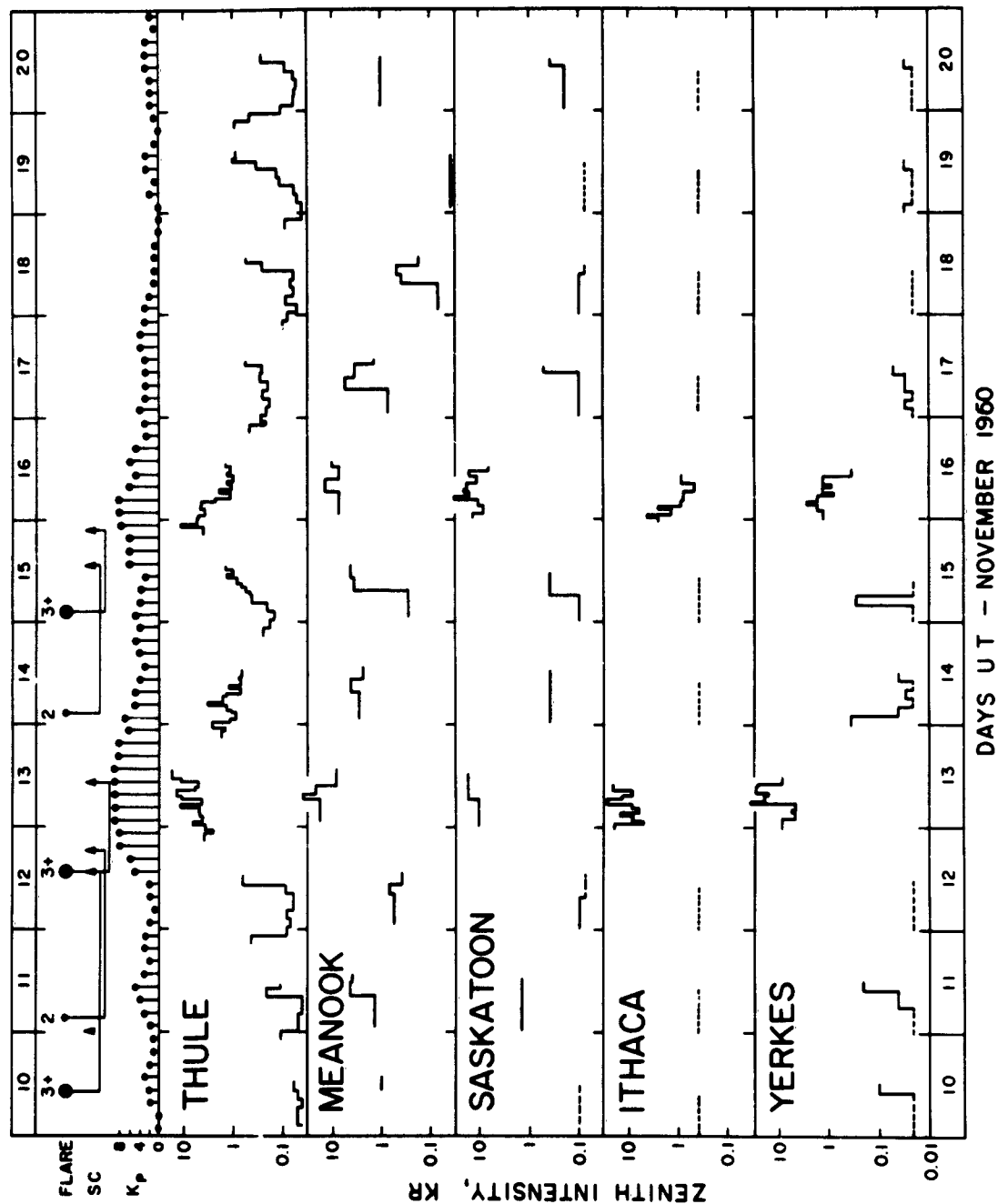


FIG. 3. Zenith intensity of 3914A emission at Thule, Meanook, Saskatoon, Ithaca and Yerkes and solar flare and magnetic data from 10 to 20 November 1960.



FIG. 4. Location of stations.

polar-glow aurora was present but it was much weaker than it was at Meanook. The intensity was much less, particularly on the 14th and 17th, than it was at Meanook. These observations suggest that the polar-glow aurora cuts off very sharply at a geomagnetic latitude of about 60° . Radio observations of the polar-cap absorption, by Reid and Leinbach,⁵ Collins, Jelly and Matthews⁶ and Nagata, Hakura and Goh,¹⁷ also indicate a very sharp cutoff at a geomagnetic latitude of about 60° . The polar-cap absorption and the polar-glow aurora appear to be very similar in geographical extent.

At both Yerkes and Ithaca, well south of the auroral zone, no polar-glow aurora was evident. Here the intensity at 3914A was high only during the main phase of the magnetic storm. Great auroral displays were observed on these nights and it is probable that all the 3914A emission at these latitudes originated from the discrete visual aurorae. During the main phase of the magnetic storms in these solar-flare events, Winckler and Bhavsar,¹⁸ Winckler, Bhavsar and Peterson,¹⁹ Freier, Ney and Winckler²⁰ and Ehmert. Erbe, Pfozter, Anger and Brown,²¹ have shown with balloon observations that energetic solar protons can penetrate down to balloon altitudes at geomagnetic latitudes as low as 52° . They think this happens because of distortions in the earth's magnetic field. In such cases polar-glow aurora would be expected at low latitudes during the main phase of the magnetic storm. It is possible, therefore, that some of the 3914A emission at Yerkes and Ithaca was due to a polar-glow auroral type of emission.

4. HEIGHT AND ORIGIN

In an earlier note, Sandford¹ suggested that the region emitting the polar-glow aurora is at or below a height of 100 km. This idea was based on the following evidence:

a) The high degree of ionization of the D region, indicating that energetic particles are present below 100 km. This is further supported by the evidence already presented showing the close similarity between the intensity variation of the polar-glow aurora and the intensity of the

cosmic-noise absorption. The latter is caused by an increase in the electron density and possibly an increase in electron-collision frequency, at D-region heights (Reid and Leinbach,⁵).

b) The lack of a twilight enhancement of the first negative band of ionized molecular nitrogen when the sun illuminates the atmosphere down to heights of 100 km in the zenith (including a screening height of 20 km, Chamberlain,²²).

c) The intensities from the metastable transitions are relatively low and their intensities do not exhibit steady changes over a period of days as the polar-glow aurora does. Below 100 km these emissions would be reduced in intensity relative to those of the normal visual aurora (above 100 km) because of collisional deactivation.

Because the polar-glow aurora is very extensive it would be difficult to obtain height measurements by triangulation techniques.

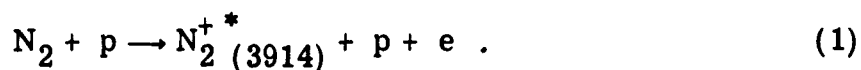
Delays as short as one hour between the onset of the solar flare and the onset of the polar-glow aurora, indicate that proton energies of at least 1 Mev are in part responsible. From cosmic-noise absorption measurements, (Reid and Leinbach,⁵) ionosonde measurements, (Gregory,²³) and balloon observations of solar cosmic rays, (Anderson and Enemark,²⁴; Anderson, Arnoldy, Hoffman, Peterson and Winckler,²⁵) it is known that protons with energies greater than 1 Mev enter the polar regions throughout the polar-cap absorption events. These protons will efficiently ionize and excite molecular nitrogen below heights of 100 km. Anderson and Enemark²⁴ have observed 100 Mev protons arriving up to nine days after a major solar flare so that the time delay between the flare and the time of arrival at the earth cannot be used as an accurate measure of the incident particle energy.

The lack of evidence of polar-glow aurora above 100 km suggests that solar proton energies greater than about 500 kev are responsible for the polar glow. The steep slope of the particle flux vs. energy spectrum measured by Anderson and Enemark²⁴ and others, indicates that solar protons with energies less than 100 Mev are primarily responsible

for the polar glow. It will, therefore, be assumed that the polar-glow aurora is caused by solar protons with energies between 0.5 and 100 Mev.

In this paper, interest is confined to the ionization and excitation of molecular nitrogen to the 0-0 band of N_2^+ . The ionization and excitation will occur at the time of the collision in a single process (Sheridan et al., ²⁶). As this excited state is an allowed transition, the 3914A quanta will be emitted almost instantaneously and the 3914A intensity will be a measure of the primary energy flux.

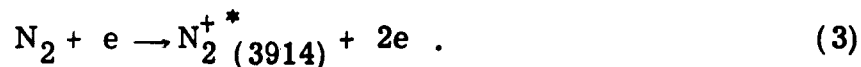
While the proton energy is above 100 kev the main reaction with molecular nitrogen will be;



Once the energy of the proton falls below 100 kev the charge exchange reaction will become important;



The secondary electrons from reaction (1) will produce further ionizations and excitations;



Some of the electrons from this reaction will carry enough energy to produce further ionizations by the same reaction. From the theoretical calculations of Bates, McDowell and Omholt²⁷ and from the experimental data in the Landolt-Börnstein Tables²⁸ it is shown that about two-thirds of the ionization and excitation is produced by reaction (3). As the major proportion of the excitation is produced by electrons the spectra will be predominately that of electron excitation rather than that of proton excitation.

In cosmic-noise-absorption measurements, the absorption is caused by the electrons produced in reactions like (1) and (3). The amount of the absorption depends on the equilibrium between electron production,

recombination and negative-ion formation. At nighttime, negative-ion formation is expected to be important (Reid and Collins,⁸). The cosmic-noise absorption is, therefore, not such a direct indication of the primary energy flux at nighttime as is the intensity of 3914A emission.

5. ENERGY AND PARTICLE FLUX OF PROTONS

If the absolute intensity of the 3914A emission can be measured it is then possible to estimate the total energy of the primary particles.

The mean absolute zenith intensity of the 5577A line was measured by Roach, McCaulley, Marovich and Purdy²⁹ for a series of stations over a wide range of geomagnetic latitudes in North America from 1957 to 1959. The mean relative zenith intensity of the 5577A line was determined, from the auroral patrol spectrographs, for a number of days before and after the November 1960 events. This data was fitted to the Roach et al.²⁹ data shown in Fig. 5. The intensity variation with geomagnetic latitude is the same for both.

These observations were all made during the sunspot maximum period. It seems reasonable to assume that the mean intensity during November 1960 is the same as it was during the period from 1957 to 1959. This comparison, therefore, was used as a calibration of the auroral patrol spectrographs. With the absolute intensity of the 5577A emission established, it is a relatively simple matter to determine the intensity of the 3914A emission. The intensity scales used in Figs. 1 and 3 have been derived in this way.

In all five events shown in Figs. 1 and 3, the zenith intensity of the 3914A band exceeds 10 kilorayleighs at the maximum of the polar-glow aurora. From a method drawn to attention by Dalgarno³⁰ the total energy of the incoming protons can be calculated if the ratio of the total cross section of ionization of N_2 , to the cross section for the ionization and excitation to the 0-0 first negative band of N_2^+ , by protons and electrons is known.

Cross sections for both these reactions have not been measured for incident proton energies in the range of 1 Mev or greater. Hooper,

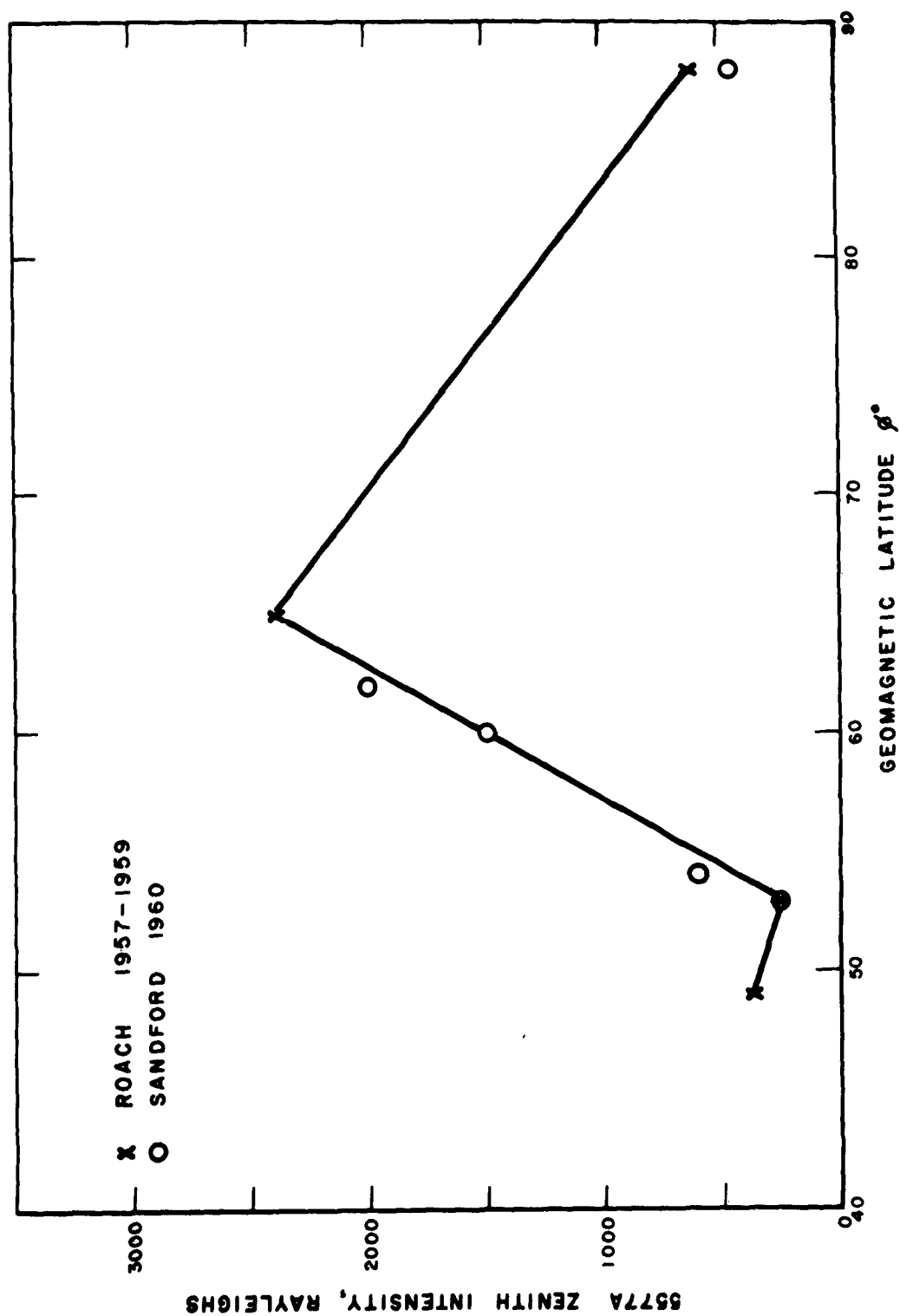


FIG. 5. The mean zenith intensity of 5577A emission vs. geomagnetic latitude from stations in this report, fitted to absolute zenith intensity measurements of 5577A reported by Roach, McCauley, Marovich and Purdy.²⁹

McDaniel, Martin and Harmer³¹ and others have shown that for proton energies above 100 kev, the cross sections for these reactions are identical for protons and electrons of the same velocity.

In order to obtain values for the reaction cross sections, it is necessary to assume values for the proton and electron energies. It has been estimated that the proton energies are between 0.5 and 100 Mev. The flux density at the lower energies is expected to be higher (Obayashi and Hakura,⁷) therefore a mean proton energy of 1 Mev is a reasonable figure. It is a little difficult to know the mean secondary electron energy. It will be assumed that the proton velocity equals the secondary electron velocity, thus the mean electron energy will be assumed to be 570 ev. This will give electron cross sections of the correct order of magnitude and greatly simplify calculations because the electron and proton cross sections will be identical. (For electrons with energies between 50 and 600 ev the cross section changes only by a factor of two.)

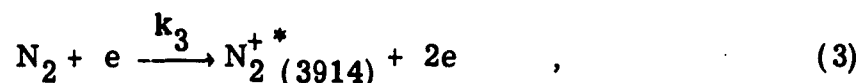
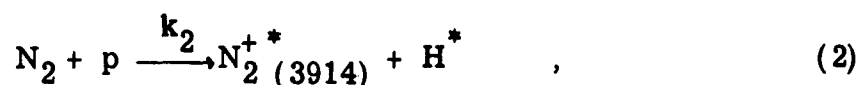
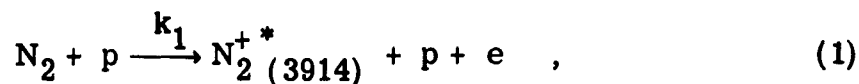
The total cross section for ionization of N_2 by electrons has been determined by Tate and Smith.³² The cross section for the ionization and excitation of the 0-0 first negative band of N_2^+ by electrons has been determined by Sheridan, Oldenberg and Carleton.²⁶ The ratio of these cross sections for electrons at 570 ev, and, therefore, for protons at 1 Mev, equals 50, thus, for every 50 ion pairs produced in N_2 , only one will be excited to the 0-0 first negative band of N_2^+ .

In the height range of 30 to 100 km, the oxygen molecule comprises about 20 percent of the atmosphere and the cross section for ionization by protons and electrons is nearly the same as for nitrogen (Hooper et al.³¹). The ratio of cross sections of total ionization to excitation of the 3914A band in the atmosphere will, therefore, be nearer to 60.

Assuming the intensity of the 3914A emission to be 10 kilorayleighs at the maximum of the polar-glow aurora, then there are 10^{10} quanta emitted at 3914A/cm² col sec. For each quantum emitted 60 ion pairs are produced, therefore, the total number of ion pairs produced is 6×10^{11} ion pairs/cm² col sec. Valentine and Curran³³ and others show

that the amount of energy necessary to produce an ion pair (assuming only ionization, excitation, and elastic scattering) is about 35 ev, this being independent of the energy or type of the ionizing particle. The total energy flux is, therefore, 2×10^{13} ev/cm² col sec.

Using a different approach it is possible to determine the particle flux. The emission of 3914A quanta will almost entirely originate from the following reactions:



where k_1 , k_2 , k_3 are the reaction rates.

The rate of production of N_2^{+*} molecules excited to the 0-0 level of the first negative band is

$$\begin{aligned} \frac{d[N_2^{+*} (3914)]}{dt} &= k_1 [N_2] [p] + k_2 [N_2] [p] + k_3 [N_2] [e] \\ &= (k_1 + k_2) [N_2] [p] + k_3 [N_2] [e] \end{aligned}$$

where $[N_2]$ is the density of the nitrogen molecules,
 $[p]$ is the density of the energetic protons,
 $[e]$ is the density of the energetic electrons.

As before it will be assumed that the incident flux is all protons of 1 Mev and that all secondary electrons have an energy of 570 ev. Since the proton energies are much greater than 100 kev the charge exchange reaction is relatively unimportant (Chamberlain,³⁴), that is,

$$k_2 \ll k_1.$$

In the basic assumptions used here, the cross section for reactions (1) and (3) are the same and two-thirds of the ions are produced by reaction (3). Since the mean energy expended in production of ion pairs by electrons and protons is the same, the effective density of the energetic secondary electrons will be twice the proton density,

$$2 [p] = [e] ,$$

then

$$\frac{d[N_2^{+*}(3914)]}{dt} = (k_1 + 2k_3) [N_2] [p] .$$

The intensity Q of the 3914A emission, expressed in number of quanta emitted, is given by

$$\begin{aligned} Q &= \int_h \frac{d[N_2^{+*}(3914)]}{dt} dh \\ &= \int_h (k_1 + 2k_3) [N_2] [p] dh , \end{aligned}$$

with the integration taken vertically along a column of 1 cm^2 section and of length h .

Protons with primary energies in the range 0.5 to 100 Mev lose 90 percent of their energy in the last 10 km or less of their path into the atmosphere. It has been assumed that the protons are monoenergetic with 1 Mev energy and it will be assumed that all their energy is lost in a uniform thin layer of thickness, Δh , equal to 10 km.

Then

$$Q = (k_1 + 2k_3) [N_2] [p] \Delta h.$$

The reaction rates k_1 and k_3 are defined as

$$\begin{aligned} k_1 &= \int \sigma_1 v_1 f(v_1) dv , \\ k_3 &= \int \sigma_3 v_3 f(v_3) dv , \end{aligned}$$

where σ_1 and σ_3 are the cross sections for reaction (1) and (3), v is the velocity of the exciting particle, and $f(v)$ is the velocity distribution of

the exciting particles. Since the primaries are monoenergetic $\int f(v)dv$ has a value of unity. The velocity of the secondary electrons is assumed equal to that of the incident protons, therefore, we can consider,

$$\sigma_1 = \sigma_3 = \sigma$$

and

$$v_1 = v_3 = v$$

then

$$k_1 = k_3 = \sigma v$$

Also

$$[p] = \frac{\Phi}{v}$$

where Φ is the proton flux/area col sec and v is the proton velocity.

Then

$$\begin{aligned} Q &= 3\sigma v \frac{\Phi}{v} [N_2] \Delta h \\ &= 3\sigma \Phi [N_2] \Delta h \end{aligned}$$

Therefore, the proton flux

$$\Phi = \frac{Q}{3\sigma [N_2] \Delta h}$$

The intensity of the 3914A emission is 10kR. The 1 Mev protons will be stopped at a height of about 90 km (Bailey,⁴) where the density of N_2 is 3.5×10^{13} molecules/cc (Chamberlain,³⁵). The cross section for 1 Mev protons equals the cross section for 570 ev electrons which equals $3 \times 10^{-18} \text{ cm}^2$ (Sheridan et al.,²⁶). The layer thickness is 10 km. Then

$$\Phi_{1\text{Mev}} \approx 3 \times 10^7 \text{ protons/cm}^2 \text{ col sec.}$$

If instead it is assumed that the proton energy is 0.1 Mev and 10 Mev respectively, assuming the secondary electron velocity equals the proton velocity and taking the appropriate values for the nitrogen density and the cross sections then

$$\Phi_{0.1 \text{ Mev}} \approx 8 \times 10^7 \text{ protons/cm}^2 \text{ col sec.}$$

and

$$\Phi_{10 \text{ Mev}} \approx 2 \times 10^6 \text{ protons/cm}^2 \text{ col sec.}$$

Because the ionosphere is in a disturbed state in these storms and because the atmospheric density varies considerably with height, the flux determined above can be considered as only an indication of the order of magnitude. It is, however, in good agreement with the values given by Obayashi and Hakura.⁷ Although it is slightly higher than their figures, it is not unreasonable when one realizes that the flux near the peak of the storm is being considered here.

The total energy flux was found to be 2×10^{13} ev/cm² col sec. If the mean proton energy is taken as 1 Mev this gives a flux of 2×10^7 protons/cm² col sec, in very good agreement with the figure of 3×10^7 protons/cm² col sec already determined.

A proton loses about 90 percent of its energy in the last 10 km of its path for stopping heights between 50 and 110 km. The intensity of the emission at 3914A is proportional to the incident particle flux. It should, thus, be possible to obtain the energy spectrum of the incoming solar cosmic rays in polar cap absorption events by measuring the intensity of the 3914A emission as a function of height with the use of rockets.

If large proton fluxes are entering the atmosphere, hydrogen lines are to be expected in the auroral spectra. The H β line will be considered as it is usually easier to observe in polar-glow aurora because the H α line is often hidden by the first positive bands of N₂.

The charge exchange reaction (2) becomes important with protons near the end of their range when their energy has dropped below 100 kev. For proton energies greater than 100 kev, Omholt³⁶ and Chamberlain^{34, 37} have shown that there will be 16 quanta of H β produced by every primary proton, independent of their initial energy. For the proton-flux values calculated earlier assuming primary proton energies of 0.1, 1 and 10 Mev, the intensity of H β has been determined and is tabulated in Table 2.

The minimum sensitivity of the patrol spectrographs varies somewhat, because it is particularly dependent on film processing techniques and on the presence of moonlight in the spectra. In good conditions, the spectrographs as used in these experiments can detect lines with an intensity of about 50 R.

In the polar-glow aurora $H\beta$ is usually visible although it is often very weak ($<100R$). The number of protons with energies of 100 kev or less, that would stop at visual-auroral heights must be relatively small or else $H\beta$ would be very much brighter. A flux of 3×10^6 protons/cm² col sec, with an energy of 100 kev will give a just detectable $H\beta$ line with an intensity of 50 R; this flux is 25 times less than that determined in Table 2. It must be assumed that either the mean proton energies are greater than 5 Mev, consistent with previous assumptions in this paper, or a significant portion of the primary energy is not carried by protons.

TABLE 2.

Proton Energy	Flux, Protons/cm ² Sec	$H\beta$ Intensity Rayleighs
0.1 Mev	8×10^7	1300
1. Mev	3×10^7	480
10. Mev	2×10^6	32

During November 13, 1960, Montalbetti and McEwen³⁸ made zenith intensity measurements of $H\beta$ at Churchill, Canada (geomagnetic latitude $\phi = 69^\circ$). These measurements are compared in Fig. 6 with the intensity of the 3914A emission measured at Thule during the same night. As these stations are very far apart (Fig. 4) detailed agreement between these observations would seem surprising. The fact that the $H\beta$ and 3914A emissions do agree in broad detail suggests that the $H\beta$ is closely associated with the polar-glow aurora, which does extend over the whole of the polar regions.

In Fig. 6 it can be seen that an intensity of 15kR at 3914A corresponds to an intensity of about 200R for $H\beta$ emission. This is consistent with a flux of protons with a mean energy of about 4 Mev agreeing favorably with the value determined above.

The absence of visual aurora over the polar cap, the intensity of the hydrogen lines and the height determinations of the polar-glow aurora, all suggest an absence of protons with energies less than 100 kev relative

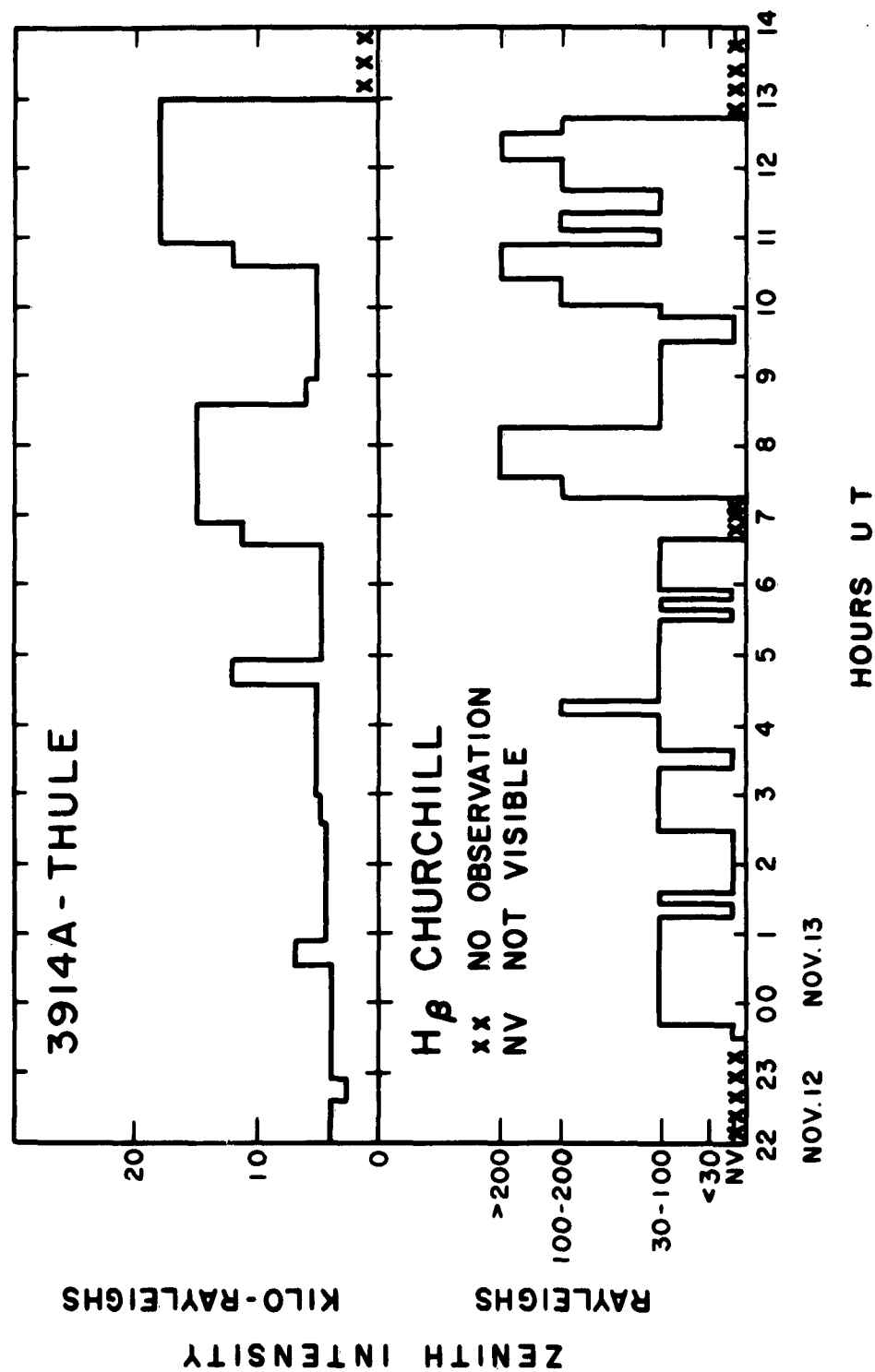


FIG. 6. The zenith intensity of 3914A emission at Thule and the zenith intensity of H β at Churchill (Montalbetti and McEwen, 38) during the night of November 12-13, 1960.

to the number with energies between 1 to 10 Mev in the polar cap absorption events. On the other hand, the proton flux determined at an energy of 1 Mev is in agreement with other workers (Obayashi and Hakura,⁷). If the proton fluxes at energies below 100 kev, estimated by Obayashi and Hakura⁷ did arrive in the polar regions, very intense hydrogen spectra would be expected. The absence of intense hydrogen spectral emission in the auroral and subauroral zones, where intense visual aurorae are observed during the peak of the storm, is consistent with the rocket observations of McIlwain³⁹ and Davis, Berg and Meredith⁴⁰ indicating visual aurora is primarily electron excited.

Bailey⁴ found that his experimental observations were best explained by a flux of protons with a differential energy spectrum which has a -5 power law for proton energies above 500 Mev and a -2 power law for energies less than 500 Mev. The work in this paper suggests that below 1 Mev the differential energy spectrum of the protons obeys a positive power law and that the maximum proton flux occurs at an energy between 1 and 10 Mev.

6. CONCLUSIONS

Solar flares that produce polar-cap absorption events also produce an extensive auroral glow which behaves like the polar-cap absorption event in time and geographical extent.

This polar-glow aurora begins several hours after the flare and reaches a peak intensity within about forty-eight hours, near the time of the sudden commencement of the associated magnetic disturbance. The emission then takes two or three days to return to normal nighttime levels. The increase to peak emission and the subsequent decay are very uniform, showing little fluctuation between spectra taken with one hour exposures.

The glow covers the polar-cap region down to a geomagnetic latitude of about 60° throughout the event and it may extend to geomagnetic latitudes of 50° during the main phase of the geomagnetic storm. Most of the emission originates below 100 km.

The polar-glow aurora shows no discrete structure. The brightest features in the visible spectrum are the first negative bands of ionized molecular nitrogen which are ionized and excited by the solar protons and secondary electrons. The intensity of the 3914A band is greater than 10 kilorayleighs at the maximum of the event.

The emission from the metastable transitions in the auroral spectrum does not show steady changes over a period of days as the polar-glow aurora does. The atomic oxygen lines at 6300A and 5577A are enhanced during the main phase of the magnetic storm, even in the absence of visual aurora, but their behavior is not the same as the 3914A emission.

The solar cosmic rays entering the polar regions are mostly protons with a maximum particle flux in the energy range of 1 to 10 Mev. There appear to be relatively few protons with energies less than 1 Mev. The great visual auroral displays observed during the main phase of the magnetic storm in the auroral and subauroral zones appear to be primarily electron excited.

During the peak of the event, the total energy flux of the arriving protons is greater than 2×10^{13} ev/cm² col sec. This corresponds to a flux of protons with a mean energy of 1 Mev, of 3×10^7 protons/cm² col sec.

ACKNOWLEDGMENTS

This work was sponsored by a National Science Foundation grant to the Arctic Institute of North America, grant 13841.

The major part of this work was carried out at the Ionospheric Physics Laboratory, Air Force Cambridge Research Laboratories, Hanscom Field, Bedford, Massachusetts.

The author wishes to gratefully acknowledge the advice and assistance of Mr. Norman J. Oliver and his staff at the Ionospheric Physics Laboratory, Air Force Cambridge Research Laboratories. He also wishes to thank Dr. A. Vallance Jones, Physics Department, University of Saskatchewan; Dr. C. Gartlein, IGY Data Center A, Cornell University, and Dr. C. Wallace, Yerkes Observatory, University of Chicago, for the loan of auroral spectrograms used in this work.

Thanks are expressed to Dr. S. Silverman, Dr. N. Carleton, Dr. T. Obayashi, and Dr. K. Champion for many useful discussions and ideas.

REFERENCES

1. B. P. SANDFORD, Nature, 190: 245, 1961.
2. B. P. SANDFORD, Ann. Geophys., 15: 445, 1959.
3. B. P. SANDFORD, J.A.T.P., 21: 182, 1961.
4. D. K. BAILEY, Proc. IRE, 47: 255, 1959.
5. G. C. REID, and H. LEINBACH, J.G.R., 64: 1801, 1959
6. C. COLLINS, D. H. JELLY and A. G. MATTHEWS, Can. J. Phys., 39: 35, 1961.
7. T. OBAYASHI and Y. HAKURA, Planet. Space Sci., 5: 59, 1961.
8. G. C. REID and C. COLLINS, J.A.T.P., 14: 63, 1959.
9. C. S. WARWICK and M. B. WOOD, Arkiv for Geofysik, 3: 457, 1961.
10. K. A. ANDERSON, Phys. Rev. Letters, 1: 335, 1958.
11. Ya. I. FELDSHTEIN, I.U.G.G. Monograph No. 7, Symposium on July 1959 Events, Helsinki, July 1960, p 126.
12. T. HATHERTON and G. G. MIDWINTER, J.G.R., 65: 1401, 1960.
13. B. P. SANDFORD, J.A.T.P., 21: 177, 1961.
14. H. LEINBACH and G. C. REID, I.U.G.G. Monograph No. 7, Symposium on July 1959 Events, Helsinki, July 1960, p 145.
15. A. H. SHAPLEY and D. TROTTER, I.U.G.G. Monograph No. 7, Symposium on July 1959 Events, Helsinki, July 1960, p 72.
16. J. BARTELS, I.U.G.G. Monograph No. 7, Symposium on July 1959 Events, Helsinki, July 1960, p 3.
17. T. NAGATA, Y. HAKURA and T. GOH, I.U.G.G. Monograph No. 7, Symposium on July 1959 Events, Helsinki, July 1960, p 135.
18. J. R. WINCKLER and P. D. BHAVSAR, J.G.R., 65: 2637, 1960.
19. J. R. WINCKLER, P. D. BHAVSAR and L. PETERSON, J.G.R., 66: 995, 1961.

REFERENCES (Contd)

20. P. S. FREIER, E. P. NEY and J. R. WINCKLER, J.G.R., 64: 685, 1959.
21. A. EHMERT, H. ERBE, G. PFOTZER, C. D. ANGER and R. R. BROWN, J.G.R., 65: 2685, 1960.
22. J. W. CHAMBERLAIN, Physics of Aurora and Airglow, Academic Press 1961, p 414.
23. J. B. GREGORY, J.G.R., 66: 2575, 1961.
24. K. A. ANDERSON and D. C. ENEMARK, J.G.R., 65: 2657, 1960.
25. K. A. ANDERSON, R. ARNOLDY, R. HOFFMAN, L. PETERSON, and J. R. WINCKLER, J.G.R., 64: 1133, 1959.
26. W. F. SHERIDAN, O. OLDENBERG and N. P. CARLETON, Abstract of Papers, 2nd. Int. Conf. on the Physics of Electronic and Atomic Collisions. W. A. Benjamin, Inc., New York, 1961, p 159.
27. D. R. BATES, M. R. C. McDOWELL and A. OMHOLT, J.A.T.P., 10: 51, 1957.
28. Landolt-Börnstein Tables, Springer-Verlag (1952) Vol. 1, Part 5, p 343.
29. F. E. ROACH, J. W. McCAULLEY, E. MAROVICH and C. M. PURDY, J.G.R., 65: 1503, 1960.
30. A. DALGARNO, (Private communication).
31. J. W. HOOPER, E. W. McDANIEL, D. W. MARTIN and D. S. HARMER, Abstract of Papers, 2nd. Int. Conf. on the Physics of Electronic and Atomic Collisions. W. A. Benjamin, Inc., New York, 1961, p 67.
32. J. T. TATE and P. T. SMITH, Phys. Rev., 39: 270, 1932.
33. J. M. VALENTINE and S. C. CURRAN, Rep. Progr. Phys., 21: 1, 1958.
34. J. W. CHAMBERLAIN, Astrophys. J., 120: 360, 1954.
35. J. W. CHAMBERLAIN, Physics of Aurora and Airglow, Academic Press 1961, p 576.

REFERENCES (Contd)

36. A. OMHOLT, Geofys. Publik, 20: No. 11, 1, 1959.
37. J. W. CHAMBERLAIN, Physics of Aurora and Airglow, Academic Press 1961, p 250.
38. R. MONTALBETTI and D. J. McEWEN, Can. J. Phys. , 39: 617, 1961.
39. C. E. McILWAIN, J.G.R. , 65: 2727, 1960.
40. L. R. DAVIS, O. E. BERG and L. H. MEREDITH, Kallman, Space Research, North Holland Pubshg. Co. , Amsterdam 1960, p 721.

IRREGULAR LUNAR REFLECTION POLARIZATION CHANGES NOTED IN THE PRESENCE OF AURORA*

J. Klobuchar, J. Aarons, H. Whitney, G. Kantor
ELECTRONICS RESEARCH DIRECTORATE
AIR FORCE CAMBRIDGE RESEARCH LABORATORIES
BEDFORD MASSACHUSETTS

ABSTRACT

Bistatic lunar reflection of 99.4-Mcps signals was used to determine the total integrated ionospheric electron density. On November 13, 1960, fast, irregular changes in the received signal polarization occurred during the time a visible aurora was observed along one leg of the bistatic path. After sunrise on the same day slow, regular Faraday polarization rotation was observed.

It is suggested that the ordinary and extraordinary ray components, which travel along slightly different paths, may have encountered small, high-velocity ionospheric irregularities, and thus have produced unusual signal phase changes.

On the mornings of November 11, 12, 13, and 14, 1960 a lunar reflection experiment was carried out between Jodrell Bank, England and Sagamore Hill, Hamilton, Massachusetts. The objective of the experiment was to determine the total integrated electron density for the two paths, particularly during sunrise at each site.

The hour angle difference between the sites is approximately $4\frac{1}{2}$ hours. Therefore, at the time of sunrise at Jodrell Bank, nighttime ionospheric conditions still exist at Sagamore Hill; and, at the time of sunrise at the Sagamore Hill station, substantially daytime conditions exist at Jodrell Bank. Analysis of the bistatic data to determine the total integrated electron density is being undertaken by G. N. Taylor at Jodrell Bank. A description of the Sagamore Hill data of November 13, 1960, showing unusual ionospheric effects, is presented here.

*Published in J. Geophys. Res., in press (Jan. 1962)

Pulses of 20 msec duration were transmitted from Jodrell Bank once each second on alternate frequencies of 99.4 and 100.6 Mcps. Linear transmitting polarization was used on a horizon-mounted 250-ft dish. Continuous FM interference made bistatic reception on 100.6 Mcps impossible. The Sagamore Hill receiver included two orthogonal, linearly polarized feeds on an equatorial mount. The feeds were positioned so that one was horizontal and the other vertical at meridian transit of the antenna. Although a slow change in received signal polarization occurred because of the differences in tracking systems, this change was small when compared with the rotation in signal polarization due to the changing electron density along the bistatic path.

On November 12, a typical record of regular Faraday polarization rotation for a normal ionosphere was obtained (see Fig. 1). In this figure, the vertical lines indicate the individual pulses; the fast fading of these pulses, which is well correlated on both polarizations, is due to the moon's apparent libration. Polarization fading was rapid at this time, reaching a maximum rate of about 11° per minute. This high rate of polarization rotation was due to a normal daytime increase in the integrated electron density along the Jodrell Bank leg of the bistatic path.¹ Ground sunrise at Jodrell Bank occurred at 0229 EST. The geomagnetic activity index K_p for the 0100-0400 EST interval on November 12, was 2, indicating a geomagnetically quiet period.

On November 13, magnetic-field variations were extremely high resulting in a K_p of 9 for the first five 3-hr periods of the day. The Sagamore Hill data from 0306 to approximately 0600 EST on November 13 showed fast, irregular fluctuations of signal strength on both polarizations (see Fig. 2). Reversals in the direction of rotation were difficult to determine but polarization changes as fast as 90° per minute were observed as compared with a maximum rate of rotation of 11° per minute on November 12. After 0600 EST slow, regular Faraday polarization rotation occurred until the end of the receiving period at 0728 EST.

During the early hours of November 13, the southern edge of the aurora extended to 48° north geomagnetic latitude.² The bistatic ray

penetrated the ionosphere through the aurora at a geomagnetic latitude of 53° (see Fig. 3). From 0306 EST (0806 UT) until approximately 0600 EST (1100 UT), the Sagamore Hill bistatic ray path was essentially in darkness with aurora present, while the Jodrell Bank ray path was sunlit with no aurora.¹ Thus, it would be expected that any unusual ionospheric effects would appear only in the bistatic data. Rapid fluctuations in polarization angle have also been noted at 400 Mcps during a previous auroral disturbance.³

On the following day, November 14, the magnetic field variations had essentially stopped. The bistatic lunar reflection data for that day showed typical Faraday polarization rotation indicating a normal increase in integrated electron density.

There are several possible explanations for the rapid polarization changes observed on November 13. One possibility is to ascribe them to changes in the magnetic field since the amount of polarization rotation is a function of the magnetic field intensity and direction and of the total number of electrons along the path. Even though the magnetic field strength variations were extremely high, they were, however, less than two percent of the total magnetic field. Unreasonably large changes in magnetic field direction would be required to produce the observed polarization fluctuations.

Changes in the total number of electrons along the path could also explain the rapid polarization changes. The total number of electrons along the monostatic path from Jodrell Bank to the moon was, however, extraordinarily low on November 13.¹ Hence, the total rotation angle of the polarization of the signal was small and it would take a large percentage of total electron changes to produce an additional ninety degrees of polarization rotation. In view of the low level of electron content, this does not seem feasible.

A more likely explanation depends on the fact that the ordinary and extraordinary waves constituting the received signal travel on slightly different paths because of the difference in refractive index. It has been

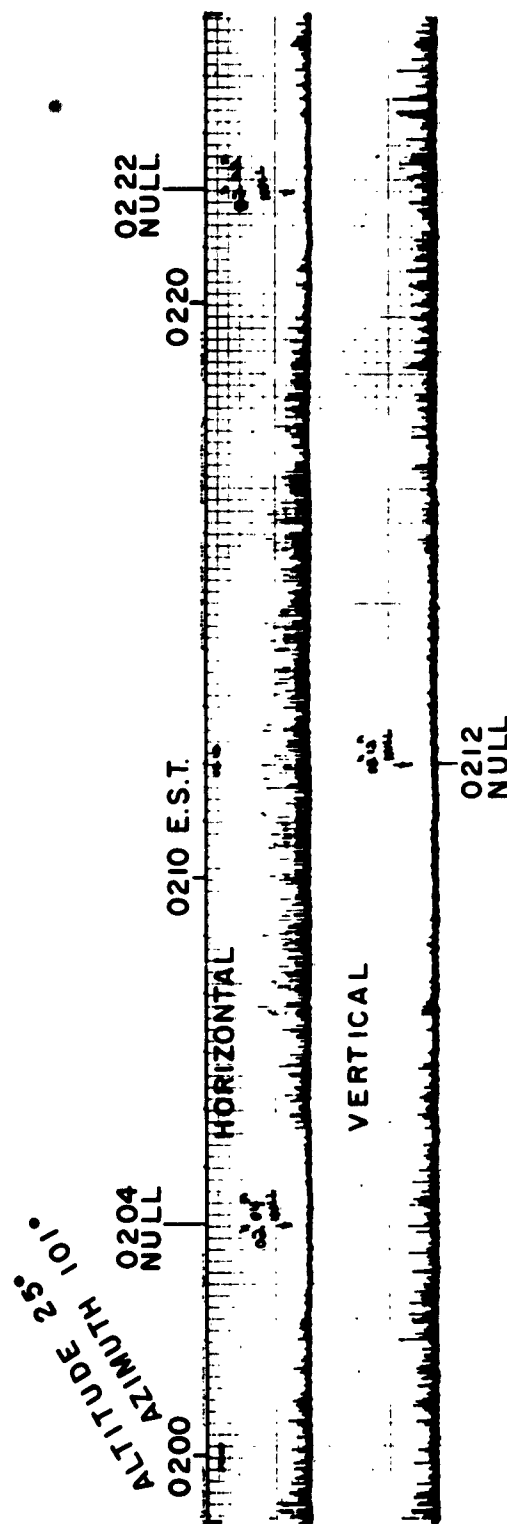
shown that drift velocities of ionospheric irregularities may increase from 100 meters per second to 1000 meters per second during geomagnetically disturbed periods.⁴ F. E. Roach and J. W. Warwick,⁵ in correlating fast scintillations with red auroral arcs, noted that the scale of irregularities was also small for this particular disturbed period. Because of the small scale of the irregularities and their increased velocity, the path differences of the two rays might be sufficiently great to account for the rapid signal phase changes. Thus, the fine scale of the irregularities could form a diffraction pattern, with the peaks and nulls of the pattern moving rapidly in the disturbed ionosphere.

ACKNOWLEDGMENTS

The authors wish to thank Mr. G. N. Taylor of the Jodrell Bank Experimental Station who operated the transmitter and analyzed the results for the quiet days. D. Knight and H. Silverman assisted with the observations at Sagamore Hill.

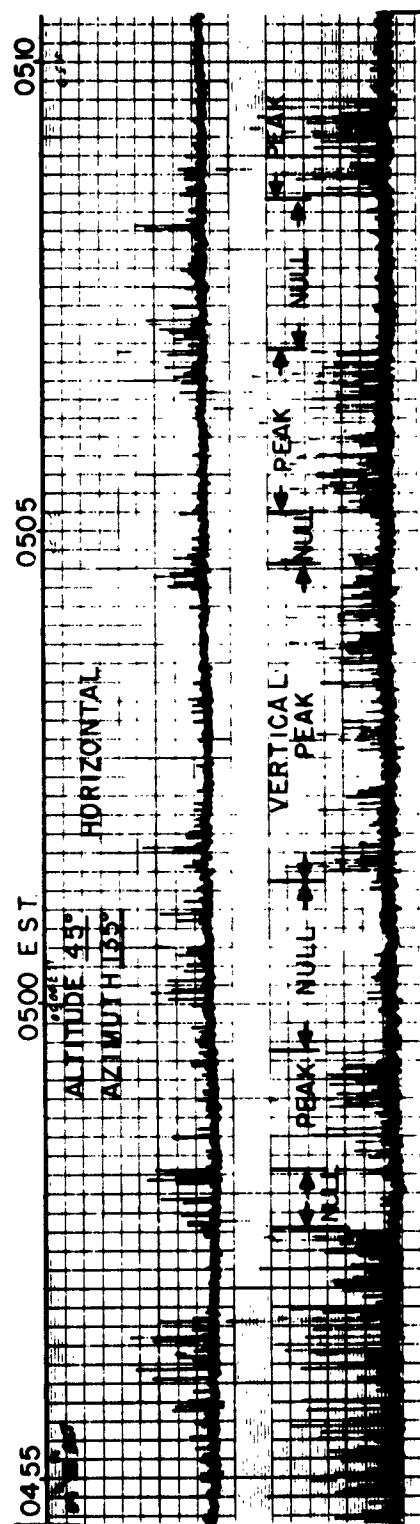
REFERENCES

1. G. N. TAYLOR, *Nature* 189: 740, March 4, 1961.
2. GARTLEIN, private communication.
3. J. C. JAMES, et al. *Nature* 185, Feb. 20, 1960.
4. H. G. BOOKER, *Proc. IRE* 46: 302, 1958
5. F. E. ROACH and J. W. WARWICK, private communication.



PEAKS AND NULLS OF FAF G NOV. 12, 1960

FIG. 1. Peaks and nulls of Faraday fading Nov. 12, 1960.



NOVEMBER 13

FIG. 2. Polarization scintillation: note irregular periods of peaks and nulls, differences in amplitudes is due to gains of two receivers.

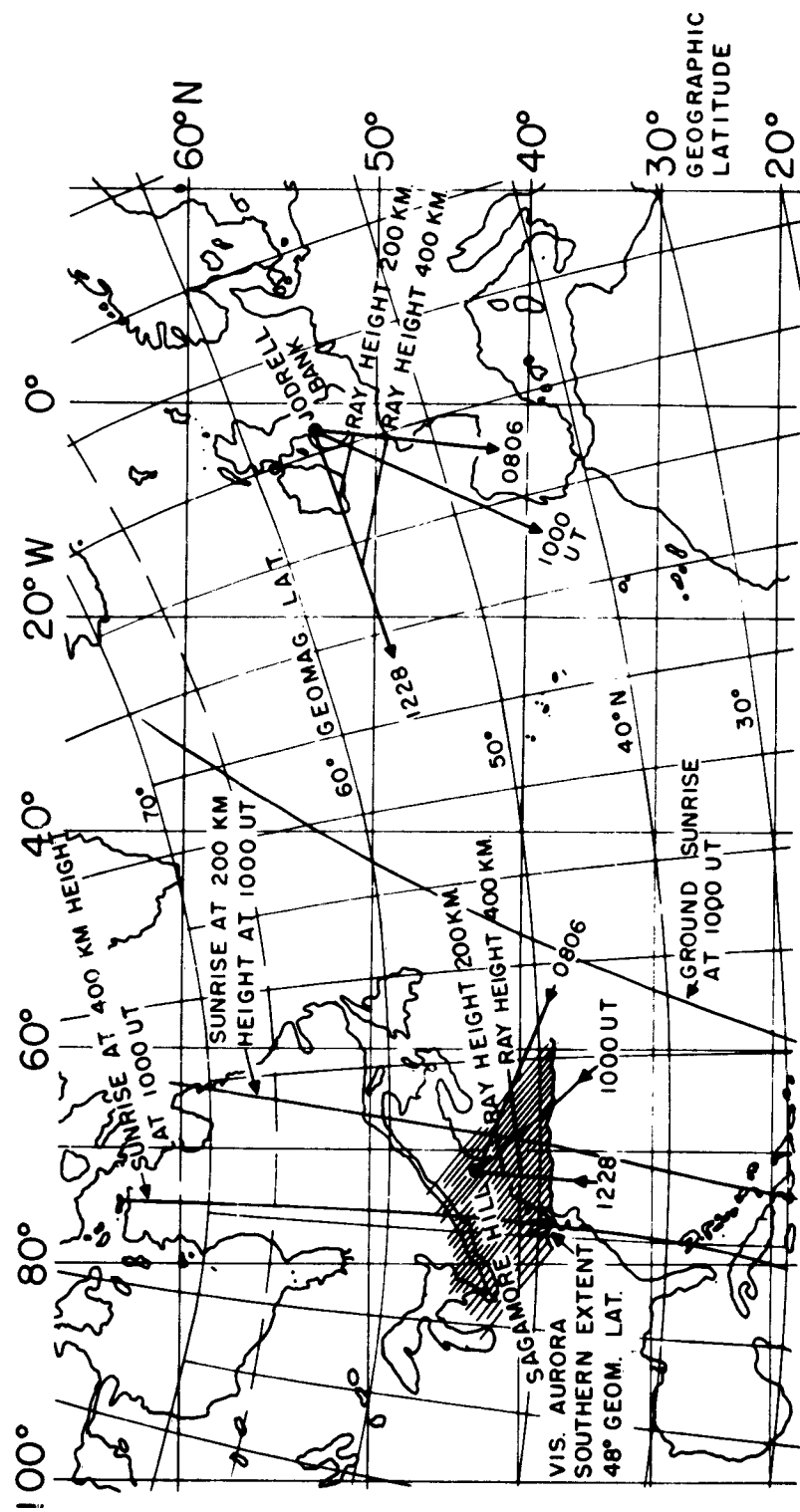


FIG. 3. Bistatic lunar path, Jodrell Bank to Sagamore Hill, Nov. 13, 1960.

EMISSION OF CARBON GROUP HEAVY NUCLEI FROM A 3+ SOLAR FLARE*

Herman Yagoda
Air Force Cambridge Research Laboratories

Robert Filz and Katsura Fukui
Emmanuel College, Boston, Mass.

Discoverer satellite XVII was launched into a polar orbit at 2042 UT on November 12, 1960, about 37 minutes after ground-level neutron monitors indicated their maximum cosmic-ray increase following a 3+ solar flare which commenced at 1325 UT. During the 50 hours between launching and successful recovery, it is estimated that the outside of the capsule received a bombardment of $\sim 2 \times 10^9$ protons of energy $E \geq 30$ Mev.¹ The instrument capsule, which carried a 772-gram block of Ilford G5 emulsion, had an apogee of 993 ± 4 km and a perigee of 188 ± 3 km. The average latitude of apogee was 20°S and the perigee occurred at 18°N . Of the 31 orbits of 96.44-min duration, a total of 0.766 day was spent above geomagnetic latitude 55°N and S.

The 10×15 cm face of the emulsion block was placed adjacent to one wall of the aluminum capsule and radiation arriving perpendicular to this plane penetrated 2.2 g cm^{-2} of condensed matter composed of light nuclei. This admitted carbon nuclei with energies in excess of 88 Mev per nucleon over a solid angle of 1.8 steradians. Owing to other instrumentation in the capsule, the rear of the block was shielded by approximately 21 g cm^{-2} of condensed matter.

After several unsuccessful attempts at full development, which caused almost every grain of silver bromide to be reduced to metallic silver, the bulk of the emulsion stack could be processed to a point where the preparations transmitted light (Fig. 1) by employing a very dilute amidol developer at near 0°C temperature and adjusted by means of a

*Published in Phys. Rev. Letters, 6 626-628 (1961)



FIG 1. Photomicrographs of three terminating flat tracks recorded in the Discoverer XVII emulsion block. The black bars define 10-micron intervals. The integral grain densities in the terminal 300 microns are as follows. A: 192 grains ($Z = 4$ or 5); B: 308 grains ($Z = 6$ or 7); and C: 871 grains ($Z \sim 20$).

sulfite-bisulfite buffer to a pH of 6.5. Details of the processing, of the flare exposure, and of further measurements on long-lived radioactive nuclides produced in the metallic components are available in a preliminary report on the Discoverer XVII flight.^{2,3}

The final ability to discern the tracks of slow, highly charged nuclei above the dense, random, single-grain background is not due in its entirety to the extremely weak development. Owing to the rapid diminution of the flare radiation following maximum, we estimate that about 50 percent of the total dose was delivered during the first hour in orbit. This intense radiation appears to have destroyed the basic sensitivity of the G5 emulsion. It is very likely that the hydrogen peroxide produced by the radiochemical decomposition of the water retained by the gelatin played a significant role. It is known that hydrogen peroxide⁴ has a powerful destructive action on the latent image produced by ionizing radiations. By diffusion into the silver bromide grains all surface latent images would be destroyed, but in the case of the largest or most sensitive grains a residual internal latent image might persist if the nuclear particle crossing the grain had a very high rate of energy loss.

Prior to development, the flown emulsion and a control piece from the same batch were exposed to polonium alpha particles. The tracks of the 5-Mev rays were readily visible on the control sheet, but could not be discerned on the flare-irradiated recording medium. Examination of the desensitized emulsion at 2000 \times magnification shows star-like structures of 3 to 6 tracks originating from a common center. The grain density and range of these associated track clusters suggests that they are the spallation products of $Z \geq 3$ commonly produced when Br, Ag, or I emulsion target nuclei are evaporated.

Systematic examination of the first three 600-micron emulsion sheets facing the thin window at 600 \times magnification shows a group of tracks which enter the stack and terminate their range by ionization. For particles making small dip angles with the emulsion plane the grain density can be measured after suitable correction for coincident background grains. The

histogram of the grain density in the terminal 300 microns of range (Fig. 2) shows a pronounced peak at 275 ± 25 grains. Most all of the light tracks have the same sense of direction and make a spatial angle with respect to the longitudinal axis of the rocket of $\leq 50^\circ$.

If we plot the logarithm of the integral grain count N as a function of the logarithm of the residual range R , tracks of varying grain density yield linear functions of essentially the same slope. This indicates that the strongly irradiated emulsion is still serving as a quantitative tool for measuring ionization. It can be shown that a line of constant grain density intersects these functions at ranges R , roughly inversely proportional to the charge Z . If we assign $Z = 4$ to the tracks with an average count of 183 ± 17 grains, then the peak at 275 ± 25 grains yields a charge of 5.9. The charge assignments for heavier nuclei, following this model, are indicated in Fig. 2.

Table 1 is a summary of the frequency of heavy primary nuclei terminations as observed on Discoverers XVII, XVIII, and at balloon elevations. The Discoverer XVIII block was exposed during a relatively

TABLE 1. Comparison of Heavy Primary Terminations in Balloon and Satellite Exposures.

Flight	Date	Altitude (km) (apogee)	$Z > 6$ terminations ($\text{cc}^{-1} \text{ day}^{-1}$)
Bemidji 532	July 29, 1960	42.5	7.78 ± 1.15
Bemidji 533	August 5, 1960	42	8.60 ± 1.04
Discoverer XVIII	December, 1960	638	8.65 ± 0.93
Discoverer XVII	November, 1960	993	900 ± 300

quiescent period of solar activity and could be developed normally. It exhibits essentially the same frequency of terminating $Z \geq 6$ particles as the balloons launched at 55°N , and the tracks enter isotropically. A comparison of the two satellite exposures indicates that during the 3+ flare the flux of $Z \geq 6$ particles capable of terminating in the detectors increased about 100-fold. The greater part of the $900 \pm 300 \text{ cc}^{-1} \text{ day}^{-1}$

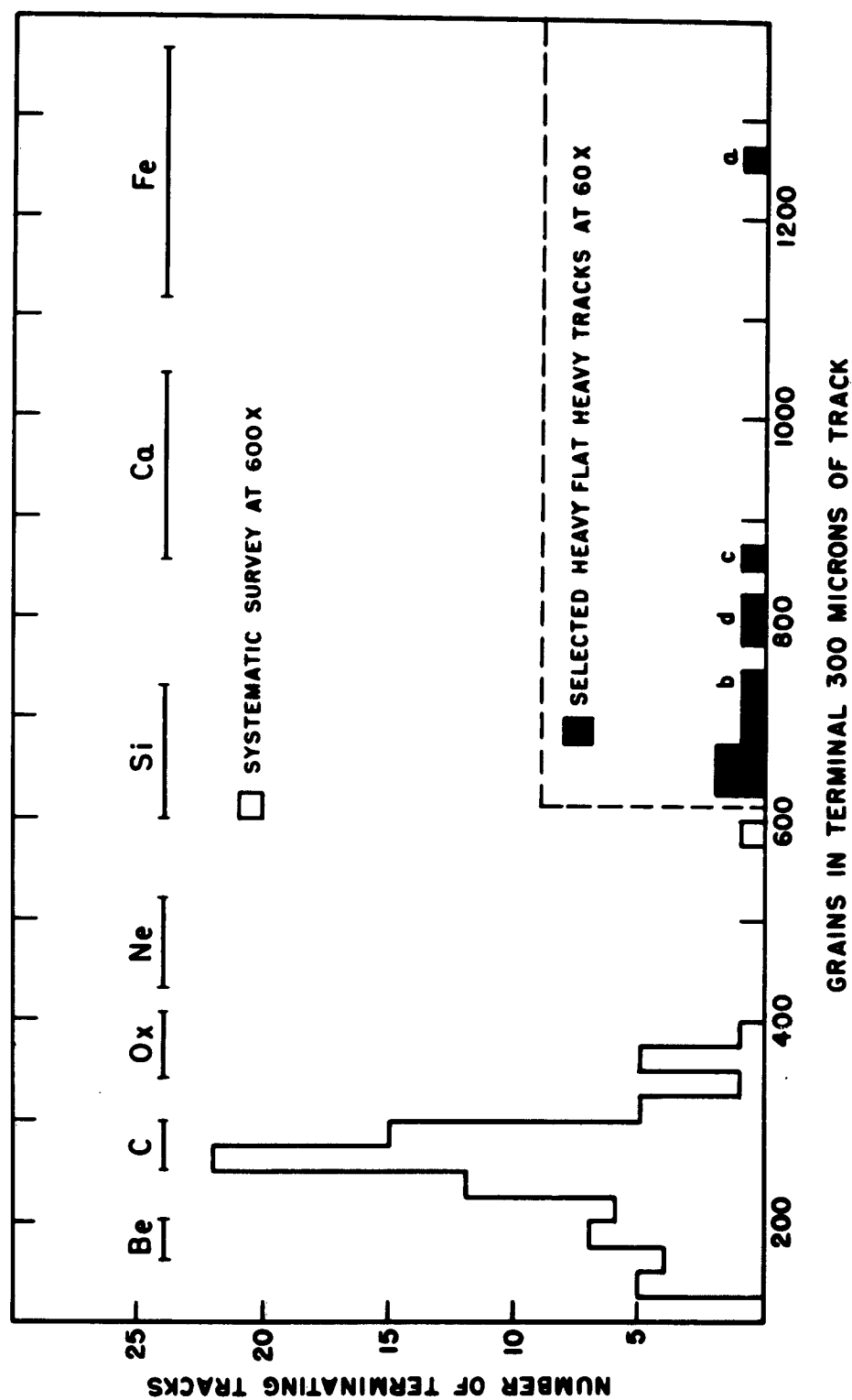


FIG 2. Histogram of relative abundance of particles based on a scale of grains in terminal 300 microns of track. The insert is not a part of the systematic survey and is included to show the gambit of the charge spectrum.

termination frequency is due to the $Z = 6 \pm 2$ group. If we assume that our low-magnification estimate⁵ of $13 \pm 3 \text{ cc}^{-1} \text{ day}^{-1}$ applies to the more conspicuous tracks of $Z \geq 10$, then the M/H ratio during a flare is ~ 70 as compared with a value of 3 for the galactic heavy primaries. The large uncertainty in the $Z \geq 6$ population is not statistical in character, but originates from the sampling position, which reaches a maximum in the first emulsion sheet facing the thin window. The over-all evidence indicates that a beam of particles of $Z = 6 \pm 2$ was emitted from the sun during the 3+ flare.

This identification is consistent with the observation by Fichtel and Guss⁶ of a flux of carbon, nitrogen, and oxygen nuclei associated with a flare of magnitude 3, detected by nuclear emulsions flown to 130 km at 1480 UT on September 3, 1960. On the other hand, Kurnosova and co-workers⁷ report an anomalously large flux of nuclei with $Z \geq 15$ associated with a Class 1 flare which occurred at 1127 UT on September 12, 1959. Their observations are based on two Cerenkov counters carried on the second U.S.S.R. cosmic rocket which responded to heavy particles with energies exceeding 1.5 Bev/nucleon. During the 17-minute period when the flux of $Z \geq 15$ increased about twelvefold, the fluxes of particles with $Z \geq 2$ and $Z \geq 5$ remained essentially normal.

REFERENCES

1. J. A. VAN ALLEN, Bull. Am. Phys. Soc. 6, 276 (1961).
2. H. YAGODA, Geophysical Research Note No. 54, Air Force Cambridge Research Laboratories, Bedford, Massachusetts, March 1961.
3. H. YAGODA, Proceedings of the Second International Space Science Symposium, Florence, Italy, April 10-14, 1961 (to be published).
4. H. YAGODA and N. KAPLAN, Phys. Rev. 73, 634 (1948).
5. K. FUKUI and H. YAGODA, Bull. Am. Phys. Soc. 6, 276 (1961).
6. C. E. FICHTEL and D. E. GUSS, Phys. Rev. Letters 6, 495 (1961).
7. L. V. KURNOSOVA, L. A. RAZORENOV, and M. L. FRADKIN, Priroda (Moscow) 1, 94-96, January 1961.

BACKSCATTER MEASUREMENTS AT 19 MCPS DURING THE NOVEMBER 1960 EVENTS

C. Malik and R. Hartke*
Electronics Research Directorate
Air Force Cambridge Research Laboratories

At the Air Force Cambridge Research Laboratories backscatter sounding station in Plum Island, Mass., auroral and ionospheric characteristics are investigated on a continuous basis. A pulse transmitter is operated at 19.39 Mcps with a peak power of 1 kw. Backscatter signals from auroras as well as ground backscatter signals, which provide information regarding the characteristics of the reflecting F2 layer, are recorded as functions of azimuth. The Yagi antenna used has a beamwidth of approximately 45° and rotates once every eight minutes.

Ground backscatter, auroras, and sporadic E returns are presented on the same display. In Figs. 1 and 2 azimuth and range plots are illustrated for each day of the November period. In the section labelled 'range,' 0 to 30 msec time delay of the signal return is plotted against the hour of the day. Since the range can and does vary with azimuth, the closest range during one complete scan has been chosen as a compromise value for the plot. In the azimuth section, directly above the range plot, hatched areas indicate the azimuths from which return was obtained during the particular hour. The vertical markings represent the total range and azimuth spread of the aurora as observed by the apparatus. Sporadic E is denoted by the sign Σ . Thus, a detailed continuous daily plot of the backscatter is displayed.

The events following the three cosmic-ray flares of November 12, 15, and 20 are of considerable interest and have therefore been studied in

* R. Hartke is employed by Wentworth Institute, Boston, Massachusetts

detail. In this note, some comparison is made between the backscatter data and related measurements made by other observers. The November 12 cosmic-ray flare of 1323 UT (0823) has been described in detail throughout this volume. A graphical picture of the ground backscatter at about this time, as seen in PPI photographs, is shown in Fig. 3. Each photograph is of 8 minutes duration and is stamped with the time of the end of the rotation. These records indicate that the SID began at 0826 EST. The 0817 and 0825 records taken before the SID show the usual gap or non-return of backscatter in the North. In this case, the absence of return is due to a lower critical frequency to the North (lower solar elevation angle). Such a gap may, however, be due in some cases to increased auroral absorption.

On the sweep which started at 0825 and ended at 0833 EST (the frame marked 0833), the backscatter is abruptly cut off at 0826, the start of the SID. For many subsequent frames there is no return. At 0848, gradually the backscatter returns begin to reappear, but complete 360-degree ground backscatter returns are not recorded until 0913. The backscatter time delay was not seriously affected by the SID. As is well known, the effect observed during the SID was primarily due to absorption in the D layer rather than to extensive height or density changes in the F2 layer.

After backscatter had reappeared, all echoes suddenly disappeared again at 1320 EST. A 10-Mcps riometer operated at Sagamore Hill¹ showed high absorption from 1323 to 1922 EST. A magnetic disturbance was also observed when the absorption began (Chernosky 1961).

In spite of the presence of optical aurora during the night of Nov. 12, auroral radar reflections were seen only sporadically. The absence of auroral echoes on the night of Nov. 12 and of auroral and backscatter echoes during the entire day of Nov. 13 was due to two factors. The first factor, the high absorption observed, would completely explain the absence of auroral returns during the evening hours. Absorption of the same magnitude has on other occasions not been sufficient to eliminate backscatter echoes during the sunlit hours. For example, equally

high absorption was recorded by the 10-Mcps riometer following the Nov. 12 flare. Nevertheless, 19-Mcps echoes were absent only during the short interval of the SID. During the period 0913 to 1320 EST on Nov. 12, the 19-Mcps echoes reappeared. Since no such echoes appear during the same time period on Nov. 13, there must be some factor in addition to the absorption which is responsible for the lack of echoes during the sunlit hours of Nov. 13. The hypothesis is advanced that the F-layer backscatter echoes were absent because the electron density was reduced at all latitudes surveyed by the radar. Ionosounders of CRPL² did observe lower critical frequencies during Nov. 13. The critical frequency was reduced in both hemispheres at geomagnetic latitudes greater than 15° . Within the geomagnetic equatorial region, the electron density was increased, however.

A comparison of the observations of November 12 and 15 is of interest. The November 15 recordings show normal backscatter in the South. There is a gap in the North, however, indicating a lower electron density in Northern regions (perhaps above 57° geomagnetic latitude).

The 'gap in the north' observations of a suitably placed low-frequency oblique sounder afford a convenient method of examining the movement of the electron density bulge during magnetic storms. This technique would show any case in which there was a deficiency of electrons in the North and an enhancement of electron density to the South.

REFERENCES

1. R. M STRAKA, personal communications.
2. J. F. BROCKMAN, Sky and Telescope, Vol. 21, July 1961.
3. E. CHERNOSKY, personal communications.

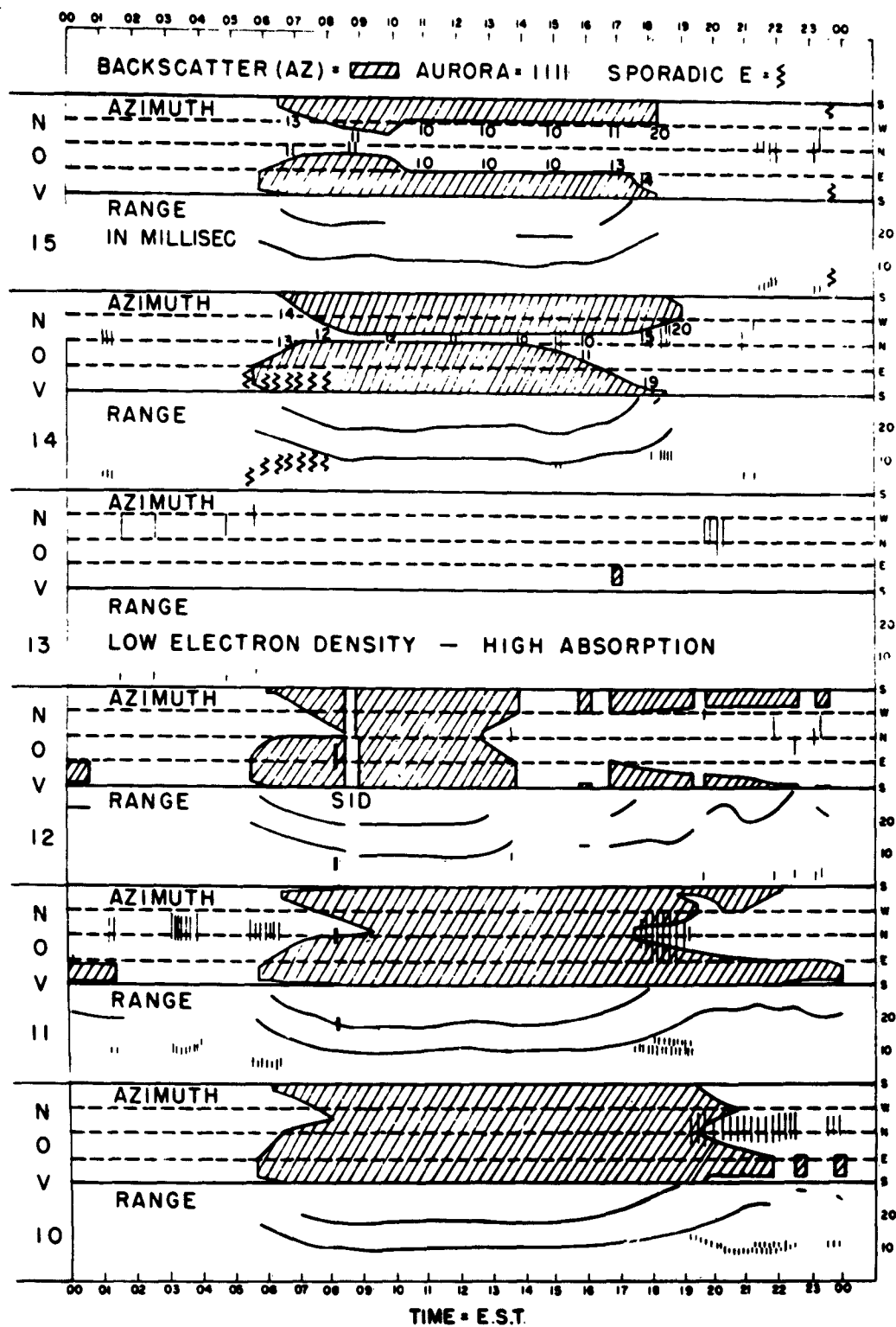


FIG. 1. Backscatter at 19.4 Mcps, Nov. 10 to 15, 1960, measured at Plum Island, Mass.

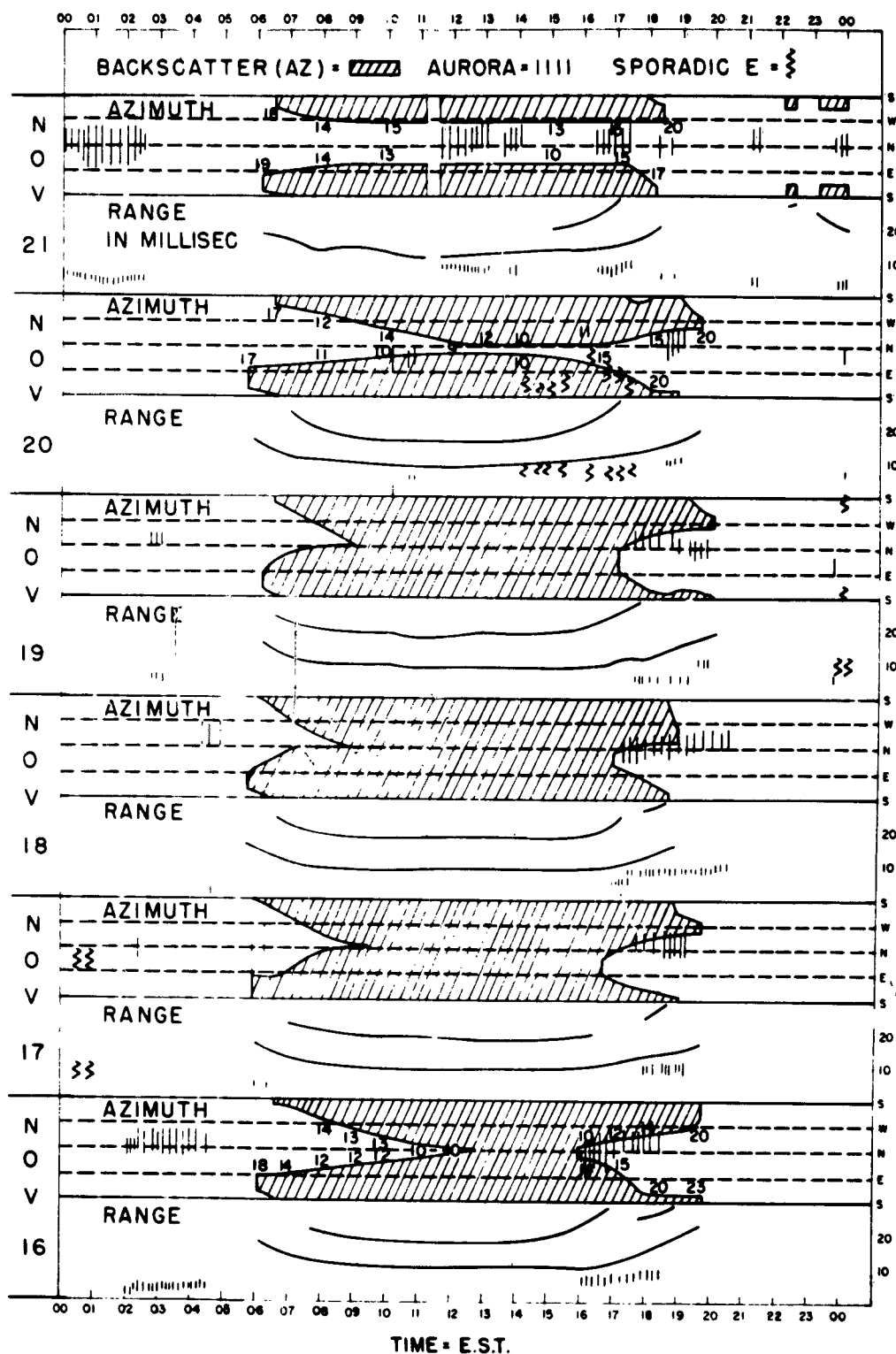


FIG. 2. Backscatter at 19.4 Mcps, Nov. 16 to 21, 1960, measured at Plum Island, Mass.

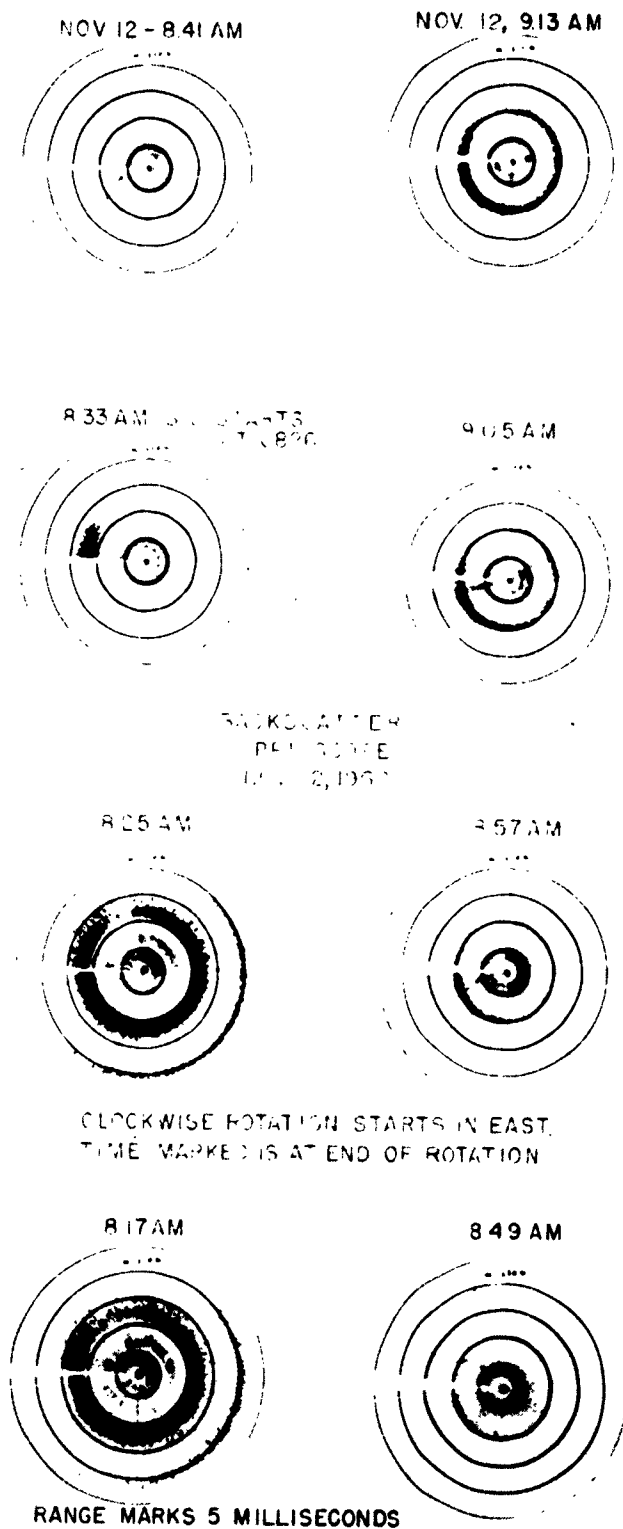


FIG. 3. Before and after PPI photographs of the cosmic-ray flare of Nov. 12, 1960

RADIATION STUDIES FROM NUCLEAR EMULSIONS
AND METALLIC COMPONENTS RECOVERED FROM
POLAR SATELLITE ORBITS*

Herman Yagoda
Air Force Cambridge Research Laboratories

ABSTRACT

Two blocks of Ilford G5 emulsion measuring 10 x 15 cm and each weighing 772 ± 2 grams have been recovered from polar satellite orbits. The one launched on Discoverer XVII was exposed to the intense solar radiation associated with the 3+ flare of 12 November 1960. By means of a special developing technique conducted at pH 6.50, which resulted in a 30-fold reduction in grain growth, it was possible to suppress the intense background of solar protons and discern the tracks of very highly charged heavy primary nuclei that stopped by ionization in the emulsion. The frequency of this category of particles with charges $Z \geq 11$ is estimated at $13 \pm 3 \text{ cc}^{-1} \text{ day}^{-1}$. A similar measurement on the Discoverer XVIII emulsions, which were placed in orbit on 7 December 1960 during a period of relatively normal solar activity, yielded a termination rate for nuclei charges $Z \geq 6$ of $8.65 \pm 0.93 \text{ cc}^{-1} \text{ day}^{-1}$. These measurements indicate that the flux of the heaviest galactic primaries remained essentially unaltered during the giant solar flare. Examination of the flare-irradiated emulsions at very high magnification shows the presence of a much larger flux of nuclei which appear to be of charge $Z = 6 \pm 2$ on the basis of tentative ionization-range identifications. A comparison of the Discoverer XVIII emulsion measurements with data from a balloon flight at 140,000 ft elevation, launched at Minnesota on 29 July 1960 and which recorded 7.8 ± 1.2 heavy primary terminating tracks $\text{cc}^{-1} \text{ day}^{-1}$, indicates that the flux of slow heavy primaries does not increase appreciably while the satellite is orbiting over the polar regions during quiescent solar conditions.

* Abstract of a paper published as GRD Research Note No. 54, March 1961.

Preliminary estimates of star production in the Discoverer XVIII emulsions show that nuclear disintegrations with three or more associated tracks accumulate with a frequency of about $6700 \pm 500 \text{ cc}^{-1} \text{ day}^{-1}$. This is about twice as large as can be anticipated from counter data and emulsions flown in rockets from sites whose geomagnetic latitudes extended between the equator and the polar regions. The slope of the integral star prong spectrum indicates a component of low-energy star-producing radiation which probably originates in the fringes of the lower Van Allen belt that the satellite grazed during apogee.

The aluminum, iron, and lead inside the satellite capsules are being analyzed by radiochemical techniques for long-lived radioactive spallation products. Preliminary reports from the Harvard Astrophysical Observatory, the Brookhaven National Laboratory and the Enrico Fermi Institute, where these studies are being conducted, indicate greatly increased yields of radionuclides in the metallic components of the satellite capsule exposed to the flare as compared with iron and stone meteorites. The yield of tritium is particularly high and the ratio of $\text{H}^3/\text{Ar}^{37}$ observed suggests that primary tritium nuclei may be accelerated during the 3+ solar flare.

RADIOACTIVITY PRODUCED IN DISCOVERER XVII
BY NOVEMBER 12, 1960
SOLAR PROTONS*

John T. Wasson
Geophysics Research Directorate
Air Force Cambridge Research Laboratories
Bedford, Massachusetts

ABSTRACT

Scintillation-spectroscopy measurements on a AgBr emulsion block from Discover XVII, which was flown during a period of high solar cosmic-ray activity on November 12, 1960, reveal a gamma-ray spectrum attributable to 8.4-day Ag^{106} . The disintegration rate, corrected to a probable production time of 2200 UT, November 12, 1960, is 14 dis sec^{-1} . If one assumes a (p, pn) cross section of 100 mb, and applies the thin-target formula for production of radioactivity, this corresponds to a total proton dosage of about $1.6 \times 10^8 \text{ protons cm}^{-2}$ within the emulsion, and to a value of 16 rads radiation dosage. An attempt to measure the gamma spectrum of 40-day Ag^{105} was unsuccessful, allowing the assignment of an upper limit on the disintegration rate of 1 dis sec^{-1} at the time of production. A search for 1.3-year Cd^{109} has been unsuccessful.

INTRODUCTION

The first observation¹ of high-energy cosmic rays generated by the sun was on February 28, 1942. The large solar cosmic-ray effect on November 12, 1960, was the eighth such event recorded, indicating an average of one such occurrence about every 3 years. The fortuitous launching of the Discoverer XVII recoverable satellite during the peak of the solar activity has provided nuclear chemists with their first chance to apply radioactivity techniques to the measurement of properties of the solar cosmic rays. The techniques involved are much the same as those utilized during recent years to investigate long- and short-term cosmic-ray intensities by studying long- and short-lived radioactivities in meteorites.

* Published in J. Geophys. Res. 66 2659-2663 (1961)

The maximum in the intensity of the November 12 cosmic-ray increase as measured by neutron monitors at middle latitude stations in North America² occurred at about 2000 UT. Discoverer XVII was launched toward the south at 2042 UT and was above the sensible atmosphere³ by about 2045 UT. It went into a polar orbit, with an apogee of 993 ± 4 km occurring at 20°S , and a perigee at 188 ± 3 km occurring at 18°N . The period was 96.4 min and the total time in orbit was 49.8 hr, after which time it was retrieved in midair over the Pacific Ocean. The next giant solar flare producing high-energy cosmic rays occurred 1 day later, on November 15, 1960.

The energy spectrum of solar cosmic rays falls rapidly with energy above a certain energy value,⁴ roughly as E^{-5} . The exact point where this rapid fall commences varies with the time after the flare, occurring at about 1 beV for prompt particles from the flare of February 23, 1956, and at about 200 MeV 19 hours after the same flare. Below these energies the spectrum changes much more slowly with energy. The lower limit on the energy is given by Winckler as about 40 MeV, although this is very uncertain. We shall assume that the primary protons that produced radioactivity in Discoverer XVII were in the energy range $45 < E < 400$ MeV, where the lower limit is given by the energy of the protons necessary to penetrate the smallest amount of absorber seen by the sample.

The geomagnetic cutoff for protons of this energy occurs at about 60° geomagnetic latitude. The earth's magnetic field was disturbed by a major magnetic storm during the exposure period, however, so we shall assume a modified cutoff latitude of 50° . A calculation on this basis indicates that the satellite was bombarded by protons in the given energy range during 45 percent of its orbit.

Since it was launched toward the south, Discoverer XVII was first above 50° latitude about 30 minutes after it was launched, or about 70 minutes after the time of the maximum cosmic-ray intensity, which occurred at about 2000 UT. According to Steljes, Carmichael and McCracken², this maximum in the neutron-monitor measurements was

the result of earth moving into a region containing magnetically trapped particles from a flare that occurred on the sun at 1320 UT. Thus, the satellite started sampling almost 8 hours after the actual occurrence of the flare on the sun.

The chemical composition of the primary components of solar cosmic particles has not been measured, but the characteristics are consistent with an assignment of a proton beam.⁴ The stellar abundance data of Aller⁵ gives a ratio of hydrogen to helium of about 7:1, which should be a lower limit for flare particles. All other elements are less abundant than hydrogen by a factor greater than 1000. This agrees well with the abundance given by Ney⁶ for galactic cosmic rays. We have assumed that all the observed radioactivity was produced by protons.

Although optical measurements on flares indicate a duration of only a few minutes, the flare particle flux at the earth lasts much longer. Neutron monitor measurements indicate a period of about 1 hour for the flux to rise and peak, at which time it falls proportional to the inverse square of the time.⁴ The data obtained from Geiger-counter measurements made on Explorer VII during the period November 12-15, 1960⁷ can be interpreted as fitting a t^{-2} decay following the November 12 flare.

RESULTS AND DISCUSSION

The observed radioactivity was produced in a AgBr emulsion block belonging to H. Yagoda, at AFCRL. This block was composed of Ilford G5 emulsion, measuring $10 \times 15 \times 1.3$ cm. Our measurements were on a total weight of 698 g (total weight flown was 772 g) of which 330 g were silver, 261 g were bromine, and the remainder was gelatin. The minimum absorber path seen by the surface of the emulsion was 2.2 g cm^{-2} , and this covered a solid angle of 3 steradians. The remaining solid angle had absorber thicknesses varying between about 5 and 25 g cm^{-2} .

Soon after the recovery of Discoverer XVII, Yagoda suggested to us that radioactivity might be detectable in his emulsion block (in which preliminary trial developments showed deep blackening from the extreme

exposure). (Subsequently a development procedure was devised which suppressed the proton and alpha track background so that the tracks of slow heavy primaries of charge $Z > 4$ could be resolved at very high magnification.) A gross gamma-ray spectrum taken on November 21 during a 1200-min count with the emulsion block sitting on the face of a 3×3 -in. NaI scintillation crystal and recorded in a 100-channel analyzer is shown in curve A of Fig. 1. Curve B was taken on November 22 during a 930-min count on an unexposed emulsion block. Curve C shows the differential spectrum obtained by subtracting the blank count from the count of the Discoverer XVII emulsion. The energy calibration was obtained from the K^{40} and Th C'' peaks in the background, and from calibration of the detection system with known gamma-ray standards.

The lower portion of Fig. 1 shows a known spectrum of 8.4-day Ag^{106} , recently published by Robinson, McGowan, and Smith.⁸ As can be seen, the energies and intensities of curve C correspond almost exactly to those given for Ag^{106} , and we attribute the entire spectrum below 1.8 Mev to that nuclide, with the possible additional contribution of an unknown species at about 1.38 Mev. We are unable to assign the high-energy peaks.

Ag^{106} was formed from Ag^{107} by a (p, pn) reaction. This type of reaction has the highest cross section of any type of reaction induced by protons of energy $45 < E < 400$ Mev incident on medium-Z targets, as indicated by data given by Caretto and Wiig,⁹ Ladenbauer and Winsberg,¹⁰ Fink and Wiig¹¹ and Meadows.¹² The other (p, pn) products from stable silver and bromine isotopes are all too short-lived to have been detected at the time of our measurements, about a week after the solar flare.

In order to obtain the total counting rate for the emulsion block, we have counted a block of KCl having the same shape as the original emulsion block, and containing 157 g K. From the known isotopic abundance and half life of K^{40} , we have calculated the efficiency of the detector with respect to 1.5-Mev gamma rays emitted in the emulsion block. The value obtained was 0.00614, or a geometrical efficiency of about 11 percent. After multiplying the peak height by a factor of 0.81 to correct for contri-

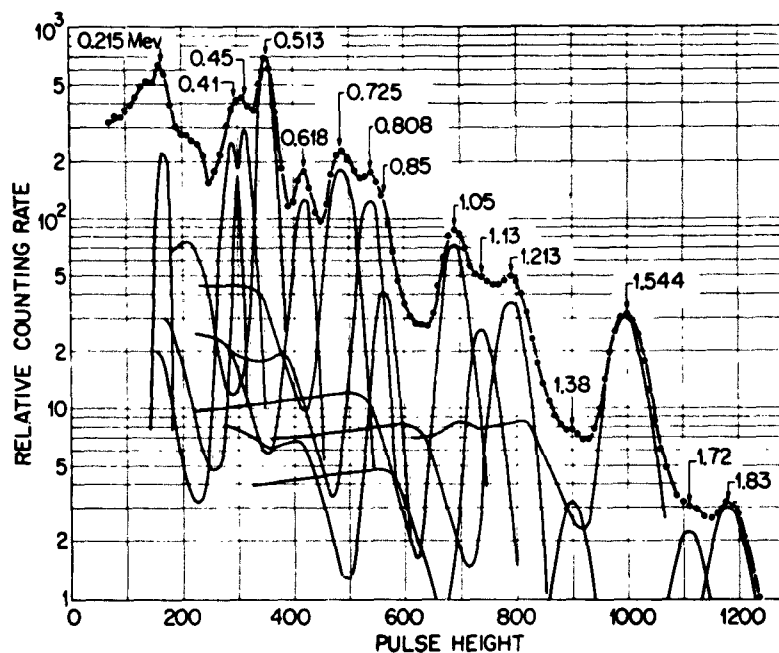
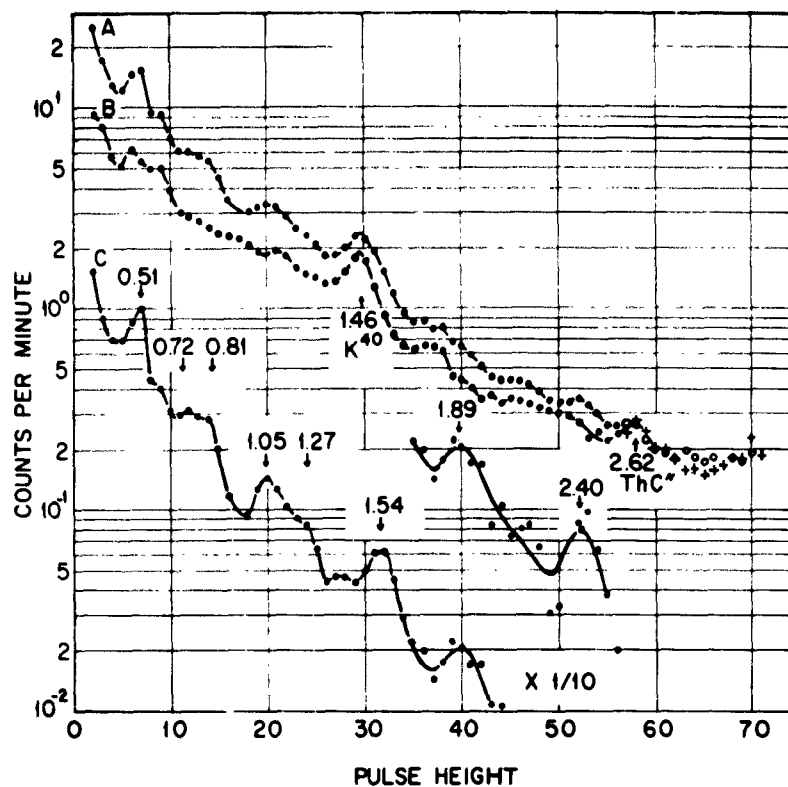


FIG. 1. The upper portion of this figure shows: A. The gross gamma spectrum of $15 \times 10 \times 1.3$ cm AgBr emulsion block from Discoverer XVII, the block resting on the face of 3×3 -in NaI detector. B. Spectrum obtained by measuring an unflown AgBr emulsion block of identical dimensions. C. Spectrum obtained by subtracting curve B from Curve A, and interpreted as 8.4-day Ag^{106} . The lower portion of the figure shows a gross spectrum of Ag^{106} given by Robinson, McGowan, and Smith.

bution from the Comptons from higher-energy gammas, by a factor 1.13 to allow for self-absorption of the gammas in the source, and allowing for the slight differences in absorption and in efficiency and peak-to-total ratios of the 1.46-Mev K^{40} gamma and the 1.54-Mev gamma, we obtain a value of 1.54 gammas sec^{-1} of the 1.54-Mev transition. This corresponds to a disintegration rate of 8.4-day Ag^{106} of 6.58 dis sec^{-1} at the time of our measurement, or 14.2 dis sec^{-1} at an assumed time of production of 2200 UT, November 12, 1960. The number of radioactive atoms of Ag^{106} that would give this disintegration rate is 1.49×10^7 atoms.

According to the preceding references given for proton-induced reactions, the (p,pn) cross section peaks at about 30 Mev, and then levels at a constant value for higher energies. The measured values vary from about 60 to 600 mb. The present case is complicated by the nuclear isomerism of Ag^{106} . The 8.4-day isomer has a 6+ spin, whereas the 24-min isomer has a 1+ spin. It is uncertain which is the ground state. However, the data of Meadows, Diamond, and Sharp¹³ and Matsuo (private communication, 1961) indicate that in this energy range the high-spin state should be formed in a higher abundance than the low-spin state. We shall assume a cross section, σ_{106} , for the production of 8.4-day Ag^{106} of 100 mb, which is independent of energy.

From the thin-target formula,

$$D_p = \frac{N_{106}}{N_{107} \sigma_{106}}$$

the given values of σ_{106} , N_{107} (the number of Ag^{107} atoms), and N_{106} (the number of Ag^{106} atoms at the time of production), we can calculate D_v , the proton dosage within the emulsion block during the flare. The value thus obtained is 1.6×10^8 protons cm^{-2} . If we assume an isotropic flux and that all protons entered through the 3-steradian 'window,' the dosage in space was 6.6×10^8 cm^{-2} . Furthermore, since the target was clearly not thin (the smallest target thickness, 4.5 g cm^{-2} is just the range of a 50-Mev proton in a AgBr medium), the stated value is only a

lower limit. In an effort to correct for the fraction of the time during which the satellite was below the geomagnetic cutoff latitude, we shall assume that it sampled 45 percent of the time corresponding to a cutoff latitude of 50° . The integrated flux is then 1.5×10^9 protons cm^{-2} .

It should be possible to obtain a value for the instantaneous flux from our value of the integrated flux. Winckler,⁴ gives the formula,

$$I = I_0 \frac{t_0^2}{t^2},$$

where t_0 is a constant equal to 1 hour, and corresponds to the beginning of the t^{-2} decay of the flux. I_0 is the flux at t_0 , and I is the flux at a time $t > t_0$. If our data are fitted to the curve obtained by assuming that Discoverer XVII started sampling 7.5 hours after the flare, an initial value for the instantaneous flux of 6.4×10^4 protons sec^{-1} is obtained. Van Allen⁷ reports fluxes measured by Explorer VII at 2330 UT on November 12 and at 0356 UT on November 13 of 2.1×10^4 and 1.1×10^4 particles $\text{cm}^{-2} \text{sec}^{-1}$. Our calculated fluxes at these times are 3.5×10^4 and 1.7×10^4 protons $\text{cm}^{-2} \text{sec}^{-1}$, in satisfactory agreement with Van Allen's results.

It is possible to calculate the radiation dosage from the value for the proton dosage within the emulsion (1.6×10^8 protons cm^{-2}). If the approximate energy of the protons entering the emulsion is 100 Mev, and they pass through an approximate absorber thickness of 8.0 g cm^{-2} , then one can calculate from range-energy relationships that the average energy loss is 50 Mev per proton. The approximate area of the emulsion having an 8 g cm^{-2} thickness is 88 cm^2 . From these numbers, plus the weight of the emulsion, 698 g, the energy dosage per gram of emulsion can be calculated. The value obtained is 1.6×10^3 ergs g^{-1} , corresponding to a radiation dosage of 16 rads. This compares with a value of about 50 rads obtained by Yagoda³ from grain-density measurements on the same emulsion. It should be noted, however, that Yagoda has measured the total radiation dosage due to all types of radiations, whereas we have only measured that fraction due to protons within the given energy limits.

Cwing to the unfortunate interpretation of our original data (top curves in Fig. 1) as indicating essentially no radioactivity, no attempts were made to find additional activities until mid-January 1961, some 2 months after the flare. Possible activities still measurable at that date included 40-day Ag^{105} , 120-day Se^{75} , and 1.3-yr Cd^{109} . Since the emulsion block had now been developed, we isolated the silver from the hypo solution and looked for Ag^{105} . An upper limit on the number of atoms of Ag^{105} on November 12, 1960, of 5×10^6 was established. On the chance that most of the radioactivity was still in the developed plates, a new count was made on about 20 percent of the original sample. No identifiable activity was observed. A search for Cd^{109} from the hypo solution that involved use of a low-background X-ray counter. (Kalkstein, unpublished material) was also unsuccessful.

The method of studying radioactivity produced by cosmic rays offers great promise for the measurement of high-intensity particle fluxes, as those produced in the Van Allen belts or during solar flares. If one takes advantage of the variation with energy of the ratio of the cross sections for various reactions, as (p,pn) and (p,p2n), then not only the flux but also the energy spectrum of these particle streams should be measurable by such techniques.

ACKNOWLEDGMENTS

I would like to express my thanks to Dr. H. Yagoda for the sample, and to him and my colleagues, Dr. P. J. Drevinsky, Dr. M. I. Kalkstein, and Mr. K. Shivanandan, for several helpful discussions. I am also grateful to Miss Anahid Thomasian and Mr. Edward C. Couble for performing chemical separations, and to Dr. R. L. Robinson for the Ag^{106} spectrum. This research was supported in part by the U. S. Atomic Energy Commission.

REFERENCES

1. S. E. FORBUSH, Three unusual cosmic-ray increases possibly due to charged particles from the sun, Phys. Rev., 70, 771, 1946.
2. J. F. STELJES, H. CARMICHAEL, and K. F. McCracken, Characteristics and fine structure of the large cosmic-ray fluctuations in November 1960, J. Geophys. Research, 66, 1363-1377, 1961.
3. H. YAGODA, Radiation studies from nuclear emulsions and metallic components recovered from polar satellite orbits, Geophysics Research Directorate Research Note No. 54, to be published in report of COSPAR meeting, Florence, April 10-14, 1961.
4. J. R. WINCKLER, Primary cosmic rays, and discussion, reprinted in NASA Technical Note, D-588, December 1960.
5. L. H. ALLER, The Atmospheres of the Sun and Stars, Ronald Press Company, New York, 1953.
6. E. P. NEY, Cosmic rays as received at the earth, Astrophys. J. Suppl., 4, 371, 1960.
7. J. A. VAN ALLEN, Explorer VII observations of solar cosmic rays, November 12-23, 1960, Bull. Am. Phys. Soc. (II), 6, 276, 1961.
8. R. L. ROBINSON, F. K. McGOWAN, and W. G. SMITH, Decays of Rh^{106} and Ag^{106} , Phys. Rev., 119, 1962, 1960.
9. A. A. CARETTO, Jr., and E. O. WIIG, Interaction of yttrium with protons of energy between 60 and 240 Mev, Phys. Rev., 115, 1238, 1959.
10. I. LADENBAUER, and L. WINSBERG, Interaction of high-energy protons and alpha particles with iodine-127, Phys. Rev., 119, 1368, 1960.
11. R. W. FINK, and E. O. WIIG, Reactions of cesium with protons at 60, 80, 100, 150, and 240 Mev, Phys. Rev., 96, 185, 1954.
12. J. W. MEADOWS, Excitation functions for proton-induced reactions with copper, Phys. Rev., 91, 885, 1953.
13. J. W. MEADOWS, R. M. DIAMOND, and R. A. SHARP, Excitation functions and yield ratios for the isomeric pairs $Br^{80, 80m}$, $Co^{58, 58m}$, and $Sc^{44, 44m}$ formed in (p, pn) reactions, Phys. Rev., 102, 190, 1956.

X-BAND 84- FT RADIO TELESCOPE

S. Basu and J. Castelli
Electronics Research Directorate
Air Force Cambridge Research Laboratories
Bedford, Massachusetts

During November 1960, personnel of AFCRL used the 84-ft radio telescope at Sagamore Hill, Hamilton, Mass. on frequencies near 9600 Mcps in an effort to determine its general usefulness at frequencies twice those of the upper useful limit for which it was designed. In all cases the sun was used as the signal source. The receiving equipment was a very stable total-power radiometer. Although this radiometer had a high noise figure, its sensitivity was sufficient for solar work.

The first series of tests were made during the period of the transit of Mercury across the sun on 7 November 1960. Multiple drifts of the sun were made in closely controlled regions on that day. It was thought that, if the path of Mercury passed over an extremely bright spot on the sun, some eclipsing of the radio energy from the sun might possibly be evident even though the ratio of the diameter of Mercury to that of the sun is about 1 to 160. The multiple drifts were compared with the results taken from artificial eclipsing of a number of solar maps available for the same day. These included a 9600-Mcps solar map made at the Sagamore Hill Radio Observatory by a method which will be described later in this paper; a 3300-Mcps solar map prepared at Stanford University; an Adler Planetarium solar photograph; and a Fraunhofer optical map. No conclusive proof of radio eclipsing of the enhanced regions was found during the transit.

During this period, studies were also undertaken to determine the actual beamwidth of the antenna at 9600 Mcps. (The theoretical value is slightly under 6.0 minutes of arc.) Many drifts of the sun were made at orientations of the feed rotated 90° from each other. The actual measured half-power beamwidth was derived by inspecting the drift curves. The

average value was found to be about 7 minutes of arc in both the E and H planes.

Although the mesh of the dish has a transmissivity of only 6 percent at 10 kMcps, the overall efficiency was estimated to be only about 15 percent. The greatest losses apparently were due to the departure of the dish shape from that of a true parabola. Concurrent with reduced main-lobe gain was the appearance of high side lobes. In spite of the high side lobes, when the 84-ft antenna was operated at 9600 Mcps, the main-lobe resolution proved very useful and made possible the construction of solar contour maps.

These contour maps were based on raw-data drifts of the sun taken at three minutes of arc separation in declination and covering the range from -18 to +18 minutes from the center of true solar declination. The drift curves are plots of antenna temperature vs. time at different declinations. In order to convert them to plots of antenna temperature vs. position on the solar disk, they must be transferred to a grid which has the same declination and hour angle as the two mutually perpendicular axes. The scale of the spacing on the declination axis must conform to the scale of the abscissa of the drift curve in order to obtain a circular disk of the sun. The center line of the solar disk is positioned on the drift curve and is then aligned with the declination axis on the prepared grid. A line is drawn parallel to the hour angle axis at the declination of the particular drift curve being used. Various antenna temperatures are marked on this line as the declination axis is gradually moved up the center line of the drift curve. The same procedure is followed with all the drift curves and, then, constant temperature points are joined by means of a smooth curve which does not cross itself at any point. These constant temperature lines are the contour lines of the solar map. The photosphere may be drawn on the grid sheet with its radius conforming to the grid scale used. Sample maps are illustrated in Figs. 1 and 2.

The high points of these maps compare reasonably well with those taken at 3300 Mcps at Stanford University. They lack some detail which

has been 'washed out' by the side lobes and the somewhat less than ideal resolution. They are offered as an indication of what can be worked out even with main-lobe beamwidths as great as 7 minutes of arc. No similar maps in this frequency range have been noted by the authors.

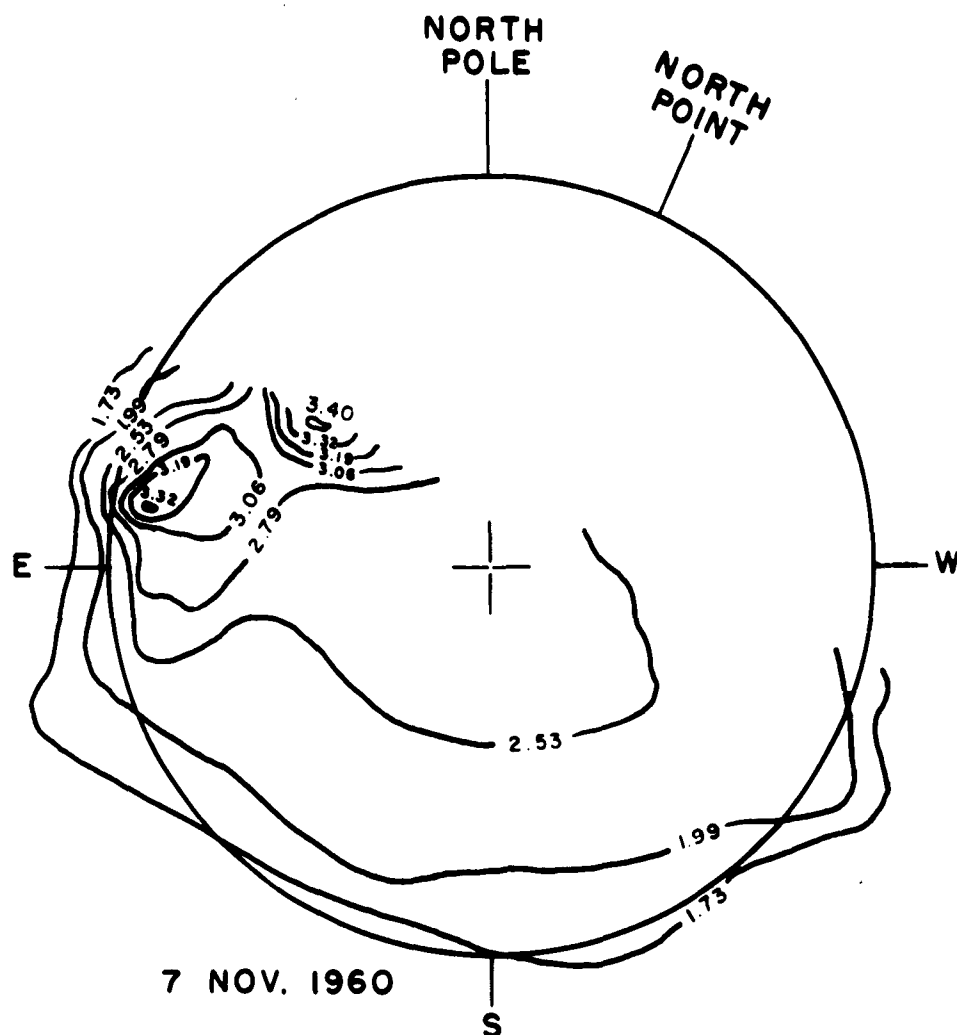


FIG. 1. Map of sun at 9600 Mcps reduced from records taken with 84-ft antenna at Air Force Radio Observatory, Hamilton, Mass. (Not corrected for antenna losses.) Time: local noon. Contour unit is 1000°K . Antenna pattern circular. Beam width approximately 7 minutes 0 seconds.

PHOTOMETRIC OBSERVATIONS OF 6300\AA O I
AT SACRAMENTO PEAK, NEW MEXICO
DURING NOVEMBER 1960

S. M. Silverman
Geophysics Research Directorate
Air Force Cambridge Research Laboratories
Bedford, Massachusetts

W. Bellew and E. Layman
Northeastern University
Boston, Massachusetts

ABSTRACT

The results of the photometric observations of 6300\AA O I at Sacramento Peak, New Mexico during November 1960 are presented. The mechanism for production of the red line is reviewed and it is concluded that the two step mechanism involving charge exchange of O^+ with O_2 and the subsequent dissociative recombination of the resulting O_2^+ can satisfactorily explain the observations during the magnetically quiet periods and during the relatively quiet periods of disturbed nights. Data relating to the largest photometric maximum of the night, at 1000 UT, are reviewed and it is concluded that for this maximum, a different mechanism must be operative.

1. INTRODUCTION

During November 1960, several active regions were present on the sun. In particular, McMath plage region 5925 appears to have been especially active from the time of its first appearance on 4 November on the east limb of the sun until 20 November when it had passed the west limb. Class 2 and 3 flares were reported on 2, 4, 5, 6, 10, 12, 13, 14, 15, 18, 19, 20, 22, 24, and 28 November. During this period three sea-level cosmic-ray increases were reported: on the 12th, 15th, and 20th. A number of other geophysical effects were also noted during the period under consideration. A summary of the major geophysical events during this period (prepared by T. Obayashi) is shown in Fig. 1. In this paper, the photometric observations of the forbidden red line of atomic oxygen

at Sacramento Peak, New Mexico will be reported. The emphasis will be on the variation of intensity with time in order that comparisons with other geophysical phenomena can be carried out.

The airglow photometer at Sacramento Peak is a modified version of the three-color birefringent photometer designed by Dunn and Manring.¹ A survey of the sky for a single color consists first, of a reading of the zenith intensity, and then of continuous scans of the azimuth at zenith angles of 40°, 55°, 70°, 75°, and 80°. Past experience at Sacramento Peak has shown that, with the exception of during very severe magnetic storms, when auroral activity is present, the oxygen red line, 6300 Å, is typically greatly enhanced and the oxygen green line, 5577 Å, is only slightly or not at all enhanced. Consequently on these nights, the observer normally makes many more surveys of the red line and only a few observations of the green line.

Before proceeding with the description of the observations it is worthwhile to present a brief description of the typical behavior of the red line at Sacramento Peak. Typically, after sunset, there is a large twilight enhancement which, after a period of hours, decreases to a relatively steady value. This value is then maintained until shortly before dawn when a rapid morning twilight enhancement occurs. Large fluctuations of intensity during the night are rare. With this behavior in mind, we may proceed to a discussion of the observations on individual nights.

Calibration of the instrument has been carried out for the green line of atomic oxygen by comparison with the National Bureau of Standards portable photometer. The calibration factor for the red line is then calculated from the green line factor by assuming that the filter characteristics for the green and red filters are the same and by using the manufacturers curve for the photomultiplier response. Both of these assumptions are in the process of being checked. The intensities, in rayleighs, given in this paper thus have a provisional character.

2. THE OBSERVATIONS

Almost every night in November for which observations are available

shows some unusual feature. Each night will be discussed separately. Plots of zenith intensity vs. time are shown in Fig. 2 for each night. In Fig. 3, the intensities for zenith and for zenith angle 80° looking south and looking approximately north northeast are shown with a logarithmic intensity scale so that comparison of the time variations in different directions may be more easily made. The north northeast is normally the direction of maximum auroral activity.

The intensity ratios of different azimuths for a trace at a given zenith angle can be readily intercompared. The intensity ratio of the 80° trace to the zenith is less reliable for instrumental reasons and because corrections for extinction and for difference in path length for auroral geometry are difficult to make. All times, unless otherwise stated, are universal time.

November 9/10 MST (Nov. 10 UT) Observations were made at 10-min intervals from 0140 to 0300, at 30-min intervals from 0500 to 0755, with no observations from 0300 to 0455. For most of the night, the behavior appears to be what would be expected. An unusual feature occurs at 0220 where the intensity of the 80° NE point is approximately 25 percent greater than expected.

November 12/13 MST (Nov. 13 UT) This is the night following the flare at 1323 UT on 12 November, which produced the first large cosmic-ray increase. The most spectacular aurora seen in years occurred at this time. Visually the initial sighting was made only 40 minutes after sunset. The first photometric maximum occurred at 0130, only 12 hours after the flare. A second maximum occurred at 0330. The greatest visual display of the night started about 0600 UT (2300 MST) and reached a peak at about 0630 UT. The maximum red line activity occurred later, about 0900 UT and reached a peak about 0945 UT. A comparison of the 80° NNE intensities with the zenith intensities indicates a movement to the south of the red line activity from 0700 (0000 MST) to about 0830 (0130 MST), and a subsequent northward movement most marked about 0930 (0230 MST). The maximum intensity in the NE was of the order of 50,000 rayleighs compared to typical values for other nights in November of the order

of 50 to 100 rayleighs. At 1000 UT the zenith and the 80° trace to the south have maxima of 5,000 rayleighs.

November 13/14 MST (Nov. 14 UT) This night exhibits a red enhancement, that is, a definitely greater intensity in the north northeast than at other azimuths. The intensity variations during the night, however, show only small fluctuations, and, in general, are similar to those of a normal night. The intensity level of about 200 rayleighs for 80° NNE is, however, some 3 to 4 times greater than those of other nights in November. What we appear to have here is a persistence of the previous night's activity. This phenomenon has also been noted for other aurorae at Sacramento Peak.

November 15/16 MST (Nov. 16 UT) Observations were made at 5 or 10 minute intervals from 0430 to 1125. The intensity variations during the night were typical of those seen on an auroral night. The maximum photometric intensity occurred at about 0500 (2200 MST) and was of the order of 2 kilorayleighs, toward the NNE and of the order of 60 rayleighs in the zenith. Other intensity maxima occurred at 0630 (2330 MST) and 0715 (0015 MST). The intensity level for the last part of the night is about 200 rayleighs for 80° NNE, about the same as for the night of November 13/14.

November 16/17 MST (Nov. 17 UT) Only four points are available for this night, from 0155 to 0355 MST. The intensities of these points are normal.

November 18/19 MST (Nov. 19 UT) Observations were made at half-hour intervals for most of the period from 0325 to 1150. The intensities fluctuated about a mean of 40 rayleighs at the zenith. There appears to have been a peak (particularly on the 80° ZNNE trace) at about 0425 UT.

November 20/21 MST (Nov. 21 UT) Observations were made at half-hour intervals from 0225 to 1155. This night shows most unusual behavior. The intensity variations are typical of auroral activity during the night. The intensity level, however, is not much greater than the normal. At least three intensity maxima are evident, at 0255, 0555 and 0725, and the largest,

at 0555, is only about 110 rayleighs for the 80° ZNNE point. The most remarkable feature of the night, however, is the lack of directionality of the variations. The entire sky appears to change in intensity at the same time and to the same extent. The typical enhancement in the north northeast is missing.

November 21/ 22 MST (Nov. 22 UT) Observations are available at half-hour intervals for almost the entire period from 0125 to 1155. The intensity fluctuations are not too marked during the night though there appears to be a maximum at 80° ZS at 0525 (2225 MST). The unusual feature of this night is an enhancement in the north northeast which disappears rapidly between 0855 and 0925.

November 22/ 23 MST (Nov. 23 UT) Observations were made at half-hour periods between 0125 and 1155. A slower than normal decline of intensity occurs for the first part of the night with a peak being present at 80° ZS at 0225, with the intensity ratio of the south to northeast being atypically high.

November 28/ 29 MST (Nov. 29 UT) Observations are available from 0155 to 1155. The intensity level during the night was somewhat higher than normal. The 80° ZS point shows a broad maximum during the night at about 0700.

The comments above give the general picture of the photometric observations of $6300 \text{ \AA} \text{ O I}$ at Sacramento Peak, New Mexico during the month of November, 1960.

3. DISCUSSION

The results given above provide us with a comparison of the red line behavior for one or two relatively quiet nights during November 1960 with the behavior during a very active period. A good deal of other data was taken throughout the world during this period and much of this is gradually appearing in the literature. In this paper, the discussion will be limited to a few points of interest and no attempt will be made to give a complete picture of the observed phenomena.

The theory for the production of the red line emission has been most fully treated by Chamberlain² and appears to be due to the following sequence of reactions:



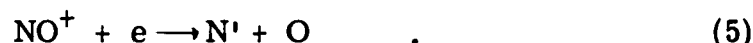
and



An alternative mechanism, proposed originally by Bates and Massey, and utilized in a recent paper by King and Roach³ makes use of the following sequence of reactions:



or,



The O' indicates an excited oxygen atom in the ¹D level, the upper state for the red line emission. For either mechanism, the dissociative recombination step is considerably faster than the other, which thereby becomes the rate determining step. Hence, if each recombination leads to the emission of one red line quantum (at either 6300 Å or 6364 Å), the emission per cubic centimeter per second is:

$$\epsilon = k_1 n(\text{O}_2)n(\text{O}^+) \quad \text{---} \quad (6)$$

or,

$$\epsilon = k_3 n(\text{N}_2)n(\text{O}^+) \quad , \quad (7)$$

depending on which mechanism is correct. The emission at 6300 Å will be 3/4 of the total.

If we now make the assumption that $n(\text{O}^+) \approx n_e$ then the integral of the emission over the height can be represented by a constant times the parameters $\overline{n(\text{O}_2)}$ and $\int n_e dh$ or $\overline{n(\text{N}_2)}$ and $\int n_e dh$, where $\overline{n(\text{O}_2)}$ or $\overline{n(\text{N}_2)}$ is related to the mean density of O₂ or N₂ and $\int n_e dh$ is the integrated electron density of the F2 layer, then the photometric intensity of 6300 Å at the ground becomes

$$Q = \frac{3}{4} k_1 \int n(O_2) n_e dh = C_1 \overline{n(O_2)} \int n_e dh, \quad (8)$$

or,

$$Q = C_2 \overline{n(O_2)} (f_o F2)^2,$$

and

$$Q = \frac{3}{4} k_3 \int n_e dh = C_3 \overline{n(N_2)} \int n_e dh, \quad (10)$$

where $f_o F2$ is the critical frequency for the F2 layer. Furthermore, if the oxygen density remains constant over the period of observation, then the airglow intensity is directly proportional to the integrated electron density.

Chamberlain's² treatment predicts that for the twilight and night, the red line intensity should vary hyperbolically with the time after ionospheric sunset. This appears to be valid under normal conditions.

For the period of the November events, however, major ionospheric storms occurred. We are interested here in seeing to what extent the theoretical predictions are valid under these conditions. We consider first the dependency on electron density. The ionospheric data from White Sands, New Mexico, show a definite decrease in the F2 critical frequency between the early morning of November 10 and the night of November 13/14.

Consequently, there must be either a decrease in the total electron content in the F2 region or a change in the electron-density profile. To decide between these two possibilities, we make use of the moon reflection experiment carried out at Jodrell Bank during this period. Ionospheric data from England show the same decrease in critical frequency as the White Sands data. In the moon reflection experiment, Faraday rotation is utilized to measure the total electron content of the ionosphere. Taylor⁴ has reported that, from the Jodrell Bank data, the total electron content of the ionosphere decreased considerably between 11 November and 14 November. Hence, it follows from comparison with the English data, that the drop in critical frequency at White Sands was associated with a drop in total electron content rather than with a change in the electron

density profile. At the same time, however, the red line intensity on 13/14 November averaged almost twice as high in the zenith as on 9/10 November. The intensity thus varies inversely with some function of the electron density. This unexpected result, apparently in contradiction to the theory, can be satisfactorily explained if during the storm there is an increase in the mean density of molecular oxygen or nitrogen, as can be seen from Eqs. (8) and (10). Seaton⁵ had proposed such an increase to explain the drop in critical frequencies during major ionospheric storms, and King and Roach³ have also used this idea in their interpretation of the aurora of 27/28 November 1959. In order to test this idea we note from Eqs. (8) and (10) that the ratio $Q/\int n_e dh$ should be equal to the density of O_2 or N_2 between the limits of integration. Calculations of the electron-density profiles from the minimum of the F layer to the height at which the electron density is a maximum at White Sands, New Mexico, are available from CRPL, National Bureau of Standards. Since the major part of the red line emission occurs below the height for which the electron density is a maximum we assume that the contribution of the integrals in Eqs. (8) and (10) above this height can be ignored. The variations in density at different heights during the November events have been obtained from satellite orbit measurements (Groves⁶; Jacchia⁷) and the form of these variations should be the same as those obtained in a plot of $Q/\int n_e dh$. In Fig. 4, this ratio is plotted for the period from 9 November to 15 November, together with the density obtained from satellite measurements (Groves⁶). It will be noted that the form of this plot is very similar to that obtained from satellite data, and that the ratio of the maximum to that on 10 November is about the same as the ratio obtained from satellite data.

We also note in Fig. 4 that, while the general form of the two curves is similar, the airglow data lag behind the satellite data by about 18 hours. The airglow curve is constructed by using the average values of the ratio during the relatively quiet parts of the night, and thus represents a nightly average. If the molecular oxygen density at these altitudes is built up during

the day and destroyed during the night by charge exchange and dissociative recombination, then the lag between the two curves could be explained. It is not yet known, however, whether this is actually the case, and comparisons for other periods need to be made before the theory outlined here can be considered satisfactory. It must be emphasized that the theory is only tentative in nature since other factors, such as large vertical movements of the electrons from day to day, could also affect the result. For the points shown in Fig. 4, the minimum heights of the electron density profile were uncorrelated with the calculated molecular densities. It is clear, however, that a more complete theory will have to take account of these factors.

It appears from the foregoing discussion that the red line intensity during the relatively quiet parts of auroral nights can, on the whole, be satisfactorily interpreted on the basis of charge exchange and subsequent dissociative recombination. We must still consider the red line behavior during the most active parts of the night. The most active period for the night of 12/13 November was between 2230 and 0330 LMT, i. e., between 0530 and 1030 UT, 13 November. On this night, the largest maximum occurred at about 0945 UT in the NNE and at about 1000 UT in the south and in the zenith, with an earlier smaller maximum at about 0630 UT, (see Fig. 3). This period corresponds to the maximum solar proton influx, reported at Kiruna as between 0700 and 1100 UT. Since this period includes hours of sunlight at Kiruna, the normal daily variation also contributes to this maximum, causing difficulty in determining the exact time of maximum. In this discussion, we shall focus attention on the maximum at 1000 UT. This maximum showed a marked difference in the time at which it occurred in the north and in the south. Furthermore, measurements by Saito⁸ on the Japanese icebreaker Soya, at 23° geomagnetic latitude, show a maximum at 1030 UT, and no maximum between 1000, when the measurements started, and 1030 UT. Measurements at Memambetsu in Hokkaido, Japan (Huruhata⁹), using primarily one-hour exposures on a patrol spectrograph, also indicate a southward movement for the maximum of the red line intensity

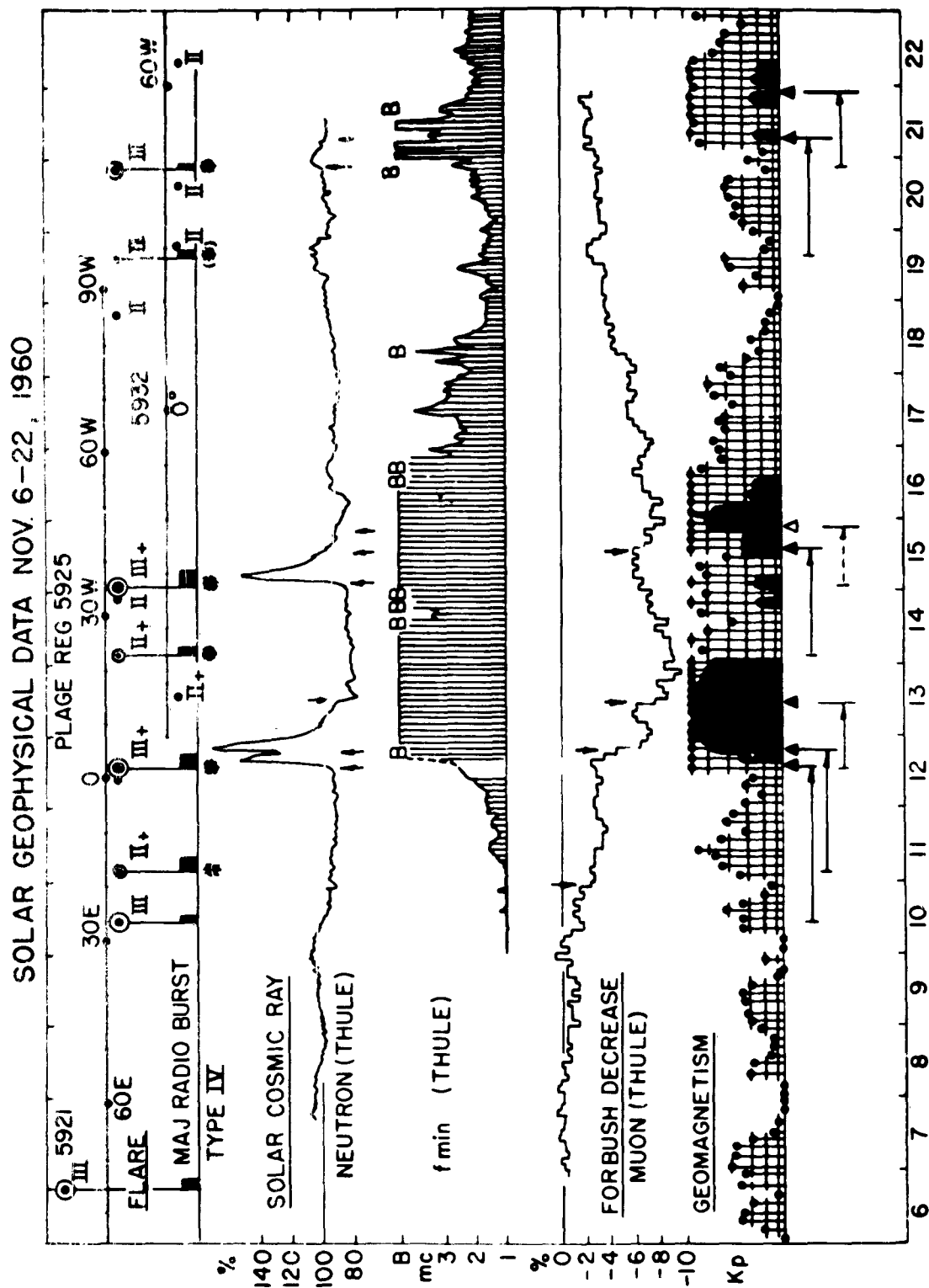
between 1000 and 1130 UT. Furthermore, the Stanford auroral radar mentioned by Leadabrand, Jaye and Dyce,¹⁰ showed unusually strong echoes from magnetic north at ranges of 1000 to 1400 km beginning at about 0130 local time (0930 UT) and continuing at ranges of 800 to 1600 km for about 30 minutes. These times correspond closely to the times for which the red line intensity observed at Sacramento Peak was at its maximum during the night.

All of the data given above indicate, therefore, that the photometric maximum at about 1000 UT must be treated differently. The strong auroral echoes indicate considerable additional ionization. Furthermore, the intensity cannot easily be interpreted using the recombination theory. As a tentative explanation of this maximum we propose that the maximum is due to corpuscular bombardment resulting from the distortion of the geomagnetic field, as proposed by Obayashi and Hakura¹¹ for polar blackouts.

The latitudinal movements for the red line intensity maximum are then similar to the movements of the southernmost extent of auroral blackouts calculated from the magnetic data by Obayashi and Hakura.

ACKNOWLEDGMENTS

The authors wish to thank the personnel of Geo-Science, Inc., who are responsible for the operation and maintenance of the Sacramento Peak airglow station. We are also indebted to J. W. Wright and G. H. Stonehocker of the Vertical Soundings Research Section, CRPL, National Bureau of Standards, Boulder, Colorado, for providing us with the White Sands electron-density profiles.



NOVEMBER 1960

FIG. 1. Solar and geophysical data, November 6 to 22, 1960.

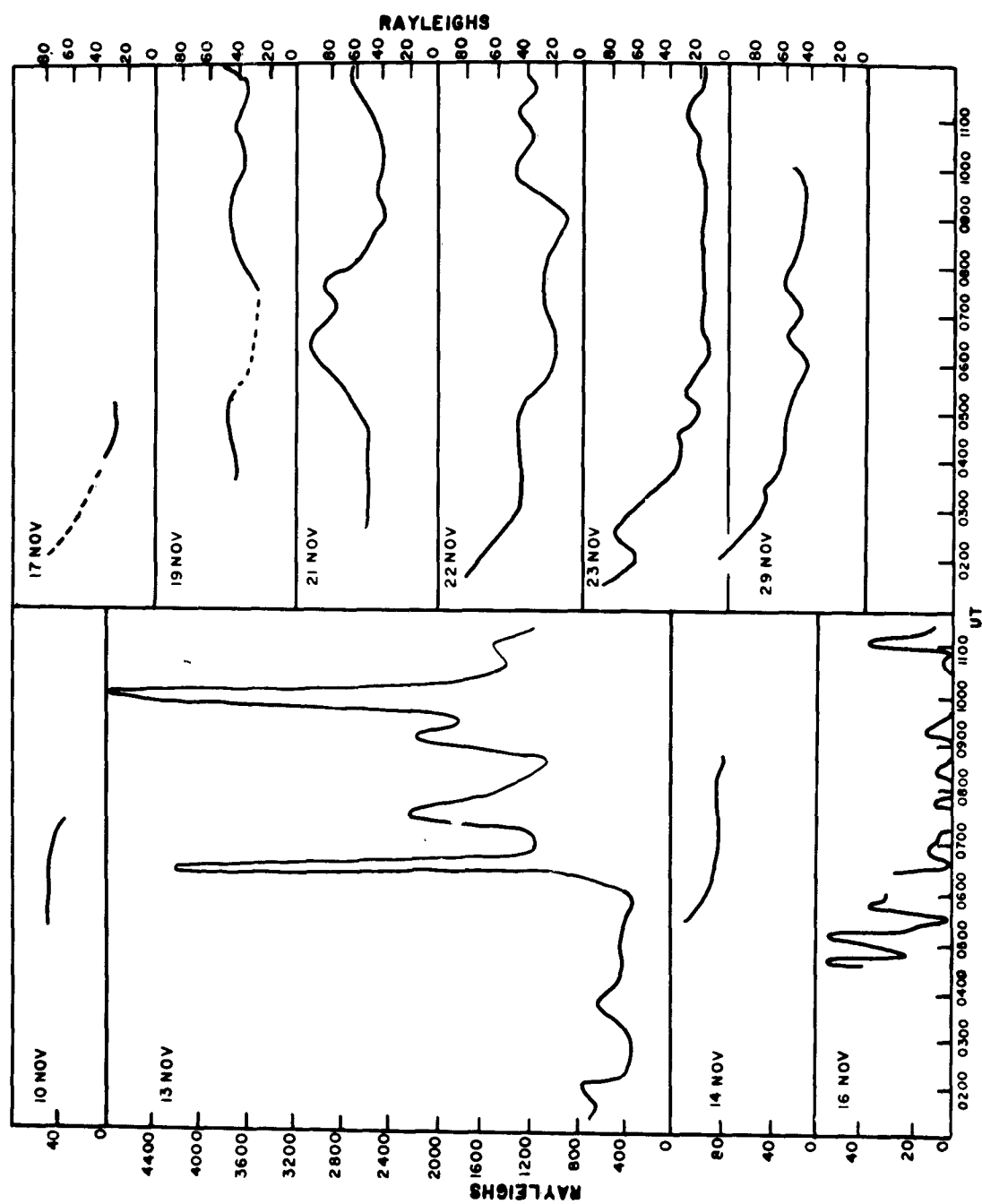


FIG. 2. Zenith intensity of 6300 Å O I from Sacramento Peak, New Mexico.

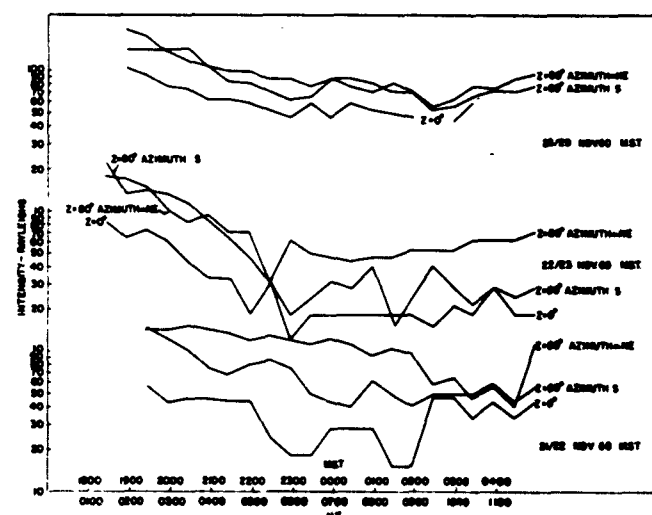
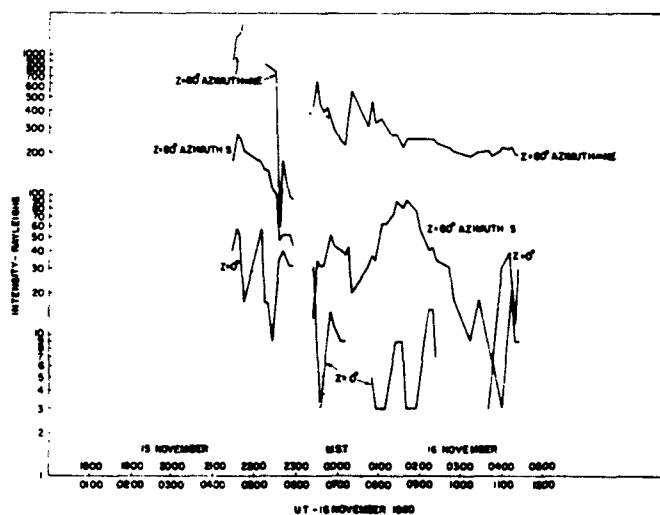
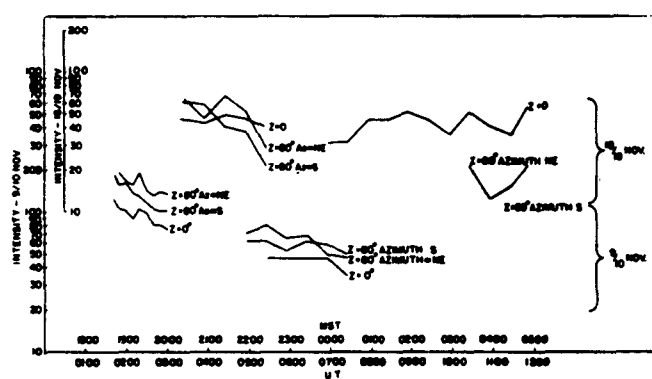
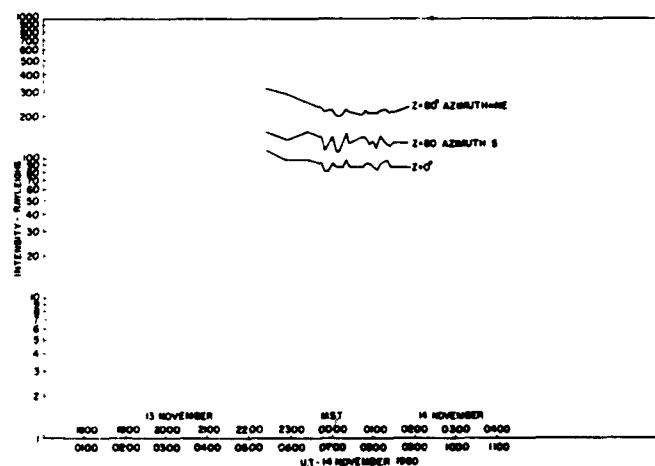
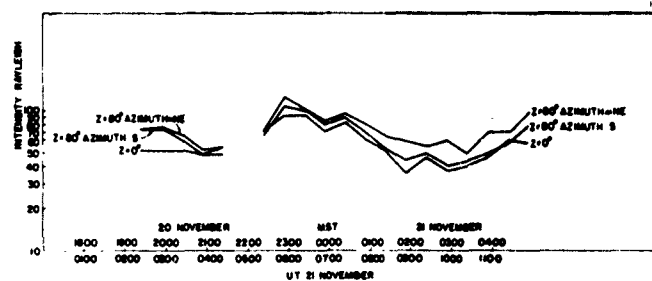
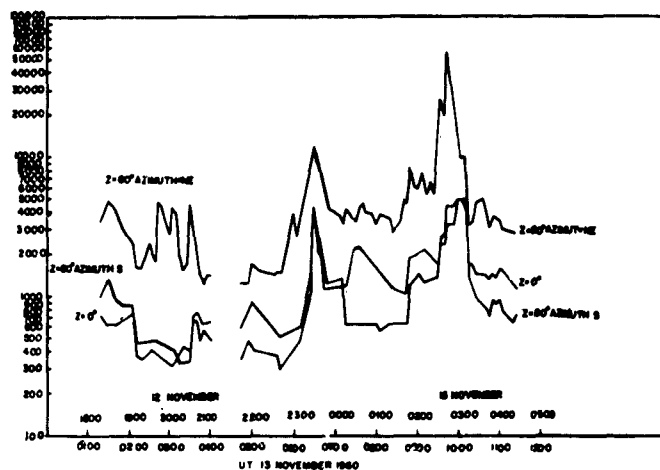


FIG. 3. Intensity of 6300 Å at zenith and 80° zenith angle looking S and NNE.

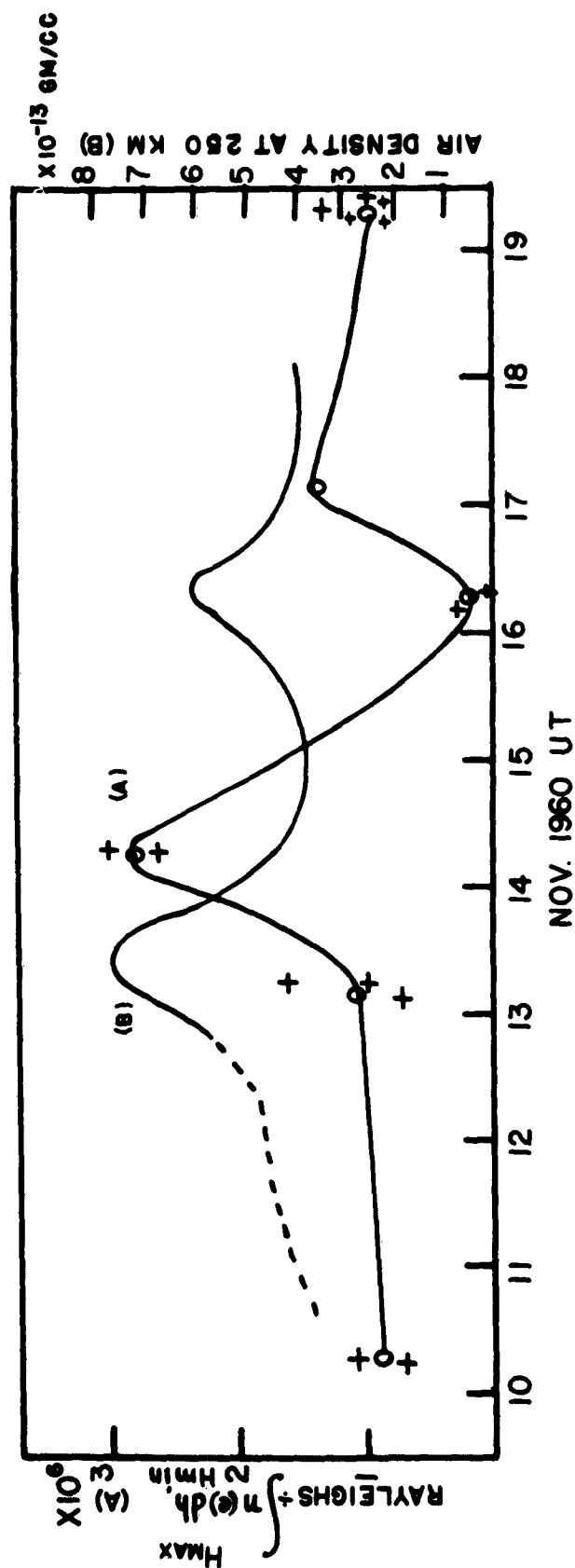


FIG. 4. Curves of atmospheric density at 250 km and the ratio of intensity of 6300 Å O I to the integrated electron density from minimum height of the F2 layer to the height of maximum electron density of the F2 layer.

REFERENCES

1. R. B. DUNN, and E. R. MANRING, Recording night sky photometer of high spectral purity, J. Opt. Soc. Amer. 46: 572-77, 1956.
2. J. CHAMBERLAIN, Oxygen red lines in the airglow I. Twilight and night excitation processes. Astrophys. J., 127: 54-66, 1958.
3. G. A. M. KING and F. E. ROACH, Relationship between red auroral arcs and ionospheric recombination. J. Res. Nat. Bur. Standards, 650: 129-135 (March-April 1961); cf. also IGY Bulletin 42, 276-282, June 1961.
4. G. N. TAYLOR, The total electron content of the ionosphere during the magnetic disturbance of November 12-13, 1960. Nature, 189: 740-1, March 4, 1961.
5. M. J. SEATON, J. Atm. and Terr. Phys., 8: 122 (1956).
6. G. V. GROVES, Conference on the November Events, Bedford, Mass., February 1961.
7. L. JACCHIA, Proc. 2nd Int. Cospar Conf., Florence, Italy, H. Kallmann-Kilj, ed., North Holland Publ. Co., Amsterdam.
8. B. SAITO, Unusual enhancement of night airglow intensity at low latitude on November 13, 1960, in press 1961.
9. M. HURUHATA, private communication, 1961.
10. R. L. LEADABRAND, W. E. JAYE, and R. B. DYCE, A note on 106.1-Mc auroral echoes detected at Stanford following the solar event of November 12, 1960. J. Geophys. Res., 66: 1069-1072, 1961.
11. T. OBAYASHI and Y. HAKURA, Enhanced ionization in the polar ionosphere caused by solar corpuscular emissions, Rep. Ionos. Space Res. Japan, 14: 1 to 40, 1960.
12. J. ORTNER, A. EGELAND, and B. HULTQVIST, The great earth storm in November 1960 as observed at Kiruna Geophysical Observatory, Scientific Report No. 1, Contract No. AF61(052)-418, 7 February, 1961.

RADIOACTIVE COBALT AND MANGANESE IN DISCOVERER XVII STAINLESS STEEL *

John T. Wasson
Geophysics Research Directorate
Air Force Cambridge Research Laboratories
Bedford, Massachusetts

ABSTRACT

Cobalt and manganese have been isolated from a stainless steel battery case carried in Discoverer XVII. This satellite was launched into orbit on November 12, 1960, at which time the Earth received an intense cosmic-ray bombardment in connection with a solar flare. Fireman, DeFelice, and Tilles² have previously found tritium and argon-37 activities in the same sample used in this investigation. Radioactive cobalt-57 was found which had a decay rate of 24 dis min^{-1} per kg of steel on November 12, 1960. This corresponds to a total of 1.3×10^7 atoms of cobalt-57 per kg, compared to 4.8×10^6 atoms of tritium per kg of steel on November 12, 1960. This clearly indicates that the tritons were not produced by an $\text{Fe}^{56}(\alpha, \text{H}^3)\text{Co}^{57}$ stripping reaction of the iron-56, which is about 64 percent abundant in the stainless steel. Detailed measurements are in progress which may reveal manganese and other cobalt activities in the sample.

The Discoverer program of recoverable satellites has allowed the use of radiochemical techniques in the study of extraatmospheric corpuscular radiation. This letter reports[†] the measurements of radioactivity due to cobalt and manganese isotopes produced by irradiation of a stainless-steel battery case flown in Discoverer XVII. This satellite was launched into a polar orbit at 2042 UT on November 12, 1960, a time when the earth was receiving an intense bombardment of solar protons associated with the 3+ solar flare which occurred at 1320 UT on the same day. The apogee of the orbit was 993 km at 20°S, and the perigee was 188 km at 18°N. The vehicle was aloft for about 50 hours. The integrated flux of protons ($E > 30 \text{ Mev}$) and alphas ($E > 120 \text{ Mev}$) measured by

* Paper delivered at the First Western National Meeting of the AGU, December 27 to 29, 1961.

† This research was supported in part by the U.S. Atomic Energy Commission under contract No. AT(49-7) - 1431.

Explorer VII during this period has been given by Van Allen¹ as about $10^9/\text{cm}^2 \text{ sec.}$

Various measurements of radioactivity present in Discoverer XVII have already appeared in the literature (Fireman, DeFelice, and Tilles;² Stoenner and Davis;³ Wasson,⁴ and others). This letter concerns the measurement of 270-day Co^{57} and its bearing on the possibility that the tritium measured in the same sample by Fireman, DeFelice, and Tilles was produced by proton stripping of solar alpha particles. It also reports upper-limit values for the nuclides, 77-day Co^{56} , 5.2-year Co^{60} , and 300-day Mn^{54} , none of which were present in measurable amounts.

The chemical handling of the stainless-steel sample is as follows. A mass of material totaling 167 g was fused by Fireman *et al.* in order to remove the hydrogen and argon. We were then given this fused sample which, due to various handling losses, totaled 150.2 g. This was dissolved in HCl, with oxidation by HNO_3 and H_2O_2 to insure that the iron was in the ferric form. The ferric chloride complex was extracted from an 8N HCl medium into isopropyl ether. (The solar protons should have produced 2.6-year Fe^{55} in good yield. The specific activity should have been quite low, however, and it would have been impossible to count the X rays from this species, which decays only by electron capture. Thus, we did not purify or count the iron fraction) The iron-free solution (predominantly Cr and Ni) was made 10N in HCl, and placed on twelve Dowex-1 anion-exchange columns, each of about 15 ml capacity. The Cr and Ni fraction (containing some Mn) was eluted with 10N HCl. The Mn fraction was eluted with 6N HCl, and the Co fraction with 4N HCl. Any ferric iron not removed by the ether extraction was left on the column. The Co was purified by placing it on a single, fresh Dowex-1 column, eluting with 10N and 6N HCl, and finally removing the Co with 4N HCl. It was then electroplated on Pt from a $\text{NH}_4\text{OH}-\text{NH}_4\text{Cl}$ medium, dried, and weighed.

The Mn fraction was taken to dryness and then dissolved in 1N HCl containing 0.2 percent H_2O_2 . This was placed with a few mg of Ti^{+4} on a Dowex 50W cation-exchange column and the column eluted with 1N HCl containing 0.2 percent H_2O_2 . The Mn was followed with a benzidine spot

test procedure, and came off a few column volumes after the Ti^{+4} . The Mn was precipitated as $MnNH_4PO_4 \cdot H_2O$, dried overnight in a desiccator, and weighed.

The stainless steel was type 304. This steel was manufactured by the Allegheny Ludlum Steel Corporation and has the following specifications: Cr, 18-20 percent; Ni, 8-12 percent; Mn, < 2 percent; Si, < 1 percent; and C, < 0.08 percent. There is no specification on Co, but a representative of Allegheny Ludlum estimated that the concentration might be about 0.15 percent. Thus, the masses of Co and Mn expected from a 150 g sample are 225 mg and < 3 g, respectively. The mass of Co electroplated was 182.3 mg, or a chemical yield of about 81 percent. This is in accordance with previously measured yields of 75 ± 10 percent obtained from this procedure. The mass of Mn counted was 152 mg, or a chemical yield of > 5 percent. We shall assume a chemical yield of Mn of 10 percent. It is not clear where the remainder of the Mn was lost, although a certain amount was definitely in the Ni-Cr fraction from the anion exchange separation.

The Co was counted on the face of a 3 in. x 3 in. NaI crystal, with the pulses sorted on a 100-channel pulse-height analyzer. No peaks due to Co^{60} or Co^{56} were visible in the singles spectrum, but a definite peak was observed at about 0.130 Mev due to the 93 percent-abundant 0.123-Mev and 7 percent-abundant 0.137-Mev gammas associated with the decay of Co^{57} (Crasemann and Manley).⁵ Figure 1 shows the spectrum obtained on September 3, 1961 along with a background spectrum. The net counting rate was 0.57 ± 0.07 cpm, corresponding to a disintegration rate of 1.35 ± 0.20 dpm. This represents a specific activity in the original sample of 24 dpm/kg on November 12, 1960, or 1.3×10^7 Co^{57} atoms/kg. The concentration of tritons found by Fireman, DeFelice and Tilles in this stainless steel sample was 4.8×10^8 tritons/kg. If these tritons were produced entirely by stripping protons from solar alpha particles, one would expect that about 64 percent, or 3.1×10^8 tritons/kg, would be produced by the $Fe^{56}(\alpha, H^3)Co^{57}$ reaction on the Fe^{56} nuclei which were 64 percent abundant in the stainless-steel sample. Our value for the con-

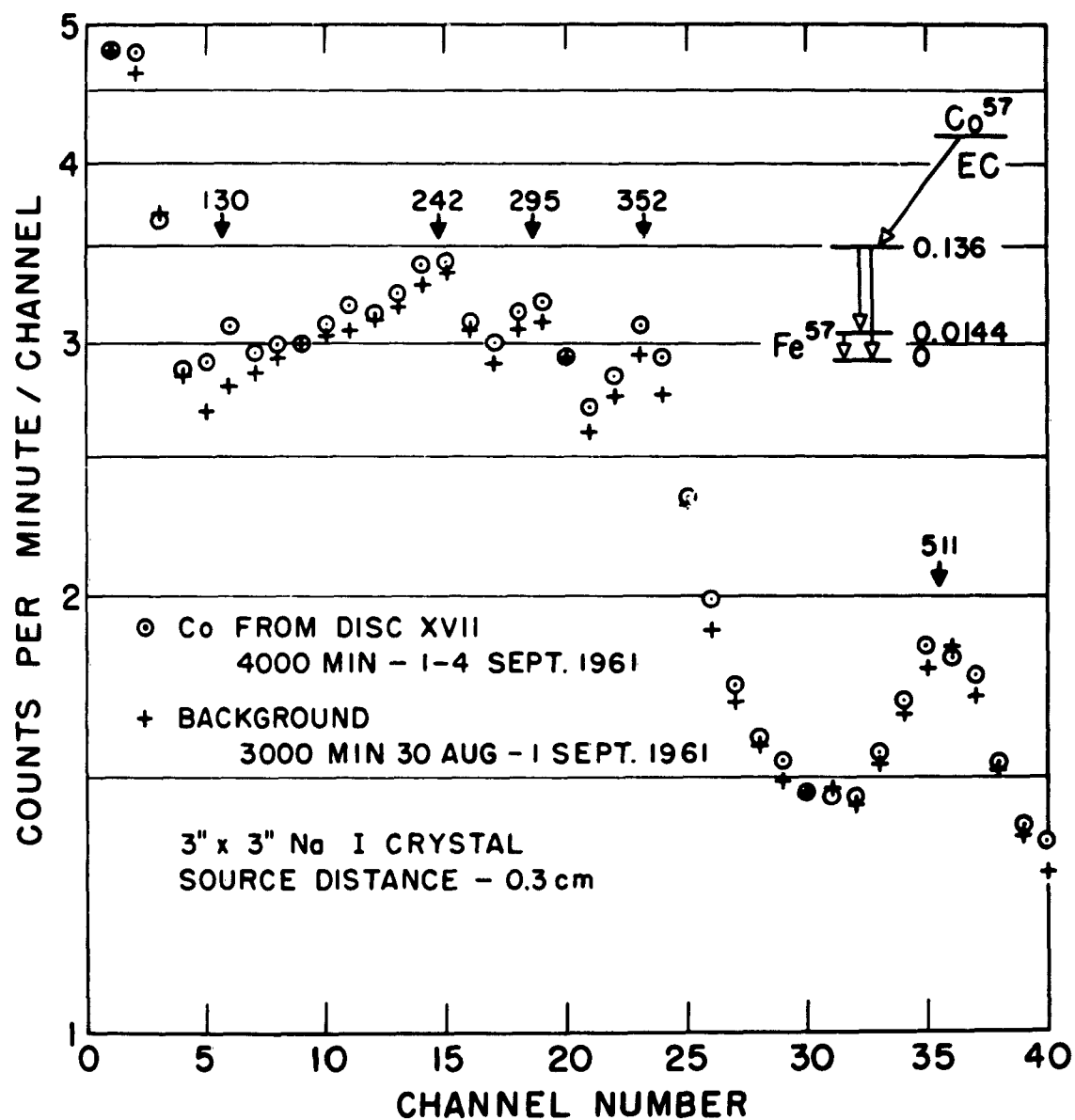


FIG. 1. Gamma-ray spectra of Co^{57} plus background (circles) and background (crosses) taken during 4000- and 3000-minute counts during August-September, 1961. The Co was chemically separated from a stainless-steel battery case carried in Discoverer XVII. A decay scheme of Co^{57} is shown in the upper right corner of the figure.

centration of Co^{57} is a factor 23 lower than that expected on the basis of this method for triton production, and this indicates that some other explanation is necessary to account for the presence of these particles in such high concentrations. Fireman, DeFelice and Tilles believe that the tritons must have been present in the original beam of particles ejected from the sun, although a small fraction may have been due to trapped tritons encountered by the vehicle as a result of its high apogee.

An alternative and more satisfactory explanation for the presence of the Co^{57} is the production of this species and 36-hour Ni^{57} by the action of protons on Ni^{58} , which is about 7 percent abundant in the stainless steel. The (p, pn) and (p, 2p) cross sections* for low-energy protons have been measured by Kaufmann⁶ ($E_p \leq 19$ Mev) and Cohen, Newman, and Handley⁷ ($E_p = 21.5$ Mev). Both of these studies show that the (p, 2p) cross section (σ_{pp}) is about three times larger than the (p, pn) cross section (σ_{pn}). If we assign constant values of $\sigma_{pp} = 450$ mb and $\sigma_{pn} = 150$ mb above a threshold energy of about 16 Mev, it is then possible to calculate the integrated flux (D_p) of protons ($E_p > 16$ Mev) that impinged on the battery case. A lower limit on this proton flux is given by the thin target formula,

$$D_p = \frac{N_{57}}{N_{58} (\sigma_{pp} + \sigma_{pn})}$$

where N_{57} is the concentration of Co^{57} , 1.3×10^7 atoms/kg, and N_{58} is the concentration of target Ni^{58} atoms, 7.4×10^{23} atoms/kg. The integrated flux is thus estimated as 2.9×10^7 protons/cm². This is a factor 5 lower than that estimated in an earlier study (Wasson⁴) on the basis of the production of 8.4-day Ag^{106} by a (p, pn) reaction on Ag^{107} in a AgBr emulsion

* The notation (p, pn) refers to a process in which a proton 'enters' a target nucleus and a proton and neutron 'leave' the nucleus, with the net result of a loss of one neutron by the target nucleus. The notation (p, 2p) refers to a similar process in which the net result is the loss of one proton by the nucleus. Cross sections are reported in units of barns ($1 \text{ b} = 10^{-24} \text{ cm}^2$) and millibarns ($1 \text{ mb} = 10^{-27} \text{ cm}^2$).

block carried on Discoverer XVII. The discrepancy between the two values is not surprising when one considers the variations in shielding associated with the different locations of the target materials within the capsule and the inherent inaccuracies involved in assuming an energy-independent production cross section (in actuality, this factor shows a strong energy dependence at energies lower than about 100 Mev).

As stated earlier, measurable intensities of gammas from Co^{60} and Co^{56} were not present in the singles gamma spectrum taken on a 3 in. x 3 in. NaI detector in conjunction with pulse-height analysis. A much more sensitive method for the measurement of these nuclides is given by the technique of gamma-gamma coincidence spectrometry circuit. Such an apparatus was assembled using two 3 in. x 3 in. NaI detectors in conjunction with single-channel analyzers and a coincidence circuit. For Co^{60} , the single-channel windows were set to cover the energy range from about 1.1 to 1.4 Mev. The efficiency of the detector system was calibrated as 0.013 count per two coincident gammas in this energy region. We estimate that the upper limit on the Co^{60} counting rate is < 0.35 coinc./hour. After considering the efficiency of the counter, the weight of the sample, and the chemical yield, we calculate a specific activity in the stainless steel of < 3.8 dpm/kg on January 25, 1962, or < 4.5 dpm/kg on November 12, 1960.

In order to count positrons, the single-channel windows were set to cover the energy region from 0.49 to 0.53 Mev. The sensitivity of the detector system for annihilation photons was calibrated as 0.10 counts per positron. We place an upper limit on the Co^{56} counting rate of < 0.42 coinc./hour, or < 4.2 positrons/hour. If we consider the weight of the sample, the chemical yield, and that Co^{56} emits positrons in only 20 percent of its decays, we arrive at a specific activity of < 2.9 dpm/kg on February 19, 1962, or < 150 dpm/kg on November 12, 1960.

We can assign an upper limit to the activity of 300-day Mn^{54} on the basis of a gamma-ray spectrum taken on October 14 to 16, 1961. The upper limit on the counting rate of < 0.15 counts/minute corresponds to a disintegration rate of < 1.2 dpm. After correcting for sample weight, the

chemical yield, and decay, we calculate a disintegration rate on November 12, 1960 of < 170 dpm/kg.

The disintegration rates and the total concentrations of radioactive nuclei for the four nuclides sought in this study are summarized in Table 1. All values are corrected for decay back to November 12, 1960. The Co^{57} was probably produced from (p, 2p) and (p, pn) reactions on Ni^{58} , as has already been discussed. It is interesting to consider possible methods for producing the other three nuclides, and to compare the necessary fluxes with that estimated from the Co^{57} activity.

TABLE 1. Comparison of the Activities and the Total Concentrations of Radioactive Nuclei for the Four Nuclides Sought in This Study. *

Nuclide	Activity, dpm/kg	Number of nuclei/kg
Co^{57}	24.	1.3×10^7
Co^{60}	< 4.5	1.7×10^7
Co^{56}	$< 150.$	2.4×10^7
Mn^{54}	$< 170.$	1.1×10^8

* All values are corrected for decay back to November 12, 1960.

There are two main mechanisms for the production of Co^{60} : proton reactions on Ni^{61} (p, 2p) or Ni^{62} (p, 2pn), or neutron capture by Co^{59} . Ni^{61} is 60 times less abundant than Ni^{58} . Ni^{62} is 17 times less abundant than Ni^{58} and the average (p, 2pn) cross section is probably at least a factor of 5 lower than σ_{pp} . Thus, the flux of protons necessary for the production of the upper-limit value of Co^{60} from Ni isotopes would be about 50 times greater than that calculated from Co^{57} production. The integrated flux of secondary thermalized neutrons (produced by proton interactions within the satellite) necessary to produce the Co^{60} can be estimated as $3.1 \times 10^7/\text{cm}^2$ on the basis of the 36-barn cross section and the amount of Co^{59} in our sample. This is considerably higher than one could expect on the basis of vehicle size and composition and the measured proton flux.

The absence of Co^{56} in concentrations higher than $\sim 2.4 \times 10^7$ atoms/kg is a rather interesting result, as Co^{56} should be produced by a (p, n) reaction on the highly abundant Fe^{56} nuclide. Thus, if the cross section for this reaction were at least 120 mb and independent of energy, then the proton flux estimated from the Co^{57} activity should produce the upper-limit value for Co^{56} . Since, however, the cross section is energy dependent with a maximum higher than 120 mb peaked in the 6- to 16-Mev region, the low concentration of Co^{56} may indicate that the energy spectrum of the protons striking the battery case was constant or rising in the region 6 to 16 Mev, before starting the steep fall ($dN/dE \approx KE^{-n}$ where $3 \leq n \leq 5$) expected at higher energies.

Manganese-54 could be produced by protons on Cr^{54} , Mn^{55} , or Fe^{56} . If it were produced from Fe^{56} by a (p, 2pn) reaction with a 50-mb cross section, then the upper limit on Mn^{54} nuclei in the battery case would indicate a maximum flux of 3.2×10^8 protons/cm², a factor of ten higher than that estimated from the Co^{57} activity.

The use of radiochemical techniques for the measurement of radioactivity of materials present in recovered satellites offers an inexpensive method for obtaining data regarding the flux and energy spectrum of protons encountered by the vehicle during its time in orbit. The large uncertainties encountered in the present work can be lowered by a large factor by reducing the shielding to a minimum and making definite measurements of a large number of nuclides produced by reactions whose excitation functions are well known.

REFERENCES

1. J.A. VAN ALLEN, Explorer VII observations of solar cosmic rays, November 12-23, 1960, Bull. Am. Phys. Soc. (II), 6: 276, 1961.
2. E.L. FIREMAN, J. DeFELICE, and D. TILLES, Solar flare tritium in a recovered satellite, Phys. Rev., 123: 1935-1936, 1961.
3. R.W. STOENNER, and R. DAVIS, Jr., Argon-37 produced in stainless steel from Discoverer XVII and XVIII and its relations to meteorites, Bull. Amer. Phys. Soc. (II), 6: 277, 1961.
4. J.T. WASSON, Radioactivity produced in Discoverer XVII by November 12, 1960 solar flare protons, J. Geophys. Res. 66: 2659-2663, 1961, pp. 115-125 in AFCRL-62-441.
5. B. CRASEMANN, and D.L. MANLEY, Radioactivity of Co^{57} , Phys. Rev., 98: 66-68, 1955.
6. S. KAUFMAN, Reactions of protons with Ni^{58} and Ni^{60} , Phys. Rev., 117: 1532-1538, 1960.
7. B.L. COHEN, E. NEWMAN, and T.H. HANDLEY, (p, pn) + (p, 2n) and (p, 2p) cross sections in medium weight elements, Phys. Rev., 99, 723-727, 1955.

MAGNETIC ACTIVITY ASSOCIATED WITH THE 12 NOVEMBER 1960 EVENT

Edwin J. Chernosky
Geophysics Research Directorate
Air Force Cambridge Research Laboratories

The geomagnetic phenomena receiving principal attention for study purposes in the November event are the Sudden Commencements (SC) and similar magnetic changes. The background magnetic activity also deserves attention and it is to this aspect that this analysis is first directed.

One worthwhile consideration related to interpretations of the event is its status as a recurrent or nonrecurrent event. A recurrent event is one which reappears at 27-day intervals, an interval corresponding to the solar rotation cycle. By reference to Bartel's "Musical" diagrams it is found that the 12-13 November dates were preceded by four intervals, 27, 54, 81 and 108 days earlier, which were definitely quiet intervals.¹ The two intervals that followed, 27 and 54 days later, were moderately quiet and quiet respectively. The Bartel's K_p values in the "Musical" diagram are for three-hour intervals of the Greenwich Day.

The observation that the great terrestrial disturbance existed in a sequence which was terrestrially quiet before and after it suggests again that the greater disturbances are not connected with recurrent events as has been noted in some studies.

Looking at the daily sequence of magnetic activity in the A_p figures there was noted an active disturbance on the 9th day preceding the great storm. The 7th to 3rd days before the onset of the storm were very quiet, however, before the gradual buildup into the big storm. This quiet period in the days before a disturbance is evidenced in statistical studies of selected disturbance and the preceding periods, although in November the increase in the daily activity was less abrupt.² The statistical cases were

selected for abruptness of onset. The daily A_p figure is derived by a linear conversion from the semi-logarithmic K_p numbers. It reaches a very high value of 280 for the 13th. (Chronological daily values of A_p are 18, 52, 11, 6, 6, 3, 5, 6, 18, 67, 280, 49, 69, 94, 18, and 5.)

Other aspects of the geomagnetic background or history are also pertinent to a complete study of any such activity. Here an evaluation of the longer term trends in horizontal magnetic intensity (H) is made. It is undertaken by a study of the successive daily mean values of H recorded at stations from polar to equatorial latitudes. These graphs are plotted from overlapping three 24-hr means centered at 1200 UT (dots), 1200 local time, and at a third hour midway in the 14 to 19 hours between the 1200 hours noted. The 24-hr means are intended to minimize the influence of the diurnal variation. The data for the month of November 1960 are shown in Fig. 1.

In the lower latitudes there is a gradual rise in H for several days prior to about the 11th of November. It is followed on the next day by the normal storm-time decrease which appears at its minimum on the 13th and reaches very low values.

Following this storm minimum there is the usual postdisturbance recovery for the several (usually 5 to 7) days following. It is during this recovery phase, however, for the first great disturbance (beginning on the 12th) that the second storm occurs (beginning on the 15th). Occurrence of the second storm before the magnetic field had returned to its prestorm, or even its mean value for the month, suggests that it and related phenomena must be considered separately, since its onset occurred under somewhat different magnetospheric conditions than did the first.

An examination in Fig. 1 of the relative intensities of the two storms shows the second storm to be less intense (does not reach as low values) at low latitudes. In progressing poleward a study of the graphs indicates the intensity of the second storm diminishes somewhat at the middle latitudes relative to the first storm. Just south of the auroral zone at Sitka there is little or no reduction of H and possibly an increase, over the mean value, during the main part of the second storm.

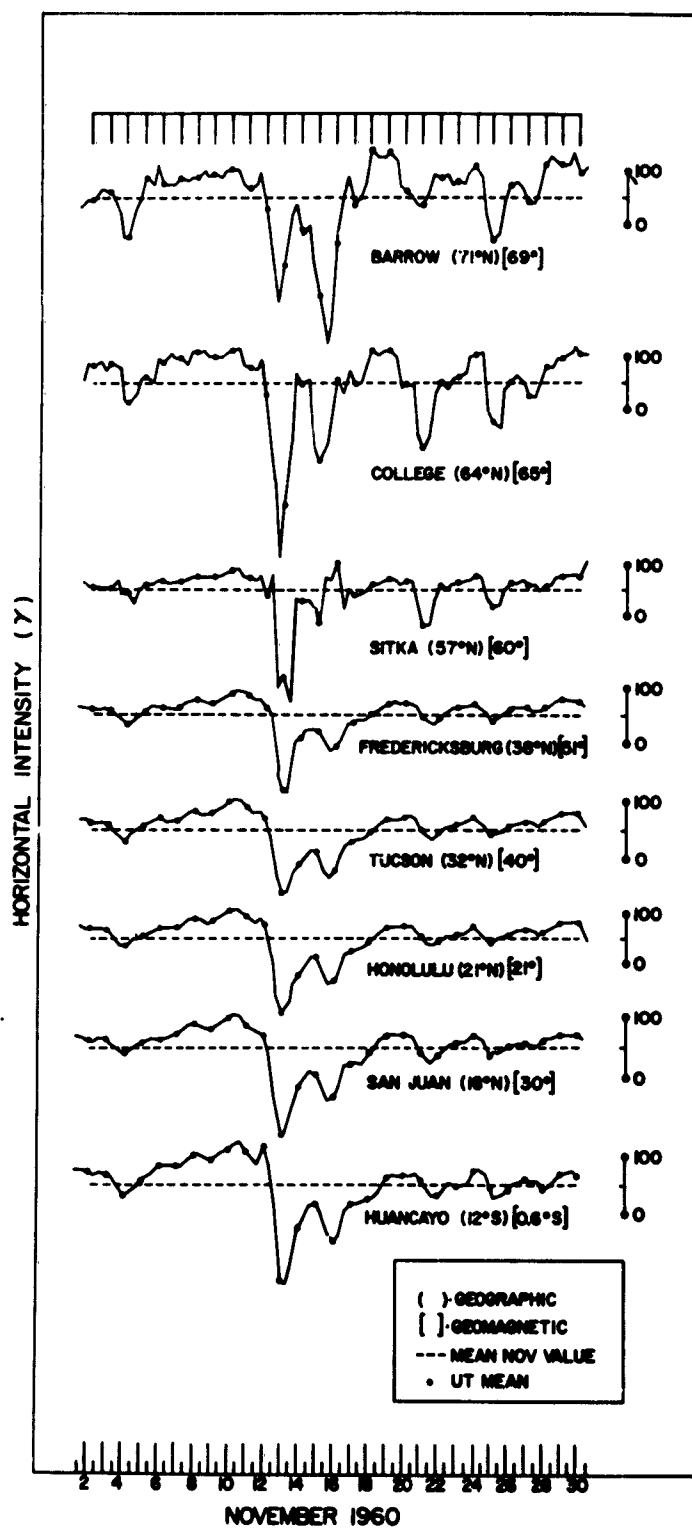


FIG. 1. Latitudinal variation in daily averages of magnetic values for November 1960.

At College, in the auroral zone, the first and second storm are related in effect as they are in the lower latitudes and attain the greatest intensities (lowest minimum values) of all the latitudes studied. At Pt. Barrow in the polar-cap zone, the second event is more intense than is the first. If this effect is not due to instrumental instability or measurement difficulties then further studies can be undertaken of effects at the polar cap responsible for the anomalies noted.

Some of the details of the onset of the first magnetic storm are shown in Fig. 2. The data are variable-area magnetograms obtained from the Vestine-Chernosky pattern magnetographs located at Godhavn, Greenland; Weston, Massachusetts; Fredericksburg, Virginia; and Huancayo, Peru. Conventional records from Honolulu provide comparison (Figs. 3 and 4).

In the variable-area records a change in the magnetic field is noted at 1325 UT on the 12th. (At Fredericksburg the film trace was being changed at this time and includes a calibration at about 1330.) The magnetic change at Huancayo shows an increase in H which can be considered similar to the onset of a magnetic 'crochet.' At 1348 a much sharper increase, which is denoted an (SC), occurs.

As a 3+ solar flare was started at 1323 UT and developed at 1325, near Central Meridian Passage (CMP), the rise at 1325 can logically be considered the beginning of a magnetic 'crochet' directly associated with the solar flare, a crochet which later merged into the following storm commencement.

The earliest observation of the association of a magnetic 'crochet' to a solar flare was at Huancayo on 8 April 1936.³ That the 'crochet' was quite pronounced can be attributed to its occurrence near local noon and the sub-solar point. The magnetic onset on 12 November occurred much earlier in the local daytime at the stations shown in Fig. 2 and this timing of occurrence was probably responsible for the small changes, which are here termed a 'crochet' also by the factor of simultaneity with the solar outburst.

While this analysis is not complete it is felt the following factors require attention.

If the flare with its associated crochet at 1325 on the 12th is related

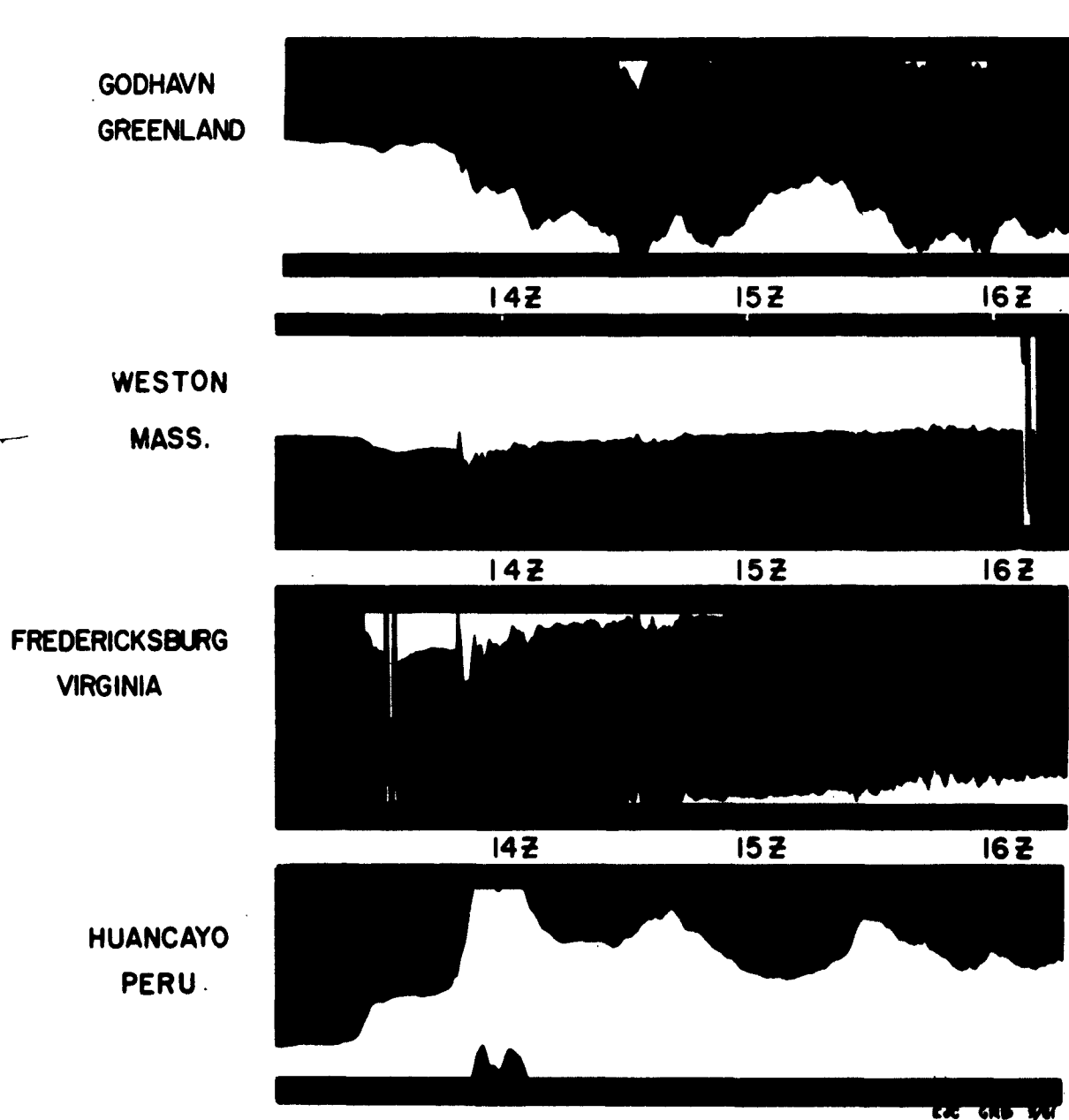


FIG. 2. Variable area magnetograms for the 12 November 1960 storm.

to the Sudden Commencement storm beginning at 1348 on the 12th, rather than the flare on the 11th, then a travel time (from sun to earth) of only 23 minutes is required for solar corpuscles as compared with travel times usually estimated at about an equivalent number of hours by that theory.⁴

This great disturbance was not a member of a recurrent sequence.

The previous history of the earth's magnetic field should be considered in the evaluation of a magnetic disturbance and related magnetospheric influences.

Differences in general character of the magnetic 'crochet' and the Storm Sudden Commencement suggest different production mechanisms for the two phenomena.

ACKNOWLEDGMENTS

Thanks are due to M. P. Hagan, J. M. Collins, and N. E. Collingwood of Physics Research Division of Emmanuel College for the computations and preparation of the graphs. The author also wishes to thank the U.S. Coast and Geodetic Survey and the Instituto Geofísico del Perú for providing the hourly magnetic values in advance of publication.

REFERENCES

1. J. BARTELS, Planetary Magnetic Three-Hour Range Indices, IAGA Committee of Characterization of Magnetic Activity, Gottingen, Germany.
2. E. J. CHERNOSKY, Changes in the Geomagnetic Field Associated with Magnetic Disturbance, Proceedings of International Conference on Earth Storms and Cosmic Rays, Kyoto, September 1961, In press.
3. O. W. TORRESON, W. E. SCOTT, F. T. DAVIES, R. S. RICHARDSON, Radio Fadeouts of April 8 and November 6, 1936 and May 25, 1937. Terrestrial Magnetism and Electricity, 41: 197-201, 1936; 42: 311, 1937.
4. S. CHAPMAN, and J. BARTEL, Geomagnetism, Chapter 24. 2, University Press, Oxford, 1951.

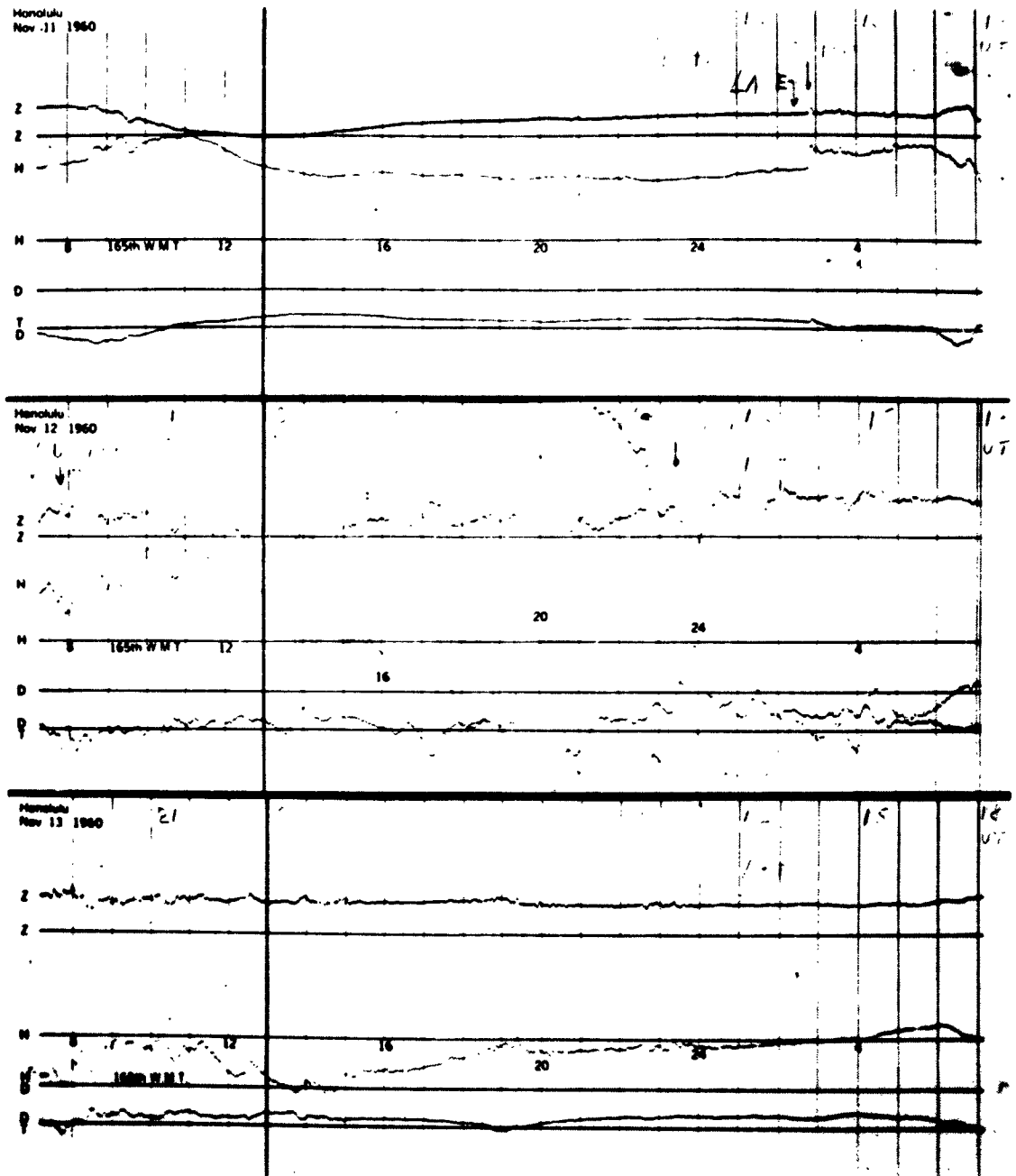


FIG. 3. Standard magnetograms from Honolulu for Nov. 11, 12, and 13, 1960.

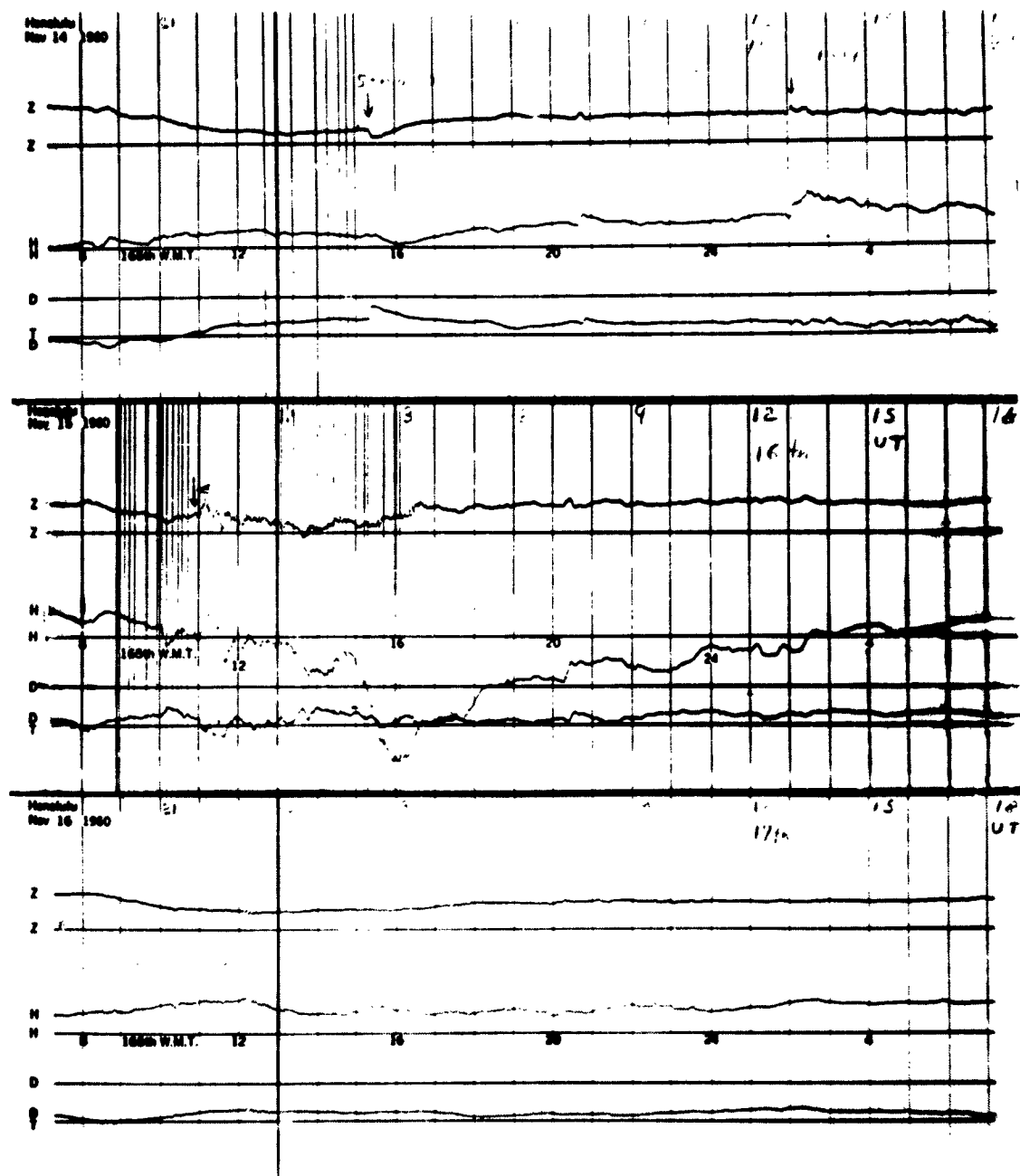


FIG. 4. Standard magnetograms from Honolulu for Nov. 14, 15, and 16, 1960.

<p>AF Cambridge Research Laboratories, Bedford, Massachusetts AFCRL STUDIES OF THE NOVEMBER 1960 SOLAR-TERRESTRIAL EVENTS, by J. Aarons and S. M. Silverman, Eds. April 1962. 162 pp. Incl. illus. AFCRL-62-441 Unclassified report</p> <p>A conference on the November 1960 solar-terrestrial events was held at the Air Force Cambridge Research Laboratories, Hanscom Field, Bedford, Massachusetts, February 15 to 17, 1961. Data on solar and geophysical observations and their theoretical interpretations by the scientific staff at AFCRL are presented. The solar-terrestrial events are unique in that they provide information on solar particles of cosmic-ray energies and on geophysical and propagation effects of the cosmic-ray flares.</p>	<p>UNCLASSIFIED</p> <p>1. Solar flares</p> <p>I. Aarons, J., Ed. II. Silverman, S. M., Ed.</p>	<p>AF Cambridge Research Laboratories, Bedford, Massachusetts AFCRL STUDIES OF THE NOVEMBER 1960 SOLAR-TERRESTRIAL EVENTS, by J. Aarons and S. M. Silverman, Eds. April 1962. 162 pp. Incl. illus. AFCRL-62-441 Unclassified report</p> <p>A conference on the November 1960 solar-terrestrial events was held at the Air Force Cambridge Research Laboratories, Hanscom Field, Bedford, Massachusetts, February 15 to 17, 1961. Data on solar and geophysical observations and their theoretical interpretations by the scientific staff at AFCRL are presented. The solar-terrestrial events are unique in that they provide information on solar particles of cosmic-ray energies and on geophysical and propagation effects of the cosmic-ray flares.</p>	<p>UNCLASSIFIED</p> <p>1. Solar flares</p> <p>I. Aarons, J., Ed. II. Silverman, S. M., Ed.</p>	<p>UNCLASSIFIED</p> <p>1. Solar flares</p> <p>I. Aarons, J., Ed. II. Silverman, S. M., Ed.</p>	<p>UNCLASSIFIED</p> <p>1. Solar flares</p> <p>I. Aarons, J., Ed. II. Silverman, S. M., Ed.</p>
<p>AF Cambridge Research Laboratories, Bedford, Massachusetts AFCRL STUDIES OF THE NOVEMBER 1960 SOLAR-TERRESTRIAL EVENTS, by J. Aarons and S. M. Silverman, Eds. April 1962. 162 pp. Incl. illus. AFCRL-62-441 Unclassified report</p> <p>A conference on the November 1960 solar-terrestrial events was held at the Air Force Cambridge Research Laboratories, Hanscom Field, Bedford, Massachusetts, February 15 to 17, 1961. Data on solar and geophysical observations and their theoretical interpretations by the scientific staff at AFCRL are presented. The solar-terrestrial events are unique in that they provide information on solar particles of cosmic-ray energies and on geophysical and propagation effects of the cosmic-ray flares.</p>	<p>UNCLASSIFIED</p> <p>1. Solar flares</p> <p>I. Aarons, J., Ed. II. Silverman, S. M., Ed.</p>	<p>AF Cambridge Research Laboratories, Bedford, Massachusetts AFCRL STUDIES OF THE NOVEMBER 1960 SOLAR-TERRESTRIAL EVENTS, by J. Aarons and S. M. Silverman, Eds. April 1962. 162 pp. Incl. illus. AFCRL-62-441 Unclassified report</p> <p>A conference on the November 1960 solar-terrestrial events was held at the Air Force Cambridge Research Laboratories, Hanscom Field, Bedford, Massachusetts, February 15 to 17, 1961. Data on solar and geophysical observations and their theoretical interpretations by the scientific staff at AFCRL are presented. The solar-terrestrial events are unique in that they provide information on solar particles of cosmic-ray energies and on geophysical and propagation effects of the cosmic-ray flares.</p>	<p>UNCLASSIFIED</p> <p>1. Solar flares</p> <p>I. Aarons, J., Ed. II. Silverman, S. M., Ed.</p>	<p>UNCLASSIFIED</p> <p>1. Solar flares</p> <p>I. Aarons, J., Ed. II. Silverman, S. M., Ed.</p>	<p>UNCLASSIFIED</p> <p>1. Solar flares</p> <p>I. Aarons, J., Ed. II. Silverman, S. M., Ed.</p>

AD	UNCLASSIFIED	AD	UNCLASSIFIED
AD	UNCLASSIFIED	AD	UNCLASSIFIED
AD	UNCLASSIFIED	AD	UNCLASSIFIED
AD	UNCLASSIFIED	AD	UNCLASSIFIED